**Naval Surface Warfare Center**
**Carderock Division**
West Bethesda, MD 20817-5700

**NSWCCD-TR-65–97/18** April 1997

Survivability, Structures, and Materials Directorate

Technical Report

# An Experimental Investigation of the Ultimate Strength of Stiffened Panels

## - Volume 1, Results and Analyses

by
Gregory J. White (USNA),
ENS Robert H. Vroman (USNR),
David P. Kihl (NSWCCD), and
Sara E. Mourning (USNA)





**DEPARTMENT OF THE NAVY**

NAVAL SURFACE WARFARE CENTER, CARDEROCK DIVISION
9500 MACARTHUR BOULEVARD
WEST BETHESDA MD 20817-5700

9100
Ser 65-43
12 May 97

From: Commander, Naval Surface Warfare Center, Carderock Division
To: Commander, Naval Sea Systems Command (SEA 03R)

Subj: RELIABILITY BASED STRUCTURAL DESIGN PROGRAM

Ref: (a) Program Element PE063564N, Project S2036-01, Milestone H5, Subtask IIC

Encl: (1) NSWCCD-TR-65–97/18, *An Experimental Investigation of the Ultimate Strength of Stiffened Panels - Volume 1, Results and Analyses*

(2) NSWCCD-TR-65–97/18, *An Experimental Investigation of the Ultimate Strength of Stiffened Panels - Volume 2, Test Data*

1. Reference (a) directed the Naval Surface Warfare Center, Carderock Division (NSWCCD) and the U.S. Naval Academy to investigate the failure mode and ultimate strength of longitudinally-stiffened plate commonly used in ship structures such as decks, bottoms, bulkheads and side shells. Enclosure (1) presents results for six grillages which were tested to collapse in the Grillage Test Fixture at the U.S. Naval Academy. Each grillage consisted of three stiffened panels (bays). They were nominally identical and represented approximately a 1/3rd scale model of typical warship deck structure. The grillages were made of longitudinal and transverse T-shaped stiffeners welded to flat plate; all pieces were made of mild steel. Three of the six specimens were tested under in-plane axial load only; the remaining three were tested under a combination of axial in-plane load and initial lateral pressure. The test specimens were fully instrumented with strain gages and displacement transducers to quantify the structural behavior up to and beyond ultimate collapse. Although representative plots of structural behavior are illustrated in Enclosure (1), a much more comprehensive series of test results is provided, for each test, in Enclosure (2).

2. The report compares test results from these panels with theoretical predictions of failure mode and stress. Data obtained from a literature search of similar tests performed at other facilities were also used for comparison. In so doing, we have evaluated the accuracy of theoretical predictions over a wide range of test conditions. A finite element model of the grillage specimen subjected to compressive axial was also constructed and compared to the test results.

3. The in-plane axial load test results were found to be between 4% and 8% higher than the theoretical prediction. The predictions are considered to be quite good and slightly conservative. The test results with lateral load were found to be 4% higher for the 5 psi case and about 20%

higher for the 10 psi and 20 psi loadings. The poorer agreement at higher pressures, although conservative, is attributed to a shortcoming in the way lateral deformations are assumed to magnify the axial in-plane stresses. The finite element results were found to accurately predict the ultimate strength of the grillage specimen, but did not produce good estimates of the overall deformations. Better agreement may be possible by modeling the stiffener attachments to the plating and including initial geometric imperfections. Results of the literature search revealed very few tests have been conducted on multi-bay specimens, and even fewer with combine in-plane and axial loads.

4. Comments or questions may be referred to the principal investigator, Dr. David P. Kihl, Code 653; telephone (301) 227-1956; e-mail, kihl@oasys.dt.navy.mil.

J. E. BEACH
By direction

Copy to:

COMNAVSEASYSCOM WASHINGTON DC
- SEA 03H (w/o encl (2))
- SEA 03H3 (w/o encl (2))
- SEA 03H3 (Engle) (w/o encl (2))
- SEA 03P (w/o encl (2))
- SEA 03P1
- SEA 03P1 (Bourne) (w/o encl (2))
- SEA 03P1 (Kadala) (w/o encl (2))
- SEA 03P1 (Nappi) (w/o encl (2))
- SEA 03P1 (Waldman) (w/o encl (2))
- SEA 03P1 (Walz) (w/o encl (2))
- SEA 03P4 (Kurzweil) (w/o encl (2))
- SEA 03P4 (Snyder) (w/o encl (2))
- SEA 03R3 (Hough) (w/o encl (2))
- SEA 03R1 (Webster) (w/o encl (2))

USNA ANNAPOLIS MD
- Dept. of Naval Architecture, Ocean, and Marine Engineering
- (White)
- (Mouring)

DTIC FORT BELVOIR VA

NAVSURFWARCEN CARDEROCKDIV BETHESDA MD
- Codes 3442 (TIC)
- 60 (w/o encl)
- 601 (w/o encl)
- 602/6091 (w/o encl)
- 65
- 65R (2 copies, encl (1)) (1 copy, encl (2))
- 65 (files, w/o encl)
- 651 (w/o encl (2))
- 651 (Adamchak)
- 653 (4 copies, encl (1)) (4 copies, encl (2))
- 653 (Kihl)
- 654 (w/o encl (2))
- 654 (Melton) (w/o encl (2))

**Naval Surface Warfare Center**
**Carderock Division**
West Bethesda, MD 20817-5700

**NSWCCD-TR-65–97/18** April 1997

Survivability, Structures, and Materials Directorate

Technical Report

# An Experimental Investigation of the Ultimate Strength of Stiffened Panels

# - Volume 1, Results and Analyses

by

Gregory J. White (USNA),

ENS Robert H. Vroman (USNR),

David P. Kihl (NSWCCD), and

Sara E. Mourning (USNA)



Enclosure (1)

# REPORT DOCUMENTATION PAGE

*Form Approved*
*OMB No. 0704-0188*



| 1. AGENCY USE ONLY *(Leave blank)* | 2. REPORT DATE | 3. REPORT TYPE AND DATES COVERED |
|---|---|---|
| | April 1997 | Final |

**4. TITLE AND SUBTITLE**
An Experimental Investigation of the Ultimate Strength of Stiffened Panels - Volume 1. Results and Analyses

**5. FUNDING NUMBERS**
PE063564N
S203601

**6. AUTHOR(S)**
Gregory J. White, Robert H. Vroman, David P. Kihl, Sara E. Mourning

**7. PERFORMING ORGANIZATION NAME(S) AND ADDRESS(ES)**
Naval Surface Warfare Center
Carderock Division
9500 MacArthur Boulevard
West Bethesda, MD 20817-5700

U.S. Naval Academy
Dept of Naval Architecture,
and Marine Engineering
121 Blake Avenue
Annapolis, MD 21402-5000

**8. PERFORMING ORGANIZATION REPORT NUMBER**
NSWCCD-TR-65-97/18

**9. SPONSORING/MONITORING AGENCY NAME(S) AND ADDRESS(ES)**
Naval Sea Systems Command (SEA 03R)
2531 Jefferson Davis Highway
Arlington, VA 22242-5160

**10. SPONSORING/MONITORING AGENCY REPORT NUMBER**

**11. SUPPLEMENTARY NOTES**

**12a. DISTRIBUTION/AVAILABILITY STATEMENT**
Approved for public release; distribution is unlimited.

**12b. DISTRIBUTION CODE**

**13. ABSTRACT** ***(Maximum 200 words)***

A series of multi-bay steel grillages were tested to collapse in the Grillage Test Fixture at the U.S. Naval Academy. The grillages were nominally 1/3-scale models of typical warship deck structures. The tests were part of a student research project investigating reliability-based design methods for stiffened panels. The six nominally identical grillage specimens were made from ordinary steel and consisted of three panels (bays) stiffened longitudinally and transversely with T-shaped stiffeners. Three specimens were tested under in-plane loads only, and three were tested with a combination of in-plane loads and initial lateral pressure. During testing, data were collected from strain gages and displacement transducers to quantify the structural behavior of the specimens under load. Theoretical predictions of failure mode and stress level are compared to observed values. The test results are also compared to results from similar tests conducted at other facilities. A finite element method analysis of the grillages subjected to compressive axial load was conducted using ABAQUS and the results compared to the test results. The data from past tests and these tests are used to evaluate the accuracy of theoretical predictions over a wide range of test conditions.

**14. SUBJECT TERMS**
steel grillage
ABAQUS
reliability-based design methods
in-plane loads
stiffened panels
T-shaped stiffeners

**15. NUMBER OF PAGES**
113

**16. PRICE CODE**

| 17. SECURITY CLASSIFICATION OF REPORT | 18. SECURITY CLASSIFICATION OF THIS PAGE | 19. SECURITY CLASSIFICATION OF ABSTRACT | 20. LIMITATION OF ABSTRACT |
|---|---|---|---|
| UNCLASSIFIED | UNCLASSIFIED | UNCLASSIFIED | SAR |

NSN 7540-01-280-5500

**Standard Form 298 (Rev. 2-89)**
Prescribed by ANSI Std. Z39-18
298-102

Table of Contents

Table of Contents (con't)



Figures

Figures (con't)

Page

Figures (con't)

Figures (con't)

Page

Figures (con't)

Page

Tables

## Administrative Information

The work described herein was performed by the Department of Naval Architecture, Ocean, and Marine Engineering at the U.S. Naval Academy (USNA) and the Structures and Composite Department, Code 65, of the Survivability, Structures, and Materials Directorate at the Naval Surface Warfare Center, Carderock Division (NSWC/CD) under the sponsorship of the Naval Sea Systems Command (SEA 03R3). This report is submitted in partial fulfillment of Milestone H5, Sub task IIC of the Reliability Based Structural Design Program PE063564N, Project S2036-01.

## Acknowledgements

The authors would like to express their gratitude to the following individuals who contributed to this effort; Mr. G. Snyder from NAVSEA 03P and Dr. J. Adamchak from NSWC/CD for their guidance and suggestions; Mr. R. Jenkins of NSWC/CD for providing the data acquisition software; and the many others, both at the USNA and NSWC/CD, who contributed during the fabrication, instrumentation and testing phases of this effort.

# Introduction

The longitudinally-stiffened plate panel forms the backbone of most of a ship's structure. It is by far the most commonly used element in a ship, appearing in decks, bottoms, bulkheads, and side shell. The primary purpose of the panel is to carry part of the longitudinal hull girder bending stress when the stiffeners are oriented longitudinally. It also serves to absorb out-of-plane (or lateral) loads and distribute these loads to the ship's primary structure. The amount of in-plane compression or tension and out-of-plane lateral loads experienced depends primarily on the location of the panel. Deck panels tend to experience large in-plane compression and tension loadings with only small lateral pressures. Bottom panels see large in-plane tension and compression loadings, but usually with very significant lateral pressures.

A typical panel, as shown in Figure 1, is bounded on each end by a transverse structure which has significantly greater stiffness in the plane of the lateral load. The sides of the panel are defined by the presence of a large structural member which has greater stiffness in bending and much greater stiffness in axial loading. Such structural members as keels, bottom girders, longitudinal bulkheads, deck girders, etc. can act as the side boundaries of the panel. When the panel is located to be in position to experience large in-plane compression, the boundary conditions for the ends can be conservatively assumed to be simply-supported. Under these same conditions, the boundary conditions along the sides can also be considered simply supported.

Three types of loads affect the panel. Negative bending loads are the lateral loads due to uniform lateral pressure which cause the plate to be in tension and the stiffener flanges to be in compression. Positive bending loads are the lateral loads which put the plating in compression

and the stiffener flange in tension. The third load type is uniform in-plane compression. This type of loading arises from the hull girder bending, and will be considered to be positive when the panel is in compression. These loads may act individually or in combination with one another.

The future of ship structural design lies in the introduction of probabilistic methods to the design process. The most common approach for introducing reliability-based design is through the use of the Load and Resistance Factor Design (LRFD) format. In this approach, partial safety factors are assigned to each of the important variables in the design equation. The partial safety factors are based on the probabilistic characteristics of the variables and the inherent uncertainty in the analytical model used as the design equation. These structural tests attempt to extend the current knowledge of the collapse behavior of typical ship orthogonally-stiffened panels (grillages) in an attempt to provide a probabilistic description of the uncertainty associated with this design approach.

## Test Description

These grillage tests were the culmination of several years of development effort between the U.S. Naval Academy (USNA) and the Carderock Division of the Naval Surface Warfare Center (NSWC/CD). The development effort was intended to put in place the capability of performing ultimate strength tests of scale model grillages under combined in-plane and lateral loads. That capability would then be used to help increase the current knowledge on the ultimate strength of stiffened panels and support student course work and research in ship structures.

This grillage testing program of six nominally identical grillages tested in two series. The first series, grillages 0494, 0894, and 1094, were loaded by in-plane compression only. The second series, grillages 0595, 0695, and 0995, were subjected to combined in-plane compressive load and uniform lateral pressure. A description of the grillage specimens, the grillage test fixture, and the testing procedure is given in the following sections.

## Test Specimens

The grillage specimens used in the test series were planned to be scaled models of the main deck of a generic warship. Because it was not possible to exactly scale the dimensions of the plating and stiffeners, standard plate and stiffener sizes were used. The sizes were chosen so that the ratio of the stiffener area to plate area and the ratio of the flexural rigidity of the plate and stiffener closely matched the baseline ship. Figure 2a shows the overall dimensions of the stiffened panels used in this series of tests while Figure 2b gives the details of the connection between the longitudinals and the transverse webs. The grillage specimens constructed at NSWC/CD, were nominally identical structures. The quality of construction in each of these grillages was intended to simulate typical shipyard standards. However, because of their small size and the nearly ideal welding conditions in the welding shop, the resulting welds were of a generally better quality than expected from a typical shipyard.

The grillages were designed to have the four longitudinal stiffeners pass continuously through cutouts in the transverse frames. The connections between the stiffeners and the frame web were provided by small steel clips butt-welded to each side of the stiffener and lap-welded

to the transverse web frame (see Figure 2b). The flange of the stiffener was also welded to the transverse frame. In order to try and ensure that failure occurred in the center bay, the plating in the two outer bays was designed to be slightly thicker. Table 1 provides the details of the geometry for the center bay portion of the grillage. The two end bays had identical dimensions with the exception that the plate thickness was increased from 3/16-inch to ¼-inch. The transition between plate thicknesses occurred one inch from the transverse web frame towards the middle of the grillage. Figure 3 is a photograph of one of the grillage specimens prior to testing. The stiffener to web connections can be seen in the photograph.

Table 1 Grillage Dimensions (Center Bay)

| Member | Grillage Number | | | | | |
|---|---|---|---|---|---|---|
| | 0494 | 0894 | 1094 | 0595 | 0695 | 0995 |
| Plate Thickness (in)[a] | 0.187 | 0.187 | 0.188 | 0.187 | 0.188 | 0.187 |
| Panel Width (in)[b] | 9.0 | 9.0 | 9.0 | 9.0 | 9.0 | 9.0 |
| Panel Length (in)[b] | 36.0 | 36.0 | 36.0 | 36.0 | 36.0 | 36.0 |
| Longitudinal Stiffener Height (in)[a] | 2.829 | 2.850 | 2.790 | 2.812 | 2.825 | 2.855 |
| Long. Stiffener Web Thickness (in)[b] | 0.114 | 0.114 | 0.114 | 0.114 | 0.114 | 0.114 |
| Long. Stiffener Flange Width (in)[a] | 1.901 | 1.865 | 1.860 | 1.875 | 1.900 | 1.865 |
| Long. Stiffener Flange Thickness (in)[a] | 0.170 | 0.168 | 0.169 | 0.172 | 0.170 | 0.166 |
| Transverse Stiffener Height (in)[b] | 9.0 | 9.0 | 9.09 | 9.0 | 9.0 | 9.0 |
| Trans. Stiffener Web Thickness (in)[b] | 0.188 | 0.188 | 0.188 | 0.188 | 0.188 | 0.188 |
| Trans. Stiffener Flange Width (in)[b] | 3.0 | 3.0 | 3.0 | 3.0 | 3.0 | 3.0 |
| Trans. Stiffener Flange Thickness (in)[b] | 0.25 | 0.25 | 0.25 | 0.25 | 0.25 | 0.25 |

[a] Dimensions are averages of the measured values for that particular grillage. Number of measurements varied on each grillage.
[b] Dimensions are nominal design values.

The material used in the construction the grillages was purchased as mild steel. This type of steel is one that has been used in warship construction. The grillages were manufactured in two different sets. The first set was constructed from a batch of steel received at NSWC in 1994. The second set was built to the same specifications, but used a batch of steel which arrived at NSWC in early 1995. Tension and compressive coupon tests were conducted at NSWC for the material used in each set of three grillages. Though both sets of steel were ordered from the same manufacturer and were purchased as "mild" steel, the strength differed between batches of steel and between the plating and the stiffeners. The results of the coupon tests are given in Table 2.

Table 2 - Material Properties

| Member | Property | Grillage Numbers | |
|---|---|---|---|
| | | 0494, 0894, & 1094 | 0595, 0695, & 0995 |
| Plate | Tensile Yield Stress | 50.7 ksi (0.027) | 51.7 ksi (0.019) |
| | Compressive Yield Stress | 46.3 ksi (0.087) | 53.4 ksi (0.026) |
| Stiffener | Tensile Yield Stress | 56.4 ksi (0.030)* | 55.8 ksi (0.089) |
| | Compressive Yield Stress | 55.1 ksi (0.002) | 57.5 ksi (0.112) |

* Mean values with coefficients of variation given in parentheses

## Apparatus Description

The grillage test fixture used in the U.S. Naval Academy Ship Structures Laboratory was specially designed by NSWC/CD based upon an earlier design used at Rhor Marine Inc., San Diego, CA, under NSWC sponsorship. The fixture is designed to apply both axial and lateral loads to a grillage. The axial load simulates the loading that would result from bending on a ship's hull. The capability to apply a lateral load simulates a hydrostatic pressure load on a ship's shell.

## Test Fixture

The test fixture, shown schematically in Figure 4, is designed to be self-reacting when applying axial compression to the test specimen. The fixture consists of a large steel reaction head connected to a large steel fixed head by two large steel I-beams (W14x82). The base of a hydraulic cylinder is attached to the fixed head and the cylinder ram is attached to a large steel loading head through a load cell and a spherical bearing. The hydraulic cylinder moves the loading head to apply compression to the grillage specimen. The other end of the grillage specimen is held by the reaction head. The force exerted against the fixed and reaction heads puts the two I-beams in tension.

The hydraulic loading mechanism is capable of applying 360,000 lbs in compression. While loading in tension is possible, the fixture was not designed to do so. The test specimen is bolted to both the reaction and the loading head, applying essentially fixed end conditions at

both ends of the grillage. The heads at both ends are able to withstand 850,000 in-lbs of moment. This moment, which resists the tendency of the deflected shape to rotate, induces the fixed-end boundary condition. The grillage specimen is also tied to four reaction links located at the ends of the transverse frames in the stiffened panel. These reaction links simulate the surrounding structure of the ship and also allow the ends of the transverse frames to translate and rotate longitudinally and transversely, but not move in the vertical plane nor rotate about the vertical axis. Each of the four reaction links is able to withstand 27,500 pounds of loading. The grillage test specimens, therefore, represent ship structure which is located away from heavy longitudinal structure.

The lateral pressure is applied to the test specimen through a rubber water bladder which pushes between the plate side of the grillage specimen and a steel pressure bed, as shown in Figure 4. The rubber diaphragm of the bladder pushes against the panel with a pressure equal to the water pressure in the bladder. The fixture is able to apply up to 40 psi over a 37 inch by 94 inch area. The four reaction links, described above, can be attached to the grillage to simulate the surrounding structure of the ship in resisting the lateral pressure loading. Figure 5a shows a view of the Grillage Test Fixture from the loading head (aft) end. Figure 5b shows a better view of the manner in which the transverse frames are attached to reaction links.

## Load Control System

The system of load application and load control is positively controlled by a personal computer operating station. The PC Integrated Control Management (PCICM) System Model

X8700, developed by Test Systems & Simulation, Inc. (TS&S), Madison Heights, MI, is able to monitor ram head position through a feedback control system. The PCICM acts as an interface between the user, parallel and serial communication, analog subsystem, and the TS&S Digital Closed Loop (DCL) Servo Controller. The X8700 system enables the user to set up DCL parameters and request desired commands for force or motion control. The DCL valve operates directly from the output of the PCICM. Communication is made through an RS485 2-wire balanced serial bus. The DCL servo controller valve is usually operated with a supply pressure of 3000 psi, although it will work with pressures between 200 psi and 3500 psi.

The in-plane compressive load is applied by a hydraulically-driven loading head. The hydraulic pressure necessary to produce desired loading is generated by a 10 hp, 1745 rpm, 440 VAC, horizontal, centrifugal, positive-displacement pump. The operating PC sends a signal with the desired head position from the servo synchro transmitter to a servo amplifier. The power transfer valve determines whether the head should be moved forward or backward. The feedback synchro on the load head sends a feedback signal back to the servo amplifier and PC which tells the head whether to continue moving or to stop.

The lateral load is applied by a rubber, water-filled bladder located under the grillage. The magnitude of the pressure is not monitored or controlled by the PC control system. A pressure gage located in the water piping line provides a visual pressure reading which is used by the operator to adjust the pressure in the system. An additional pressure sensor provides the bladder pressure signal to the data acquisition system. During testing, any variation in the pressure must be manually corrected by adjusting the needle valves in the water supply and discharge lines.

## Data Acquisition System

The data acquisition system used in these experiments is quite versatile, allowing several types of data to be gathered into one system. A NEFF 470 data acquisition system provides conditioning, amplification and converts the data signals from the various measuring instruments into a format usable by the computer system. This system consists of two NEFF 470 chassis, each capable of accommodating 64 channels for a total capacity of 128 data channels. Sixteen cards are inserted into each chassis; each of these cards is able to handle four data channels. For the test setup, one card (four channels) was allocated for the load cell and loading head position. A separate card handled the pressure transducer and two others were dedicated to supporting the five string potentiometers. Fifteen cards were allocated to the sixty strain gages.

The PC-based data acquisition program, developed by NSWC/CD, is capable of acquiring information from strain gages, potentiometers, pressure transducers, and load cells. For the tests performed at USNA, only strain gages, potentiometers, and load cells were used. Calibration of the gages and resistors is simplified by an on-screen monitor that displays the calibration values as each shunt resistor is applied to each strain bridge. Moreover, the setup of the data system allows the characteristics of each strain gage or potentiometer to be fed directly into the program -- nominal manufacturer values do not necessarily have to be used.

The strain gage locations for the first three tests are shown in Figure 6. The remaining three tests had the same strain gage locations except that gages in the forward and aft bays at midspan were moved to the quarter points nearest the center bay (see notes on Figure 6). The

strain gages were placed in these specific locations to assess uniformity of load across the grillage, identify specific buckling modes, and identify load shedding from the plate to the stiffener when the plate buckled. Two different strain gage sizes were used on each grillage specimen. The gages placed on the stiffener flanges were CEA-06-125UW-350 gages and those placed on the plate were CEA-06-250UW-350. The gages were attached to the plating using M Bond AE-10 epoxy. The most important gages for data analysis are in the center panel of the bay between the transverse frames. At the longitudinal center of the panel, gages 35, 37, and 39 on the top of the plate correspond to the gages 36, 38, and 40 at the bottom of the plate. Gages 32, 33, 34 and 42, 43, 44 on the top of the stiffener flanges are located so that the rotation of the stiffener flange could be monitored. Also, by comparing gages 33 with 31 and gages 43 with 41, it is possible to estimate the amount of bending in the stiffener. The gages in the end bays were used to monitor the loading of the grillage and later to monitor the post-collapse behavior of the stiffeners in the end bays.

The displacement measurements are taken by computer monitored string potentiometers and manually monitored analog dial gages. Two string potentiometers were used to measure end shortening and three were used to measure vertical displacements These potentiometers were scanned by the data acquisition computer every second during the loading and unloading processes. The string potentiometers used for this experiment worked well in one direction but showed a significant delay and error in unloading. A similar delay on reloading produces a hysteresis in the plotted output. Care must be taken when attempting to draw conclusions from the output data of the string potentiometers. The visual dial gages used to measure deflections did not seem to experience any similar errors in unloading. However, the limitations of a

visually-read analog dial gage are quite obvious when compared to continuously scanned potentiometers. Future tests will include a more reliable method of continuous displacement measurement.

The data acquisition program proved to be quite useful during testing. Real time monitoring of the loading and the strains in the grillage facilitates the determination of the loading and unloading points during the testing. In addition, the software provides real time graphing function aids which are useful in visually evaluating the relationship between any two data inputs; e.g., load and end shortening.

## Residual Stress Measurements

During the manufacturing of the grillage specimens, residual stress measurements were taken across the span of the center plate. These measurements quantify the effects of welding the stiffeners to the plating on the distribution of stress in the longitudinal direction. Fifteen pairs of points were marked along the plate side and eleven pairs were marked on the stiffener side (the missing points on the stiffener side corresponded to the locations of the stiffeners). The longitudinal distance (nominally 10 inches) between pairs of points were measured once when the plate was weld free, after the stiffeners were tack-welded to the plate, and again after the stiffener welds were completed. Changes in the distance between pairs of points were measured with a Whitmore Gage which is a high precision device for measuring small changes in length over a large gage length. Strain at a given location was calculated by dividing the change in length by the nominal gage length. During each set of readings, a separate plate was measured

to account for any thermal effects. Residual stress was then calculated by simply multiplying the residual strain by an elastic modulus of 30,000,000 psi.

Using pairs of points on each side of the plate, the average axial stress and the average bending stress in the plate were determined for each condition. Figure 7 shows the average axial residual stress across the midspan for all six grillages. Figure 8 shows the average bending residual stress across the midspan of the center bay for the six grillages. The figures show the residual stresses which were induced into the center plate between the time the plate was initially weld-free and when it was fully welded (completely fabricated). In general, the magnitudes of the axial stresses were larger than those of the bending stresses. Also, the magnitude of the stresses were in the range that is considered typical for welded steel structures.[1] That range is generally between 5% and 20% of the material yield stress. Near the edges of the plate the measured residual stresses are very large. This is most likely due to the manner in which the plates were held during the welding process.

## Test Procedure

Efforts were made to place the grillage into the fixture as level as possible. This precaution reduces any effects of load eccentricities or induced bending. All four corners were surveyed and the vertical position of each corner was controlled by adjusting the length of the reaction link turnbuckles. The end plates of the grillage were then drilled to match the holes in the reaction and loading heads, and bolts were installed.

The vertical position of the grillage specimen in the test fixture was set so that the center

of the hydraulic cylinder was aligned at a position ¼-inch above the top surface of the plating (stiffener side). This position was chosen in an attempt to account for the shift in the neutral axis caused by the progressive yielding of the stiffener-plate combination. It is approximately halfway between the locations of the elastic neutral axis and the plastic neutral axis. Figure 9 provides details of the stiffener-plate geometry. The sensitivity of the ultimate strength of the grillage to the initial vertical position of the grillage is thought to be very small. This is due to the very large mass and stiffness of the loading head, the presence of the spherical bearing between the hydraulic cylinder and the loading head, and the fact that the end plates of the grillage were bolted to the loading and reaction heads.

Extensive measurements of initial deformations were made once the grillage was properly leveled and attached to the testing rig. The survey was carried out using a surveyor's transit and a calibrated measuring stick with a bubble gage attached to insure the stick was held in a vertical plane. Twenty-four longitudinal points were measured along each of the stiffeners. Three columns of 24 points per column were measured longitudinally along each of the three bays in the plate. Additionally, a row of 24 points were taken at the outermost edge of the plates (outboard of the stiffener). Table 3 details the maximum deflections measured in each of the grillages. Figure 10 is an example of a contour plot of the initial deflections for one of the grillage specimens.

Table 3 - Non-dimensionalized Initial Deformations

| Grillage # | Stiffener[a] | Plating[b] |
|---|---|---|
| 0494 | -423.5 | -94.7 |
| 0894 | 327.3 | 85.7 |
| 1094 | 720.0 | -150.0 |
| 0595 | 720.0 | -200.0 |
| 0695 | 360.0 | 90.0 |
| 0995 | 327.3 | 75.0 |

[a]Stiffener deformations are non-dimensionalized by dividing into frame spacing - $a/\delta_s$
[b]Plating deformations are non-dimensionalized by dividing into plate width - $b/\delta_p$

The normal procedure for testing called for an initial compressive axial load of approximately 1000 pounds to be applied. This would get most of the play out of the axial components. The bolts connecting the grillage end plates to the loading and reaction heads would then be tightened. A lateral pressure of about 10 psi would then be applied while the strain gages were monitored to insure all strains remained small. This would remove any vertical play and would allow for the calibration of the lateral pressure. The pressure would then be removed and all the recording instruments would be re-zeroed. All of the axial loading during the testing was done using displacement control. By applying a specified amount of axial displacement and monitoring the load as measured by the load cell, fine control could be maintained over the entire range of the tests. Displacement control is also safer than trying to control use load control. The

hydraulic cylinder used to apply the loads has a maximum stroke length of 8 inches, but the grillage fixture has only 4 inches of clearance between the loading head and the lateral pressure bed. Because of the very fast response time of the load control system it would be difficult to keep the loading head from ramming the pressure bed when the grillage collapsed.

All of the grillages were tested to collapse and well into the post-buckling range. As shown in the time history plot of the loading sequence for grillage 1094 (Figure 11), several loading and unloadings were performed. It is apparent from the time history that the grillage was continuing to carry a significant portion of the ultimate load (on the order of 60%) even after it had surpassed its ultimate load capacity.

Figure 12 is the Load-End Shortening plot for grillage 1094 and shows the typical pattern associated with these grillage panels. The plot also shows the difficulties resulting from using string potentiometers to measure the shortening of the grillage. The hysteresis seen in each unloading sequence is a result of the string potentiometer's delay in responding to reversal of the direction of the change in length.

The Load-End Shortening plot shows the number of loading and unloadings conducted during the test. By periodically unloading the grillage and reapplying the load, the linearity of the grillage response and the magnitude of permanent deformations can be determined. After the first loading, all subsequent unloadings show an offset loading line with nominally the same slope. This is very difficult to determine from Figure 12 because of the hysteresis problem.

## Test Results

The buckling of longitudinally-stiffened panels is a complex process involving an interaction between the effects of the geometry of the stiffener and plate, the material properties of each, and the effect of each on the compressive strength of the other. With two sources of possible loading, axial compression and lateral pressure, the types of panel failure can be grouped into one of three possible modes.[2] A Mode I type of failure is the result of compressive failure of the stiffener flange. In general this is characterized by a deflection of the stiffener in the direction of the plating (negative bending) and a definite "S" pattern of a local plastic buckling mechanism in the stiffener flange. Lateral torsional buckling, also known as *tripping*, is another possible failure mechanism which can be classified as a Mode I failure. Tripping is characterized by a distinct rotation of the stiffener about the line connecting the stiffener to the plate. Depending on the thickness of the stiffener web and the flexural rigidity of the plating, there may be some deformation of both the stiffener web and the surrounding plating as the stiffener rolls over.

Bending which causes the stiffener to deflect in the direction of the stiffener flange and deformations in the direction of the stiffener flange are identified as positive. Positive bending or deflections of the stiffener tend to initiate a Mode II type of failure. Mode II failure is distinguished by compressive failure of the plate and a progressive failure of the stiffeners as the plate flange becomes less and less effective. The physical characteristics of a Mode II failure are a positive deflection of the stiffener in a single half-wave and a characteristic pattern of large deflections in the plating in a number of half-waves approximately equal to the plate aspect ratio.

The plate deflection in one bay between stiffeners induces an alternating pattern of deflections in the adjacent bays.

A Mode III type of failure is not typically found in ship structures near amidships, but is the result of simultaneous failure of the stiffener flange in tension and the plating in compression. This mode is normally driven by a large magnitude lateral load on the structure which induces large positive bending. At low levels of in-plane compression it is possible to have tension in the stiffener flange and compression in the plating.

In the laboratory, the distinction between Mode I and Mode II failure is not readily apparent at the time of the ultimate load. This is because the magnitude of the deflections and the amount of rotation or bending is relatively small and not clearly evident. In all the tests conducted in this series, the panels were loaded well beyond the ultimate load so that large deformations and clear patterns of failure could be observed. However, to be sure of the condition at the time of the ultimate load, a careful check of the strain gage data was performed. The data analysis to determine the mode of panel failure was accomplished by looking at a series of strain gages at set loading or time intervals. Whichever gage shows equivalent stresses that exceed the yield stress of the element first will determine the type of failure mode. Mode I failure shows the stiffener flange at yield first and Mode II shows the compressive yield of the plating first.

Table 4 provides a summary of grillage collapse loads, stresses, and failure modes. A short summary of each grillage test is given below, more detailed data on each test is available in the test data book[3] which contains strain gage plots, deflection measurements, dial gage readings, photographs, and computer files of the collected data.

Table 4 - Summary of Collapse Parameters

| Grillage # | Ultimate Compressive Load (lbs) | Ultimate Stress $\sigma_{ult}$ (psi) | Lateral Pressure (psi) | $\phi_{exp}$ [a] | Failure Mode |
|---|---|---|---|---|---|
| 0494 | 325,857 | 37,225 | 0 | 0.764 | Mode II |
| 0894 | 300,812 | 34,481 | 0 | 0.708 | Mode II |
| 1094 | 312,414 | 35,772 | 0 | 0.735 | Mode II |
| 0595 | 315,663 | 36,104 | 5 | 0.662 | Mode II |
| 0695 | 305,994 | 38,835 | 10 | 0.638 | Mode II |
| 0995 | 296,356 | 34,020 | 20 | 0.624 | Mode II |

[a] The ratio of the ultimate stress to the weighted mean compressive yield stress of the plate and stiffener combination

## In-plane Load Only Tests

### Grillage 0494

Grillage 0494 collapsed by Mode II failure, a compression failure of the plating. This determination was made by an evaluation of the stress/strain relationships in the center bay. At common loading increments, the plating was the first element to reach the yield stress of the material. The experimental ultimate collapse stress was 37,225 psi with no applied lateral pressure. The collapse occurred between the transverse frames in the center bay. A characteristic

positive bending of the grillage towards the stiffeners was observed. Photographs of the fully developed collapse from the above, below, and the side of the grillage are shown in Figures 13a, 13b, and 13c. Figure 13d shows a detail of the longitudinal stiffeners in the center bay. Note the rotation of the two stiffeners to the left (the center two stiffeners) and the pronounced "S" shape of all three stiffeners. This is an indication of stiffener buckling which was ultimately the cause of the panel collapse. However, the large deflections in the plating indicate that plate buckling likely preceded and caused the collapse of the stiffeners. Figure 14a shows the load history for the test of grillage 0494. Figure 14b shows the plot of load versus end shortening of the grillage. For this test the only means available for measuring the end shortening was the position of the loading head as read directly from the load control system. After this test we recognized the need for a continuous readout of the end shortening fed directly into the data acquisition system. All of the remaining tests used one or more means of directly measuring the end shortening.

Figure 15 shows the strain versus applied load for the strain gages in the center bay at midspan. Figure 15a shows the gages on the stiffener side and Figure 15b, the gages on the plate side. Note that there is a significant amount of permanent deformation well before the ultimate load is achieved and that the stiffener side is experiencing much higher levels of compression. This indicates that the plate was deflecting towards the plate side (negative deflection). Also note that the level of strain is significantly larger in the center strain gage than in the two outer gages. The plate had reached the approximate yield strain (1800 μ-in/in) at a load of slightly less than 300,000 lbs. Figure 16 shows the strain gages on the two adjacent stiffeners; Figure 16a to the port side and Figure 16b to the starboard side. The level of strain is higher in the gage further

from the center plate on both stiffeners indicating that the stiffener flanges are bowing in towards the center bay. Also note that the level of strain is much lower in the stiffener flanges than in the plating clearly indicating a Mode II failure. Figures 17a and 17b show the contours of measured deflections before and after the testing, respectively.

Grillage 0894

Grillage 0894 collapsed by Mode II failure, a compression failure of the plating. The experimental ultimate collapse stress was 34,481 psi. No lateral pressure was applied. Collapse occurred first in the center bay between the transverse frames. Positive bending towards the stiffeners was observed. Figures 18a, 18b, and 18c show the grillage specimen after testing. Note the alternating pattern of the plate deflection in adjacent panels of plating between stiffeners. Also of note is the fact that the maximum deflection of the stiffeners and plating does not occur at the midspan of the center bay, but rather just forward of midspan (Figure 18b). The center bay failed as a result of the plate buckling and the stiffeners ultimately carrying more of the axial load until they too failed. Because of the fixed end boundaries at each end of the panel, the deflection of the center bay panel in the direction of the stiffeners caused a negative bending moment in the two end bays. The negative moments induced a failure of the stiffener flanges in compression - a Mode I failure. The characteristic "S" shape local failure mechanism of the stiffener flange can be seen in Figure 18d. This figure shows the stiffeners in the aft bay and the amount of deflection and rotation they experienced.

Figure 19a shows the history of the loading for this test. Again the test specimen was loaded well beyond its ultimate buckling capacity. The plot of load versus end shortening is

shown in Figure 19b. These data were taken using the string potentiometers and show the characteristic hysteresis on load reversals.

Figure 20a is a plot of strain versus load for the strain gages located across the center bay at midspan on the stiffener side. Figure 20b shows the measured strains at the same positions on the plate side. The plate side shows higher levels of compressive strain than the stiffener side at the same loading levels. Once the maximum load is reached, the stiffener side goes into tension and the plate side into compression, indicating a large amount of plate bending in the direction of the stiffener (see Figure 18a). The strains in the stiffeners on either side of the center bay are shown in Figures 21a and 21b. Note that the strains in the plating are considerably higher than the strains in the stiffener flanges at equivalent loading levels. Based on the strains measured in the plating, it is possible to observe that the plating deflected in the direction of the stiffeners and took on a significant level of permanent set prior to the panel reaching its ultimate capacity. Based on the differences in strain across the flanges of the stiffeners, it is possible to conclude that the stiffeners failed after the plate and they adopted a shape which had each stiffener bowing away from the center plate. Figure 22a shows the initial deflections of the panel and Figure 22b shows the final deflections.

Grillage 1094

Grillage 1094 also collapsed by a Mode II failure. The ultimate collapse stress was 35,772 psi. No lateral pressure was applied during this test. Collapse occurred in the center bay between the transverse frames with an alternating pattern of deflections noted in the plating. Figure 23a shows the center bay of the test specimen after testing. Note the pattern of deflections

in the plating and the apparent rotation of the stiffener flanges. Figure 23b shows the same region, but on the plate side of the panel. The amount of deflection of the plating and stiffeners can be seen in Figure 23c. The location of the plate failure is similar to that on Grillage 0494, but the pattern of plate deflection is mirror imaged (on Grillage 0494, the plate deflects down on the edge vice up on Grillage 1094). Figure 23d is a detail of the plate deflections at the center bay of Grillage 1094.

During this test we attempted to collect date on the stress field in one of the end bays using photo-elasticity. Figure 24a shows the light source and camera set up during the testing. Figure 24b is a photograph of the photo-elastic sheet which had been bonded to the plating. A pattern of color changes was observed but difficulty with the bonding material limited our ability to interpret the results. As a result of the difficulty with the photo-elastic equipment on this test, we decided to not use it again for the remainder of the tests.

Figure 25a shows a plot of the measured strains on the stiffener side of the center panel at the midspan of the center bay. Notice that the strains become more and more compressive with increased loading until about 280,000 lbs of applied compressive load. At that point, the strains start to go in the tensile direction. This indicates the formation of a large half-wave in the plate in the direction of the stiffeners. Figure 25b shows the strains for the paired gages on the plate side. These gages show a sudden increase in compression at about the same loading point as in Figure 25a.

Figure 26a and 26b show the strains across the two stiffeners adjacent to the center panel. The edge of the flange closest to the center panel on both stiffeners is experiencing the most compression indicating that both stiffeners are deflecting away from the center panel. Also note

that just prior to collapse (around 290,000 lbs of applied load) the strains in the stiffener flange are much smaller than those in the plating. This confirms the Mode II collapse mechanism observed during the testing. Figures 27a and 27b provide the contour plots of initial and final deflections, respectively, for this grillage. The very large upward deflection at the midspan of the center panel in Figure 27b correlates with the strain gage readings taken at the same location.

## Combined Loads

Three tests were conducted in order to evaluate the effect of lateral pressure on the ultimate strength of the grillages. In all cases the lateral pressure was applied first while the ends of the grillage were held in a constant position. As the in-plane load was applied, the lateral pressure was monitored and manually adjusted to try and maintain a constant pressure on the test specimen. The lateral pressure was applied to the plate side of the grillage thus forcing a "positive" bending and an upward (positive) deflection of the plate and stiffeners.

### Grillage 0595

Grillage 0595 was loaded with a constant 5 psi of uniform lateral pressure. The ultimate collapse stress was 36,104 psi and the failure was, as expected, a Mode II mechanism. The uniform lateral pressure caused an initial deflection at the midspan of the stiffeners of 0.011-inches and an initial deflection of the midspan of the center plate of 0.015-inches. The collapse started in the center panel of the center bay and proceeded outward to the stiffeners. Figure 28a shows the port side of Grillage 0595 in the Test Fixture after collapse. Figure 28b shows the

pattern of deformation experienced by the stiffeners and the plating. Figure 28c is a detail of the deflection pattern. Note how the pattern alternates across the grillage and how the web of the stiffeners are affected by the plate deformation. The failure of the stiffener flanges in the forward bay can be seen in Figure 28d. The combination of the fixed end boundary conditions at the grillage ends and the upward deflection of the stiffeners in the center bay put the stiffener flanges in the end bays in compression and cause a local buckling mechanism.

Figure 29a provides the load history for the test and Figure 29b is the Load versus End Shortening plot for the grillage. This plot was developed from manually-read digital dial gages attached to the pressure bed which measured the loading head movement. It was not clear from the data on end shortening if this manner of collecting data appropriately accounted for stretching of the tension beams of the test fixture under loading. As a result, the next two tests used a combination of means for evaluating the end shortening.

Figures 30a and 30b show the measured strains on the stiffener side and plate side, respectively, of the center panel at midspan. Note that the levels of strain across the plate are nearly the same and only after the ultimate load is reached is there an obvious difference between the strains in the center and those on each side. Figure 30b shows that, at about 300,000 lbs of applied compressive load, the maximum strains were slightly less than -2000 μ-in/in. The stiffener side of the plating was experiencing similar strains. However, Figures 31a and 31b indicate that, at the same loading point, the strains experienced in the stiffeners were on the order of -1200 μ-in/in. This pattern is similar to that seen in the tests where no lateral pressure was applied and is an indication of a Mode II failure. The main difference with the earlier tests is that the stiffeners started with a small amount of tension in the flanges as a result of the lateral

pressure. The top and bottom surfaces of the plating did not show the same kind of characteristic. This is likely due to the relatively large distance from the elastic neutral axis to the top surface of the stiffener flange. Figures 32a and 32b are the deflection contours for the initial and final measurements, respectively. The pattern shown in Figure 32b is very similar to that seen in earlier tests (see Figure 27b).

Grillage 0695

Grillage 0695 was loaded with a constant 10 psi of uniform lateral pressure. The ultimate collapse stress was 34,835 psi and the failure was, again, a Mode II mechanism. The uniform lateral pressure caused an initial deflection at the midspan of the inboard port stiffener of 0.009 inches and the inboard starboard stiffener of 0.015 inches. The initial deflection of the midspan of the center plate was 0.019 inches. The collapse started in the center panel of the center bay and proceeded outward to the stiffeners. Figure 33a shows the stiffener side of the center bay of Grillage 0695 in the Test Fixture after collapse. Note that the strain gages in the center panel are right at the peak of the downward deflection. Figure 33b shows the starboard side of the grillage and clearly shows the rotation of the transverse frame and the peal deflection of the stiffeners. Figure 33c is a detail of the deflection pattern on the plate side of the grillage. Strain gages 35, 37, and 39 are not at the deepest point of the deflection. The rotation of the stiffener flanges in the center bay can be seen in Figure 33d. The local buckling of the plate between the stiffeners affects the stiffener web - causing it to bulge away from the upward deflection of the plate. This in turn causes the stiffener flange to rotate towards the center of the panel.

Figure 34a provides the load history for the test and Figure 34b is the Load versus End

Shortening plot for the grillage. Three different means of measuring the end shortening were used. First was the head position as measured by an LVDT in the hydraulic cylinder. This measurement is used to control the position of the loading head and thus the applied force. It does not reflect the stretching that the main tension beams of the test fixture undergo as the load is increased. The data identified as "String Pots" is the average of two string potentiometers, one on each side of the grillage specimen. The string pots measure the relative positions of the loading head to the reaction head. This should give an accurate measure of the change in length of the grillage specimen. The difficulty is that the string pots lose an undetermined level of accuracy each time they are loaded and unloaded. As in earlier tests, two digital dial gages were mounted on the pressure bed (fixed to the lab floor) and measured the movement of the loading head. The data points labeled "Dial Gage Readings" represent the average values for the two gages. The String Potentiometers could arguable be considered the most accurate as they are directly measuring the quantity of interest. The dial gages are fixed to the pressure bed which is in turn fixed to the floor. The reaction head is also fixed to the pressure bed, but there may be some movement or slipping in those connections. The overall difference between the three methods is on the order of 100 mils. The change in length of the tension beams under the maximum load is estimated to be about 60 mils.

Figure 35a shows the measured strains on the stiffener side of the plate in the center panel of the middle section at the mid-span length. The strain remain linear in the plating almost up to the peak load (305,994 lbs). There is little difference in the strains across the plate up to almost 300,000 lbs of load. Figure 35b shows the strains at the corresponding positions on the plating side. The point of departure from linearity is nearly the same as in Figure 35a, but the

plate side goes into tension while the stiffener side goes to compression. This indicates a downward deflection of the plating at this point. The strains in the adjacent stiffeners are shown in Figures 36a and 36b. The port stiffener shown in Figure 36a experiences transverse bending towards the center panel at relatively low loads. The maximum strain seen in the stiffener flange is relatively small, indicating a Mode II type of failure. The starboard stiffener in Figure 36b shows similar characteristics, but experiences a decrease in the compressive strains after the ultimate load has been reached. Figures 37a and 37b show the plots of the deflection contours for the initial and final measurements, respectively. The pattern shown in Figure 37b is very similar to that seen in earlier tests (see Figure 32b and 27b).

Grillage 0995

Grillage 0995 was loaded with a constant 20 psi of uniform lateral pressure. The ultimate collapse stress was 34,020 psi and the failure was by a Mode II mechanism. The uniform lateral pressure caused an initial deflection at the midspan of the inboard port stiffener of 0.014-inches and the inboard starboard stiffener of 0.028-inches. The initial deflection of the midspan of the center plate of 0.038-inches. The collapse started in the center panel of the center bay and proceeded outward to the stiffeners. Figure 38a shows the center bay of Grillage 0995 in the Test Fixture after collapse. Figure 38b shows the deformation experienced by the stiffeners and the plating. Figure 38c is a view of the deflection pattern on the plating side of Grillage 0995. Note how the pattern is the mirror image of that seen on Grillage 0695 (Figure 33c). The closeup view of the starboard stiffener in Figure 38d shows the amount of deflection experienced by the stiffener compared to that seen in the plate.

Figure 39a provides the load history for the test and Figure 39b is the Load versus End Shortening plot for the grillage. The maximum load in this case did not reach 300,000 lbs, though the amount of post-buckling strength appears to be the same as in earlier tests. The end shortening in Figure 39b was measured using the string potentiometers and the loading head LVDT. At the peak load there is a difference of almost 190 mils. As in the earlier cases, about 60 to 80 mils can be attributed to the stretching of the tension beams under the loading. Some loss in accuracy happens to the string pots on successive loading and unloadings. This is seen in the plot of the string pot data where the curve greatly flattens out. It is safe to say though, that the amount of end shortening at failure is less than that experience by earlier tests.

The measured strains in the plating of the center panel at midspan are shown in Figure 40. The strains on the stiffener side appear in Figure 40a where it can be seen that the linearity is lost at a load of about 150,000 lbs. By the second unloading (about 250,000 lbs), there is a significant amount of plastic deformation. There is a change in the strain pattern on the stiffener side of the plate prior to reaching the ultimate load. The two outside gages initially start to become more tensile, then suddenly turn more compressive while the center gage continues to become more tensile. The gages in Figure 40b show more and more compressive strain as the load is increased. Again, there is some permanent set at the time of the second unloading. However, at about the same point that there was a significant change in the corresponding gages on the other side of the plate, the plating side simply became more compressive. Ultimately the amount of compression on the plate surface indicates some amount of bending.

The measured strains in the stiffeners are shown in Figure 41. The port stiffener in Figure 41a shows a lower level of strain than observed in the plating. Also, the stiffener flange

remained elastic and did not adopt any lateral deflection until the ultimate load was nearly reached. This is due, in part, to the tensile strain originally induced in the stiffener flanges by the lateral pressure. The pattern is similar in the starboard stiffener shown in Figure 41b. However, there is some plastic deformation prior to the ultimate load and some lateral deflection away from the center panel here. It is interesting to note that after the ultimate load was reached the starboard stiffener adopted a lateral deflection towards the center panel.

Figures 42a and 42b show the plots of the deflection contours for the initial and final measurements, respectively. The pattern shown in Figure 37b is very similar to that seen in earlier tests (see Figure 32b and 27b).

## Discussion of Results

The results of the six tests performed as a part of this study represent a valuable collection of information on the performance of ship-type grillages under combined loads. The authors are very interested in how well the test results compare with available analytical algorithms for predicting panel collapse and how well the data compares to data from similar experiments performed throughout the world. It is also possible to use finite element methods (FEM) to do "numerical" testing of ship grillages.

## Comparison To Theory

A number of theoretical algorithms for determining the ultimate strength of stiffened

panels have been proposed over the years. One of the more recent, and comprehensive, is that developed under the guidance and sponsorship of the Merrison Committee which became the UK LRFD Code for steel box girder bridges, BS5400.[4] A thorough discussion of the algorithm is provided by Hughes in Chapter 14 of his book.[2] The book describes the development of the algorithm based on determining the level of stress in the stiffener flange and the plate between stiffeners under actions of combined loads. In a comparison of several algorithms for stiffened panels, Hughes et al[5], recommended using this British "Standard Algorithm" for ship structures.

The algorithm treats the stiffened panel as a series of beam-columns and evaluates the three possible failure modes discussed earlier in this report. The ultimate stress is determined to be that amount of applied in-plane compressive stress needed to raise the level of stress in the stiffener or plate to a prescribed level. The stress in the plate or stiffener is the result of the combined in-plane loads (axial and transverse) and lateral pressure. The fundamental form of the relationship for the determining the stress for all three failure modes is

Total Stress = Axial Stress + Bending Stress + Stress Due to Deflection Under Lateral Load

The axial stress is due to the in-plane axial load, the bending stress is due to the lateral pressure, and the third term is induced stress as the result of the deflection under the lateral load causing the in-plane load to have an induced eccentricity. This induced stress is the well known "P-$\Delta$" effect. For the case of a Mode II failure, the equation used by the algorithm is

$$\sigma_2 = \sigma_{X,tr} + \frac{M_0}{Z_{p,tr}} + \frac{\sigma_{X,tr} A_{tr} (\delta_0 + \Delta)}{Z_{p,tr}} \phi + \frac{\sigma_{X,tr} A_{tr} \Delta_p}{Z_{p,tr}} \quad (1)$$

The axial stress component $\sigma_{X,tr}$ is the axial load divided by the *transformed* area of the stiffener. The transformed area is a correction which accounts for the real behavior of welded steel plates and is based on the "secant modulus" concept. $A_{tr}$ is the transformed area of the stiffener and plating and $z_{p,tr}$ is the section modulus of the transformed section to the plating. The effect of the lateral pressure is felt through the value of $M_o$, the central bending moment due to the lateral pressure, and $\delta_o$, the central deflection of the beam-column under the lateral load. Any load eccentricity or initial deflection of the stiffener is accounted for by the value of $\Delta$ in the third term. The magnification factor, $\phi$, is intended to account for the increasing induced stress as the axial load approaches the critical buckling load for a column. The last term is another induced stress that results from an eccentricity which develops as the neutral axis of the beam-column moves from its initial location to the final location (full plastic neutral axis).

All six tests were evaluated using a computer program based on the "standard" algorithm. In Table 5, the theoretical ultimate stress (Mode II failure) for the section is provided as is the ratio of the ultimate stress to the weighted mean of the compressive yield stresses, $\phi_{II}$. Figure 43 shows the relationship between the theoretical values for the ultimate stress ratio, $\phi_{II}$, and the experimental values for the ultimate stress ratio, $\phi_{exp}$. Perfect correlation would have the data points all falling on the solid diagonal line. Note that the theoretical values are all less than the experimental values, indicating that the theory is conservative. This is consistent with Hughes et al[5] who found that the "standard" algorithm tended to underestimate the failure stress by about

10% for Mode II. The dashed lines represent roughly a 10% error margin about the perfect correlation line.

Table 5 - Results of Theoretical Algorithm for Mode II

| Test Number | Lateral Pressure (psi) | Theoretical Ultimate Stress (psi) | Ultimate Stress Ratio $\phi_{II}$ |
|---|---|---|---|
| 0494 | 0 | 35,657 | 0.732 |
| 0894 | 0 | 32,002 | 0.657 |
| 1094 | 0 | 33,114 | 0.680 |
| 0595 | 5 | 34,635 | 0.635 |
| 0695 | 10 | 32,248 | 0.591 |
| 0995 | 20 | 28,819 | 0.528 |

There are some differences between the values in Table 5 and those presented by Vroman[6] for the same tests. Vroman originally evaluated the standard algorithm using the "nominal" dimensions of the specimens. Later analysis of the test data also revealed that an incorrect value of plate yield stress and incorrect stiffener initial deformations were also used. As the "standard" algorithm is very sensitive to both of those quantities, there have been some changes in the values in Table 5 and Figure 43.

The three tests conducted with "in-plane loads only" show some scatter which needs to

be explained. Though nominally the same grillage, there were some differences in the "as tested" dimensions and significant differences in the initial deformations of the stiffeners. The data point farthest to the right in Figure 43 represents Grillage 0484. The initial deflections of Grillage 0484 were in the direction which would be considered negative, i.e., towards the plating. This has the effect of making the panel stronger in Mode II. The other two in-plane only tests were about 7.5% low which is consistent with other results.[5] Further analysis of Figure 43 shows that, as expected, there is an apparent decrease in the experimental collapse stress as the lateral pressure is increased. There is also a change in the theoretical stress ratio. It continues to under predict the experimental values but the margin increases with increasing lateral pressure. It appears that the "standard" algorithm is not handling the effect of lateral pressure very well. The effect is small for low pressures but increases with larger pressure.

By looking at the test data for deflections under the lateral loading, it is possible to identify a possible source of the increasing error. The "standard" algorithm assumes that the beam-column has a plate flange that bends under the uniform pressure at the same rate as the rest of the stiffener. Thus, the deflection under uniform lateral pressure ($\delta_o$ in Equation 1) is calculated from simple mechanics as:

$$\delta_0 = \frac{5Pba^4}{384E_sI} \qquad (2)$$

where $P$ is the lateral pressure, $b$ is the plate flange width, $a$ is the panel length, $E_s$ is the elastic modulus of the stiffener, and $I$ is the vertical moment of inertial of the beam-column. While Equation (2) is commonly used and widely accepted, it does not account for the relative

deformation of the plate flange with respect to the stiffener web. Some of the energy from the lateral pressure goes into deforming the plating and is not available to cause deflection of the beam column. Table 6 shows the measured deformations for the central plating and the port-inboard stiffener of Grillage 0995 at 5, 10, and 20 psi of lateral pressure. For comparison the deflection according to Equation (2) is also provided.

Table 6 - Stiffener and Plate Deflections on Grillage 0995

| Lateral Pressure (psi) | As Measured | | Equation (2) (in) |
|---|---|---|---|
| | Stiffener (in) | Plating (in) | |
| 5 | 0.060 | 0.010 | 0.011 |
| 10 | 0.011 | 0.019 | 0.022 |
| 20 | 0.024 | 0.038 | 0.045 |

As seen in Table 6, the actual deflection of the stiffener under the uniform lateral pressure is about one half of that calculated by Equation (2). Because the standard algorithm uses Equation (2) to determine one of the most important values in the "P-D" effect term of Equation (1), the algorithm will find that the beam-column fails at a lower in-plane load than it actually does. We are currently investigating a means to account for this so that the "standard" algorithm will provide better results in cases of large lateral pressures.

## Comparison to Historical Test Results

A database of historical tests on stiffened panels was developed as part of the USNA research effort during the course of the stiffened panel testing. Through an extensive literature search, 101 tests were found which reported enough information to make them useful to the database. These data were from eight separate test series conducted at five different locations over a 30 year period. Faulkner[1], Horne, et al[7,8], Kondo, et al[9], Rampetstreiter, et al[10], Smith[11], and Murray[12] detail the particulars of each test. Fifteen additional experiments discussed by Hughes[2] and completed in Australia in 1977 were not included because we were unable to obtain the original references and Hughes did not provide enough information to include them in the database.

Of the total of 101 tests, 18 conducted by Faulkner and identified as the "Student Series" were subsequently dropped from the database. Faulkner reported that the tests were conducted for demonstration purposes and not for data collection. As a result, he did not have as much confidence in the results as he did with his 28 other tests. Of the remaining 83 tests, only 11 were conducted on tests specimens with more than one bay. Only eight of the 83 tests were conducted with combined in-plane axial force and lateral pressure. Finally, only four of the 83 tests were both multi-bay and combined-load tests. The six tests conducted at USNA make a significant addition to the overall database of information on stiffened panel ultimate strength. Including the USNA tests raises the number of multi-bay tests to 17, the number of combined load tests to 11, and almost doubles the total of multi-bay tests conducted with combined loads.

The theoretical ultimate stress ratio of each grillage was determined using the "standard"

algorithm discussed in the previous section. Figure 44 compares the theoretical stress ratio to the experimental results. As in Figure 43, the solid line represents a perfect correlation between theory and experiment. Any data points falling below the solid line indicate a conservative theoretical estimate or a safe prediction.

Several important inferences can be made from Figure 44 regarding stiffened panel testing, the theoretical algorithm, and the effects of geometry on panel strength. Each test series points to one or more important issues about stiffened panel design and strength. The following discussion considers the relationships of boundary end conditions, combined axial and lateral loading, the theoretical algorithm, and panel geometry to Figure 44.

Horne[7,8] conducted his series of tests using two approaches to boundary end conditions: one-half of his tests were fixed-end and the other half were pinned-end. The resulting relationships between these two procedures show that a pinned-end model is under conservative whereas a fixed-end model is over conservative. This conclusion agrees with reality, as the end boundary conditions of a panel in a ship's structure are neither entirely fixed nor pinned. Rather, an actual panel is somewhere between these two extremes; although it is not ideal either, a simply-supported end condition is used in the theoretical model for this very reason. Similarly, two series of tests were conducted at Lehigh University's Fritz Engineering Laboratory (Rampetstreiter et al[10], Kondo and Ostapenko[9]), one fixed-end and one pinned-end. The delineation between these boundary conditions in Figure 44 is not distinct. However, this discrepancy should not discount Horne's results. Many of the Lehigh tests were subjected to combined lateral and axial loading. As discussed later in greater detail, the effect of lateral pressure on a stiffened plate tends to change the strength characteristics of a grillage.

The net result of the boundary condition data shows the necessity for multi-bay testing. In single-bay testing such as Horne's, the effects of the end restraints are extremely influential on the strength of the panel. However, a three-, four-, or five-bay grillage allows the experimenter to discount the end bays and concentrate the analysis on the inner bays where the boundary conditions of the panel more closely resemble the actual end conditions in a ship's structure. The USNA tests discussed in this report are examples of a multi-bay test. The data show that the USNA tests yielded reasonable results with good correlation between experiment and theory.

The effect of lateral pressure on the strength of a stiffened panel is not well understood. Intuitively, one would think that lateral pressure on a panel combined with axial loading would tend to decrease the overall strength of the panel. The plate bending caused by the lateral load usually induces a simple half-wave pattern as one would expect. Depending on the aspect ratio of the plate, this pattern will not likely match the critical buckling mode shape for the plate and therefore may actually increase the plate critical buckling stress. The lateral pressure does cause the stiffeners to deflect in a sinusoidal half wave, inducing another component of stress in the panel (the P-$\Delta$ term in Equation (1)). However, if the failure mode for the panel is the plate-induced Mode II failure, moderate levels of lateral pressure may have almost no overall effect on strength. This is due to the possibility that the increase in the plate critical buckling stress may more than offset the increased stress from the P-$\Delta$ effect.

Figure 45 provides some insight into this situation. As stated earlier, there are only eleven tests in the database which include lateral pressure with in-plane compression. The two data points from the Lehigh test series near the bottom of the chart (identified as *T14* and *T15*) were

conducted on single-bay panels with fixed-end boundary conditions. Both tests had nominally identical geometry and both were loaded with 13 psi of uniform lateral pressure. The difference in experimental results is a result of some quantity which was not reported and we believe test *T15* was an anomaly. The other Lehigh test near the bottom, *T13*, was another nearly identical panel, with the same boundary conditions, but loaded with 6.5 psi of lateral pressure. This test has a considerably higher experimental strength than that noted for test *T14*. Another Lehigh test, *T6*, was also loaded at 6.5 psi, but used pinned-end boundary conditions. Lateral pressure would induce more deflection in a pinned-end beam-column and would thus reduce the ultimate stress ratio.

Conclusions are hard to draw from Smith's tests. All of his tests were very large scale grillages with 5 bays longitudinally and 11 stiffeners across the width. Test *1b* had a plate aspect ratio of 2, relatively thick plating, and a larger stiffener than the rest of the tests. Test *1b* was loaded with 15 psi of lateral pressure. Test *3a* had a lower experimental stress ratio than test *1b* but was only loaded with 3 psi of lateral pressure. However, test *3a* had an aspect ratio of 5, the thinnest plating in the test series, and a smaller stiffener. The ratio of the stiffener to plate area was the lowest in the series, 0.265. Tests *2a* and *4b* were subjected to lateral pressures of 7 psi and 8 psi, respectively. Both grillages had high aspect ratios (5 and 4, respectively), but 2a had thicker plating and larger stiffeners. The stiffener area to plate area ratio was larger for 2a (0.453 to 0.317) which tends to give more strength in a Mode II failure mechanism.

Vroman[6] looked at a variety of dimensional and non-dimensional parameters associated with these tests in an attempt to establish some meaningful relationships for evaluating stiffened panel strength. The difficulty is that some important data are often not reported. Stiffened panel

strength is very sensitive to initial stiffener deflection, yet Horne et al[7,8] reported no initial deflections. Table 7 gives the reader an idea of the range the test parameters covered. For the purpose of clarifying Table 7, the following definitions are provided.

$$StiffenerAreaRatio\ \gamma = \frac{A_{stiffener}}{bt}$$

$$PlateSlenderness\ \beta = \frac{b}{t}\sqrt{\frac{\sigma_{yield\text{-}plate}}{E}}$$

$$ColumnSlenderness\ \lambda = \frac{a}{\pi}\sqrt{\frac{A\sigma_{yield\text{-}stiffener}}{EI}}$$

$$PlateAspectRatio\ \alpha = \frac{a}{b}$$

The range of values seen in Table 7 make the kind of macroscopic comparisons Vroman[6] tried, very difficult. It quickly becomes obvious that even the kind of global look attempted in Figures 43 to 45 is going to miss things. The advantage of the way in which those figures are generated is that the theoretical "standard" algorithm takes into account all of the important variables and allows us to see the effect of each on the ultimate strength.

Hughes et al[5] found that the ultimate strength of longitudinally stiffened panels was most affected by the yield strength of the plating, the plating thickness, and the initial deflection of the plating. We concur with this finding but also feel that the ratio of the stiffener area to the plate area is an important parameter. If the plating is thick and the stiffener is small, the panel will fail near the yield strength of the plating. If the plating is thin and the stiffener is sturdy, the panel fails near the yield strength of the stiffener. Figure 46 attempts to show this effect. The lines drawn in Figure 46 are intended to show the general trend of the data for different groups. Because so many other parameters have an effect on the ultimate strength, there is a lot of scatter. However, we believe that the trend is exhibited in the figure.

Table 7 - Dimensionless Parameters for Historical Test Database

| Test Series | Plate Slenderness $\beta$ | Column Slenderness $\lambda$ | Stiffener Area Ratio $\gamma$ | Aspect Ratio $\alpha$ |
|---|---|---|---|---|
| Faulkner-Parametric Series | 0.99-4.25 | 0.267-1.281 | 0.300-0.715 | 1.50-8.80 |
| Faulkner-Weld Series | 2.00-2.15 | 0.601-0.656 | 0.562 | 4.32 |
| Horne-Fixed End | 0.88-2.25 | 0.238-0.383 | 0.333-1.168 | 2.00-6.00 |
| Horne-Pinned End | 0.82-2.32 | 0.534-0.925 | 0.333-1.168 | 4.00-13.50 |
| Lehigh-Fixed End | 2.17 | 0.640 | 0.187-0.281 | 3.80 |
| Lehigh- Pinned End | 1.45-2.17 | 0.543-0.574 | 0.187 | 1.30-5.85 |
| Murray | 2.05-2.56 | 0.457-1.093 | 0.150-0.500 | 2.79-7.44 |
| Smith | 1.41-3.65 | 0.203-0.665 | 0.135-0.458 | 2.00-5.00 |
| USNA | 1.89-2.02 | 0.435-0.448 | 0.384 | 4.00 |

## Comparison to Finite Element Analysis

The objective of this part of the project was to see if a numerical modeling technique could be used to accurately predict the structural stability of a tee-stiffened panel subjected to in-plane loading. Test results of the stiffened panels (with in-plane loads only) were compared to

results from this numerical model.

The finite element analysis (FEA) software, ABAQUS, was used to perform a non-linear analysis of the stiffened panels subjected to in-plane compressive loading. The plate was modeled with 4-node, doubly curved shell (SR5) elements which allow for reduced integration and hourglass control (see Figure 47). The majority of the plate elements are 3 inches x 6 inches in dimension with thicknesses of 1/4 inch (outer plates) and 3/16 inch (center plate). The stiffeners and frames were modeled with two-node, linear beam (B31) elements which allow for bending, stretching, and torsion. The beam elements for frames and stiffeners were 6 inches and 3 inches in length, respectively. The elements are connected by multi-point constraints (MPCs). Mainly, link constraints were used to connect the stiffener nodes to the plate nodes and frame nodes to the plate nodes. A link constraint provides a pinned-rigid link between two nodes.

The boundary conditions for the loaded edge of the model were imposed by constraining all degrees of freedom except in the $u_y$ (longitudinal) direction. At the opposite end of the grillage, fixed-end constraints were imposed, constraining all six degrees of freedom. The connections between transverse frame ends and the reaction links were modeled by constraining the edge of the plate only in the $u_z$ (out-of-plane) direction.

Elastic material properties were defined to be equal to the nominal values for mild steel: Young's modulus, $E = 30{,}000{,}000$ psi and Poisson's ratio, $\nu = 0.3$. Material properties in the plastic region were determined from compression coupon tests performed at NSWC. These tests showed that mild steel displays an almost perfectly elastic-plastic behavior under compression. Figure 48 shows a plot of the results for the coupon test of the plating used in the center bay of the grillage.

The non-linear FEA was performed using two different methods. These methods were

an attempt to capture the post-buckling behavior. Post-buckling occurred after the plate yielded and began to lose strength; the FEA became very complicated at this point. The first method was the boundary-displacement method which displaced the loaded edge a given amount. The maximum end-displacement was determined to be approximately 0.144 inches and represents the end-displacement at the point of buckling. The second method was the "RIKS" method which solves simultaneously for load and displacement. This solution technique is very sensitive to mesh imperfections. Several different approaches were developed to perturb the mesh. One approach involved writing a FORTRAN code to perturb the mesh into a single half-wave in the longitudinal and transverse directions with the ratio of the panel length to the maximum deflection equal to 750. In a second approach, the mesh was preloaded in a separate step which created a perturbed mesh.

The post-buckling behavior was not modeled very well by either of the two approaches. Due to the high sensitivity to the mesh imperfections, the best results from RIKS were not as good as the results from the boundary-displacement method. The RIKS method may have been more successful with more time to determine the appropriate mesh imperfections. The boundary-displacement method can determine the peak load (ultimate strength) but cannot progress pass this point where the load reduces while the end-shortening increases. The halt in the analysis at the ultimate strength suggests that the model is exhibiting the expected behavior of the grillage. Since the grillage ultimate strength is of most concern to the structural designer, the lack of post-buckling behavior is not detrimental to this analytical method.

The results from the FEA compared reasonably well to the experimental tests of the grillages. Patterns of displacements, similar to those observed in the experiments, were found by the FEA, as shown in Figure 49. Figure 50 is a contour plot of the vertical displacements in

the center plate. Maximum deflections were found in the longitudinal center of the plate. There were three positive peak values found: 0.016 inches on the two edges and 0.0142 inches at the center. The model exhibited a half-wave pattern between these maximum values across the width. These multiple half-wave patterns were seen during the testing of the grillages. We do not have good data to compare these results to because of the difficulty we had in getting good values from the dial gages used in the first three tests. However, the typical levels of vertical displacement observed during the testing were significantly larger than the values found from the FEA results.

In general, the FEA analysis tended to give displacements which were smaller than those observed during the testing. A comparison of the load versus end-shortening results for the FEA run and Grillage 1094 is shown in Figure 51. The FEA load versus end-shortening plot is based on longitudinal displacements between nodes 18 and 294. The total load from the FEA is found to be 329,354 lbs when the solution fails at an end-shortening of 0.144 inches. The data for Grillage 1094 were developed from the string potentiometers used to measure end-shortening. Later experience with the string potentiometers and other measuring devices has caused us to discontinue using the string potentiometers in this application. The level of non-linearity in the string potentiometers is unacceptable and accounts for some of the difference in slope between the FEA and Grillage 1094 seen in Figure 51. It should be noted that the average ultimate load of the three in-plane load only grillage tests (0494, 0894, & 1094) was 313,027 lbs. This represents a difference of about 5.2% from the FEA results, well within acceptable tolerances for FEA.

Figure 52 is a contour plot of the FEA-based stresses in the center plate under peak loads. The maximum stresses in the center plate are about 47,000 psi and are located at the connections

between the frame and the plate in the bays between the stiffeners. The stress in the center of the plate is 44,200 psi. The average mid-thickness experimental stresses in the center of the plate for the first three grillages (0494, 0894, & 1094) is about 47,700 psi. This value was taken from the strain gage plots as the point at which the strain started to go highly non-linear.

Comparisons between the FEA and experimental test results show that non-linear FEA is a viable method to predict the ultimate strength of a stiffened panel. Post-buckling behavior is much harder to predict due to the solution's high sensitivity to the initial imperfections. However, the post-buckling behavior is not as critical to the designer as the determination of the ultimate strength. Further experimental tests are needed to validate the vertical displacements predicted by ABAQUS. One such method would be to replace the manually read dial gages with digital dial gages. At the exact point of ultimate load, the experimental displacement values would then be available for comparison to the analytical values.

One area of suggested future research is the use of FEA to increase the stiffened panel test database. Currently, there is only a very limited database available for the development of a reliability-based design of stiffened panels. The database could be increased with new experiments and testing; however, these would be very costly and time-consuming. An alternative to testing would be the development of an analytical tool. If Finite Element models can be validated, FEA would be an inexpensive alternative for building a larger database. Validation would be performed by comparing experimental results to FEA results of other panel tests currently available in literature.

# Conclusions and Recommendations

One of the purposes of the test program on stiffened panels conducted at USNA was to develop sufficient information so that a measure of the modeling error in stiffened panel design equations could be developed. In reliability-based design, a *statistical* measure of this error is needed in order to effectively develop the required partial safety factors for the design equation. The partial safety factors are statistically-based values which direct the design equation into producing a design with the desired level of safety or reliability. Physical testing is the primary source of the type of information needed for determining the modeling error. Vroman[6] used the results from the first three USNA tests and the database of historical tests to conduct a statistical investigation of the error associated with using the beam-column analytical model for stiffened plates. Though he was able to use some, it is evident that there is not nearly enough of the multi-bay tests under combined loads for a really solid statistical analysis.

Some conclusions about the behavior of stiffened panels under various load and boundary conditions can be drawn from the database of information. The first is that the results of testing single bay panels are highly dependent on the boundary conditions applied at the loaded edge. When fixed-end conditions are applied, the results of the testing tend to give a higher ultimate strength than when pinned-end conditions are applied. This is likely the result of the effective length of the beam-columns with the different boundary conditions. In general, the multi-bay tests tend to fall somewhere between the two extremes of pin and fixed-ended as expected. The real-world ship structure is not truly modeled by either of the extreme boundary conditions. The conclusion drawn here is that all future testing of stiffened panels modeling ship structures should be done with multi-bay test specimens.

The effect of the lateral pressure on the ultimate strength of stiffened panels is still not well understood. It is apparent that the presence of moderate amounts of lateral pressure causes a decrease in the ultimate strength. However, if the level of lateral pressure is relatively small, it seems to have no effect on the ultimate strength. This tendency is strongly affected by the yield strength of the plate material, the aspect ratio of the plate between stiffeners, and the relative thickness of the plating. The strength of the panel seems to be driven by the stiffener size and bending stiffness. However, there is not a sufficient number of tests covering a range of stiffener geometries to make a quantitative assessment regarding the role of the relative sizes of stiffener and plating. Further investigation in this area is needed.

Surprisingly, the initial deflection of the plating has little to do with the ultimate strength of the panel due to the fact that the usual form of initial deflection of plating is a single longitudinal and transverse wave. This mode shape is actually much stronger in axial compression than the preferred mode shape. The net result is an increase in axial strength of the plating with initial deflection. This idea ties in with the effect of lateral pressure, which also tends to induce an initial deflection of the plate in a one half-wave pattern. However, initial deflections of the stiffener are important in both determining the failure mode as well as the failure load. Typically, any initial deflection tends to push the stiffener in a direction which corresponds to a primary failure mode shape. The relationship between stiffener geometry and the tolerance allowed on initial deflections is an area which needs further investigation.

Attempts to reproduce the experimental results using a Finite Element Analysis (FEA) program met with some success. While we were not able to model the post-buckling behavior of the grillage, we were able to predict the average ultimate strength reasonably well. The levels of stress and pattern of highly stressed areas of the grillage were modeled very well by the FEA.

However, there was a noticeable difference in the magnitudes of the deflections predicted by the FEA and those observed during the testing. We feel that, with further work in this area, particularly in modeling the stiffener attachments to the plating and including initial geometric imperfections of the grillages, the FEA method will be able to accurately predict the ultimate strength of the panel. Whether or not the cost and effort involved produce results which are significantly better than other less difficult analytical methods (e.g., "standard" algorithm) remains to be seen.

Finally, the total database of available tests on grillage structures is not sufficient to develop the kind of statistical information needed for the development of reliability-based design of ship structures. A series of experiments looking at the effects of stiffener size (and stiffness) with respect to plate thickness and stiffener spacing is needed. This sort of testing may provide the base information needed to truly optimize the design of the stiffened panel - the most common element in a ship's structure.

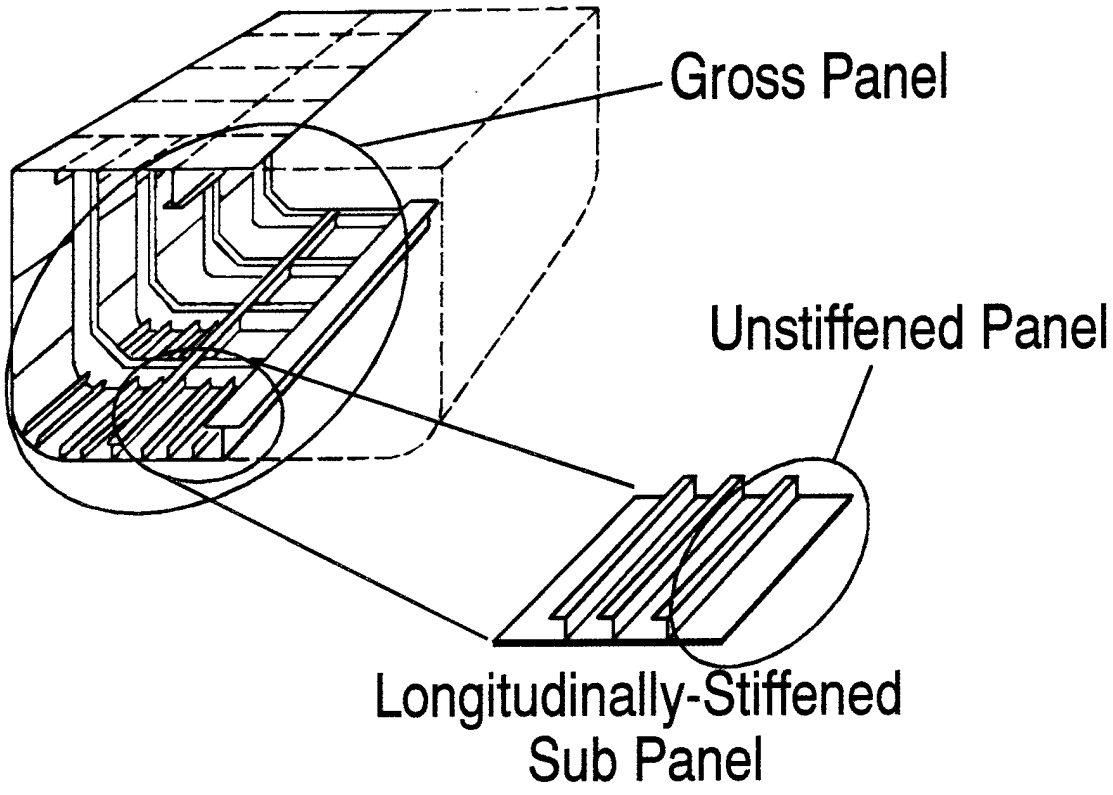


Figure 1 - Definitions for Stiffened Panels (Hughes, 1988)

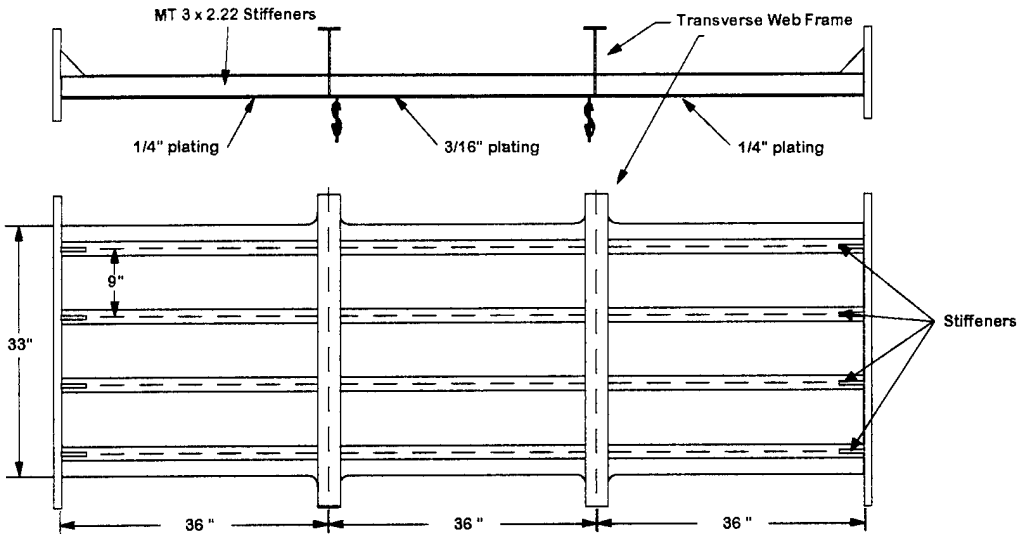


Figure 2a - Dimensions of the Grillage Specimens

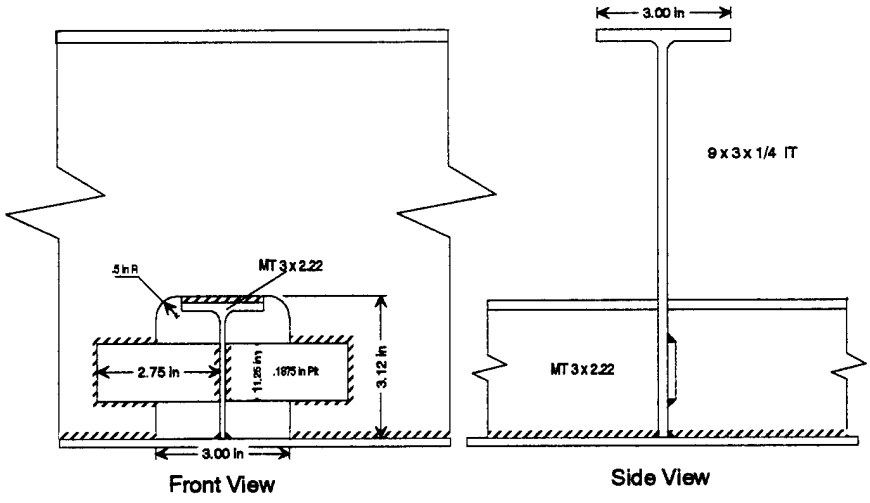


Figure 2b - Web-Stiffener Connection Details

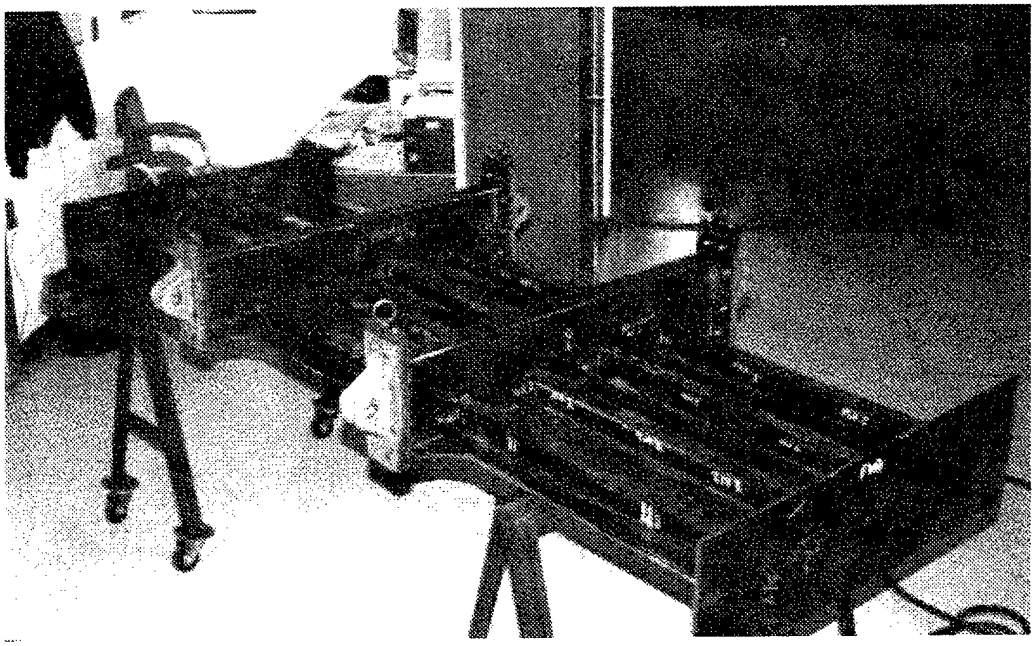

Figure 3 - Typical Grillage Specimen Before Testing

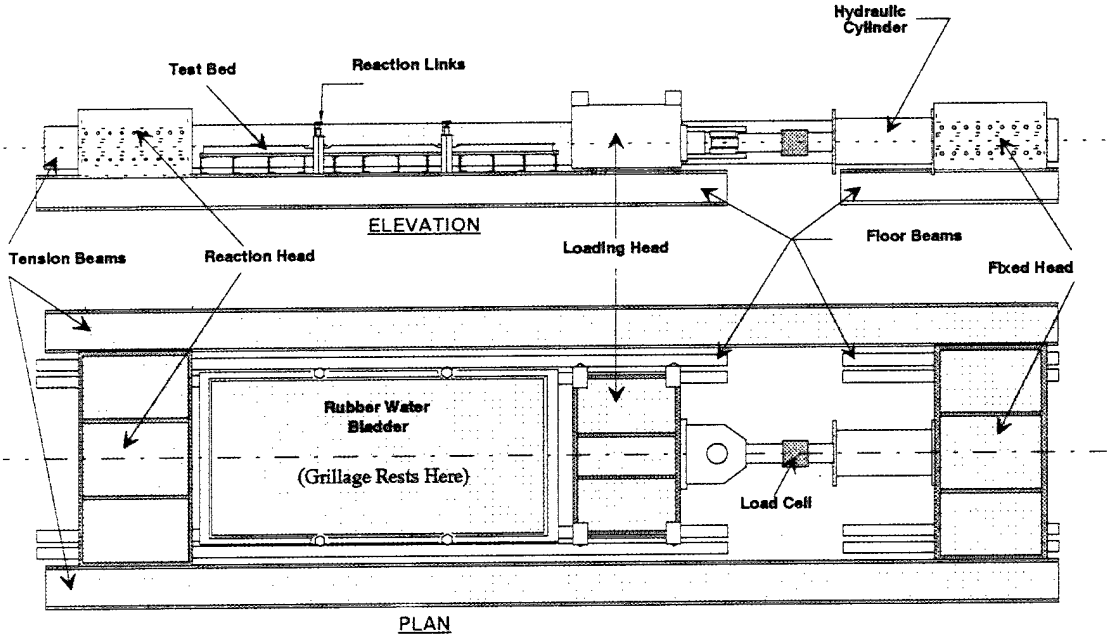


Figure 4 - Schematic of the USNA Grillage Test Fixture.

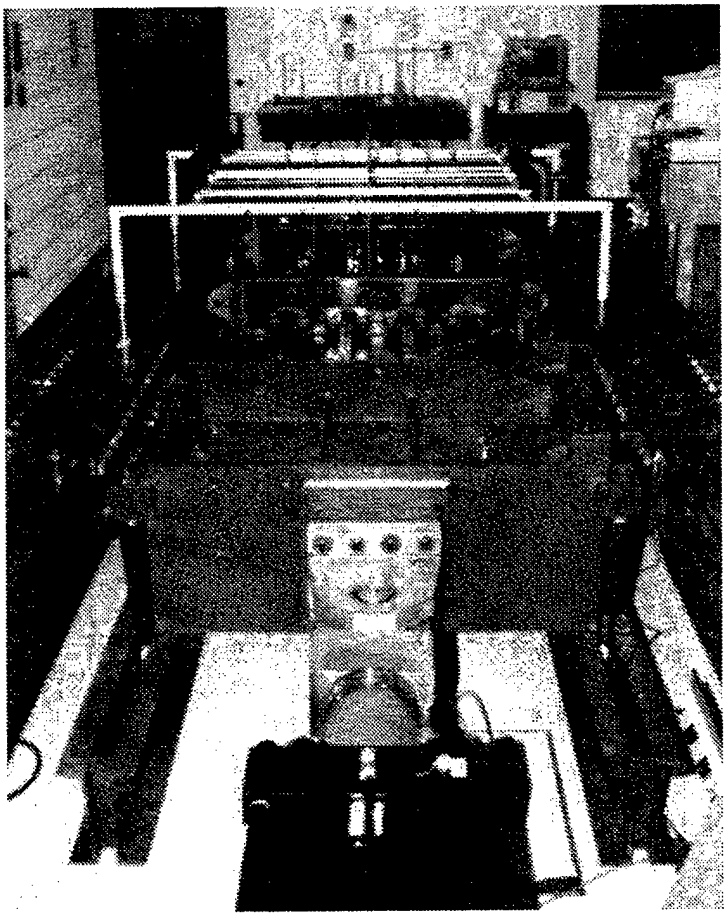

Figure 5a - View of Grillage Test Fixture from the loading head (aft) end.

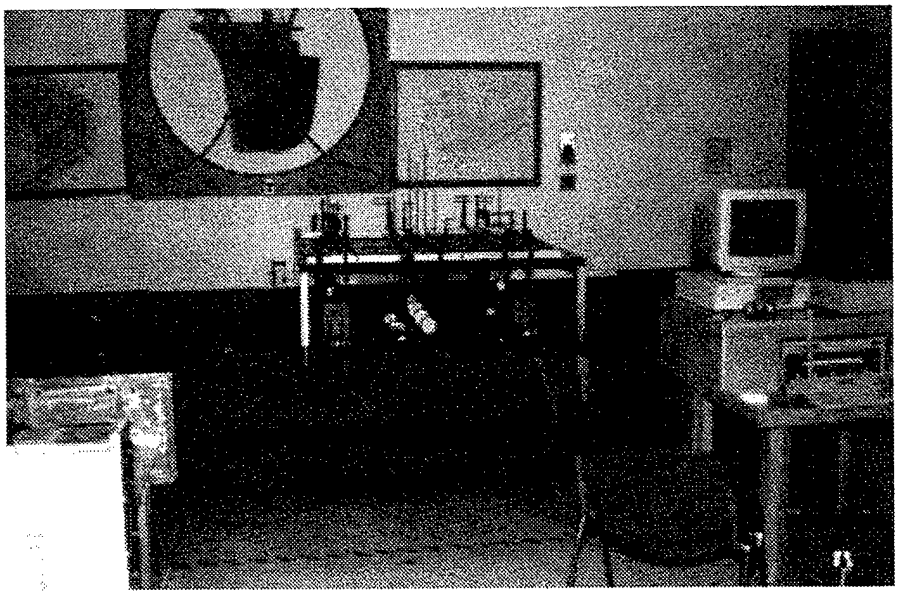

Figure 5b - View of the Stbd. Side of the Grillage Test Fixture

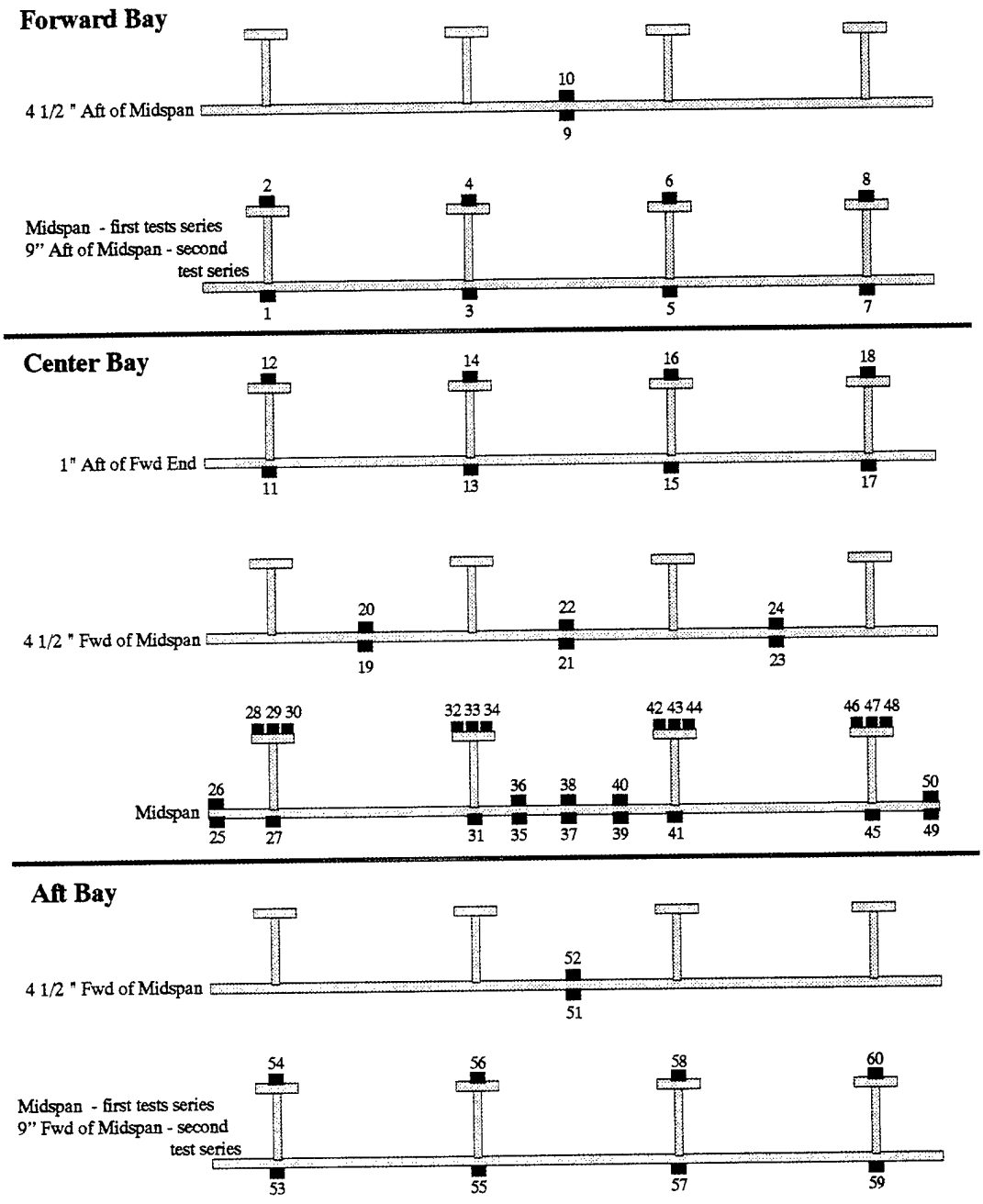


Figure 6 - Strain gage locations for test series.

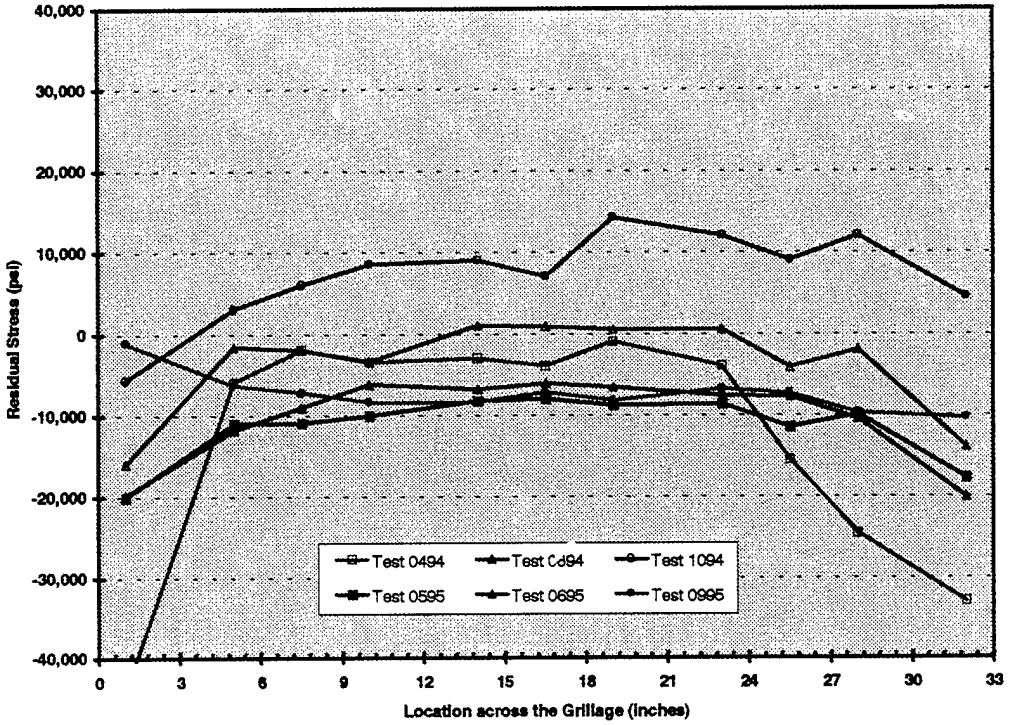


Figure 7 - Residual Stress Measurements - Average Axial Stress

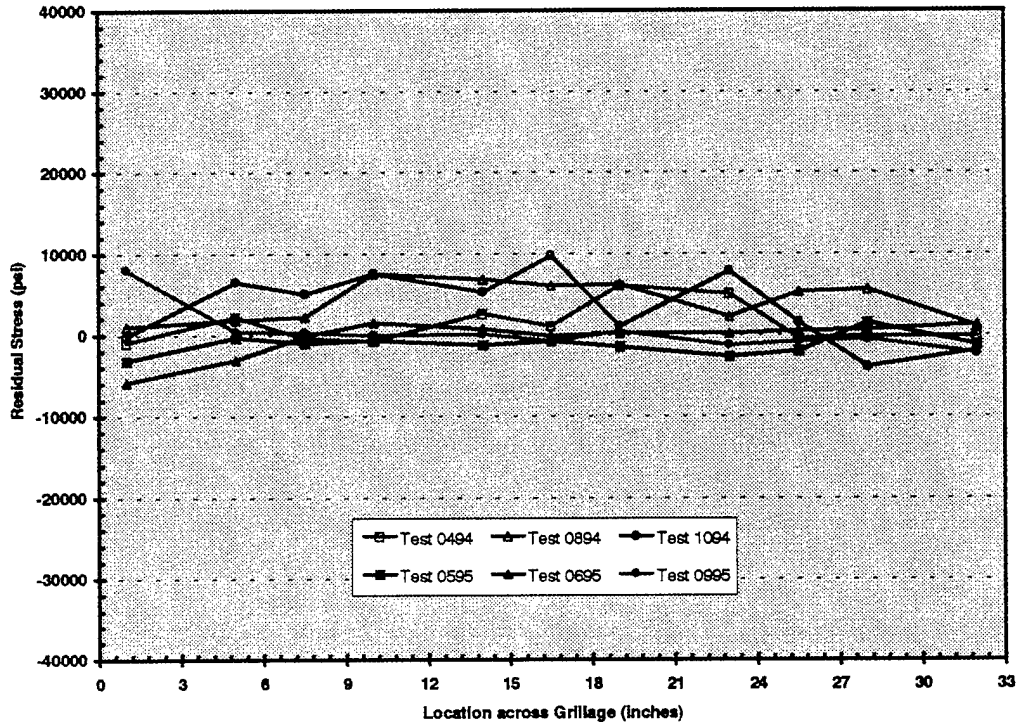


Figure 8 - Residual Stress Measurements - Average Bending Stress

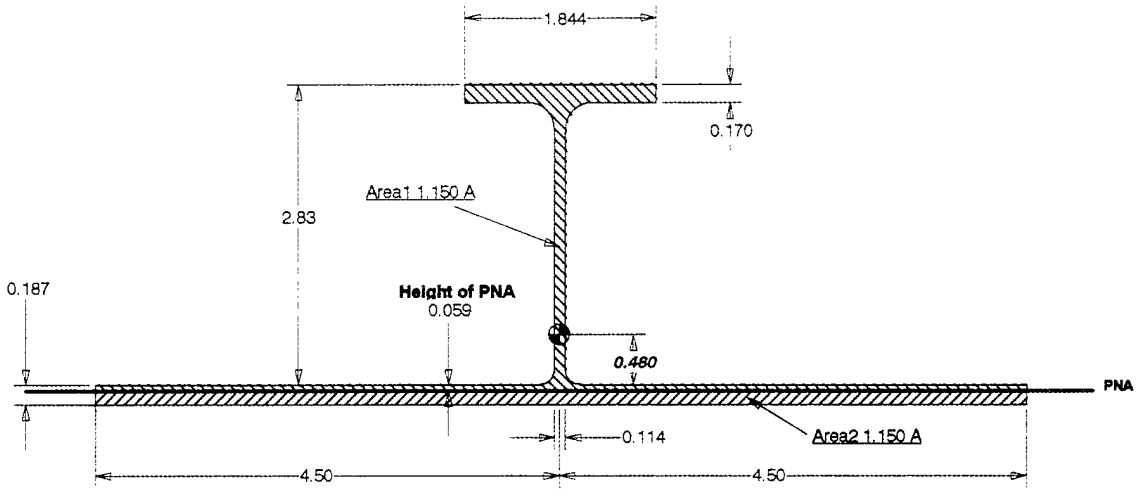


Figure 9 - Geometry of the Stiffener-Plate Cross-section.

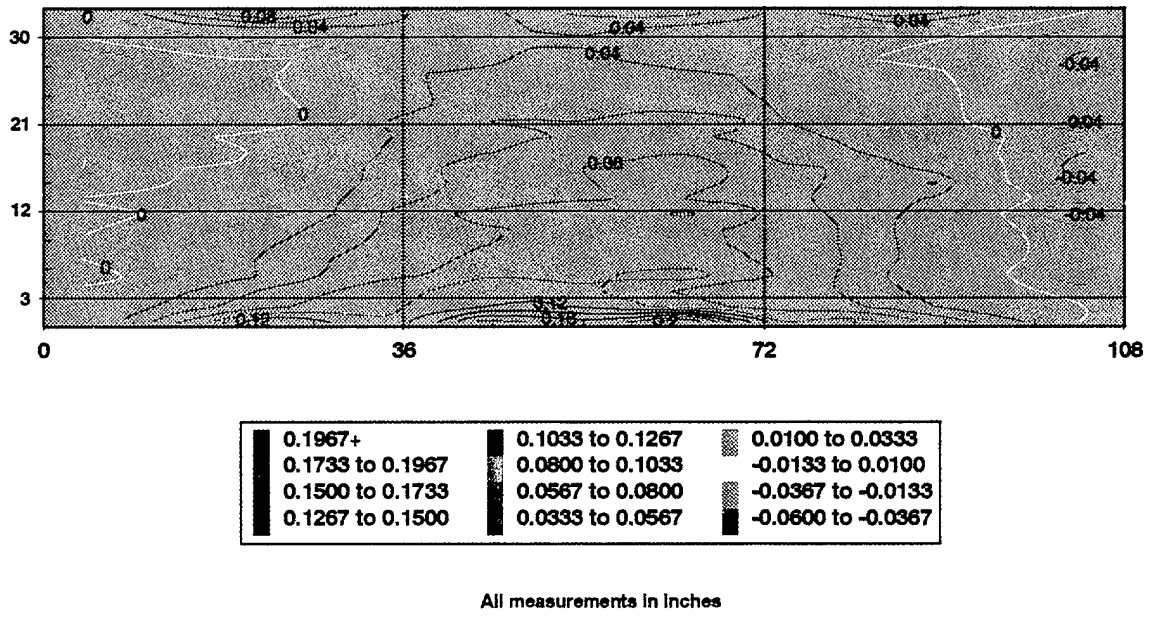


Figure 10 - Contour Plot of the Initial Deflections of Grillage Specimen 0894.

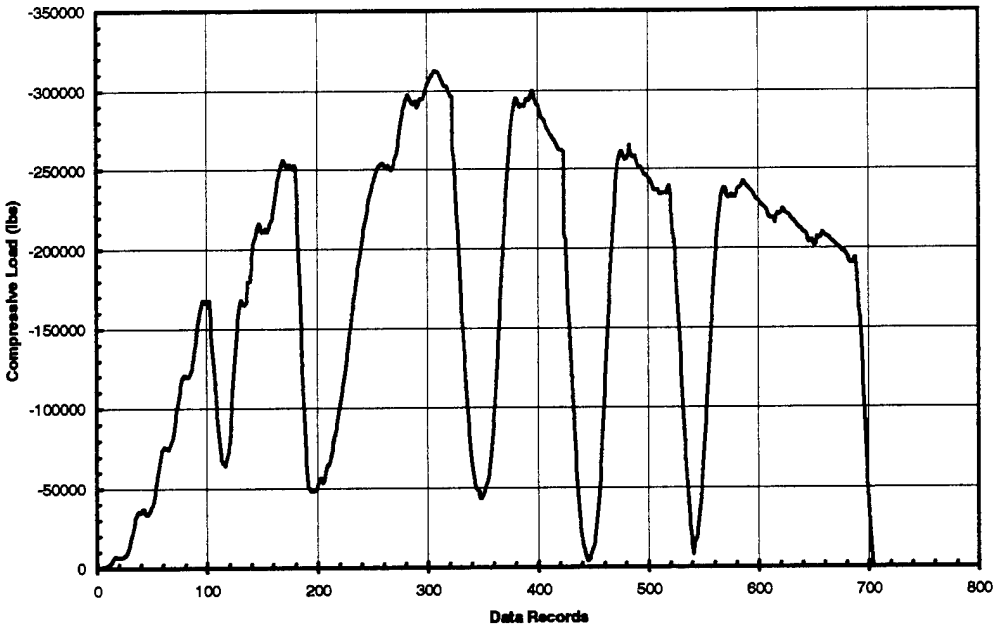


Figure 11 - Load History for Grillage 1094

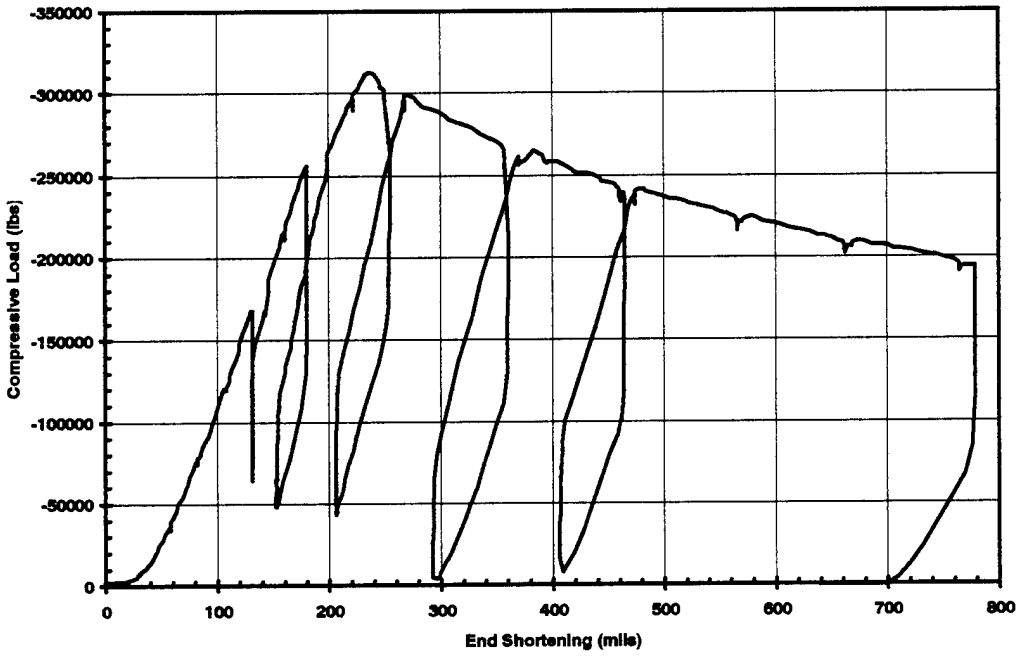


Figure 12 - Load vs. End Shortening for Grillage 1094

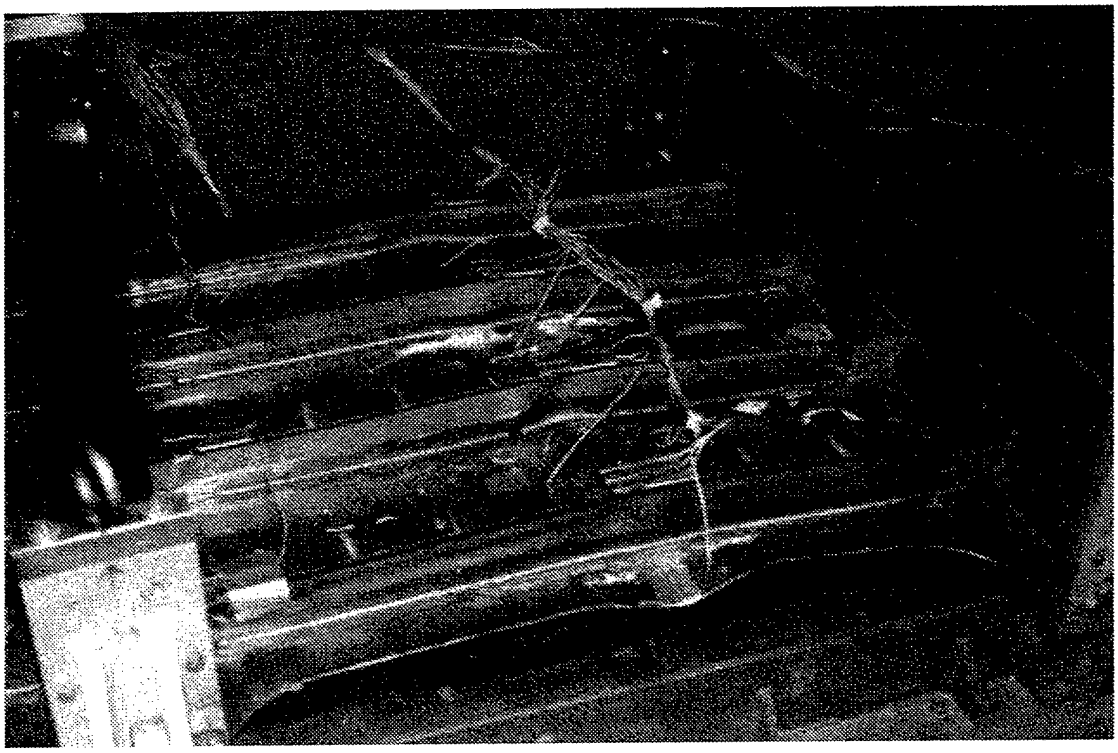

Figure 13a - Grillage 0494 in Test Fixture after Collapse

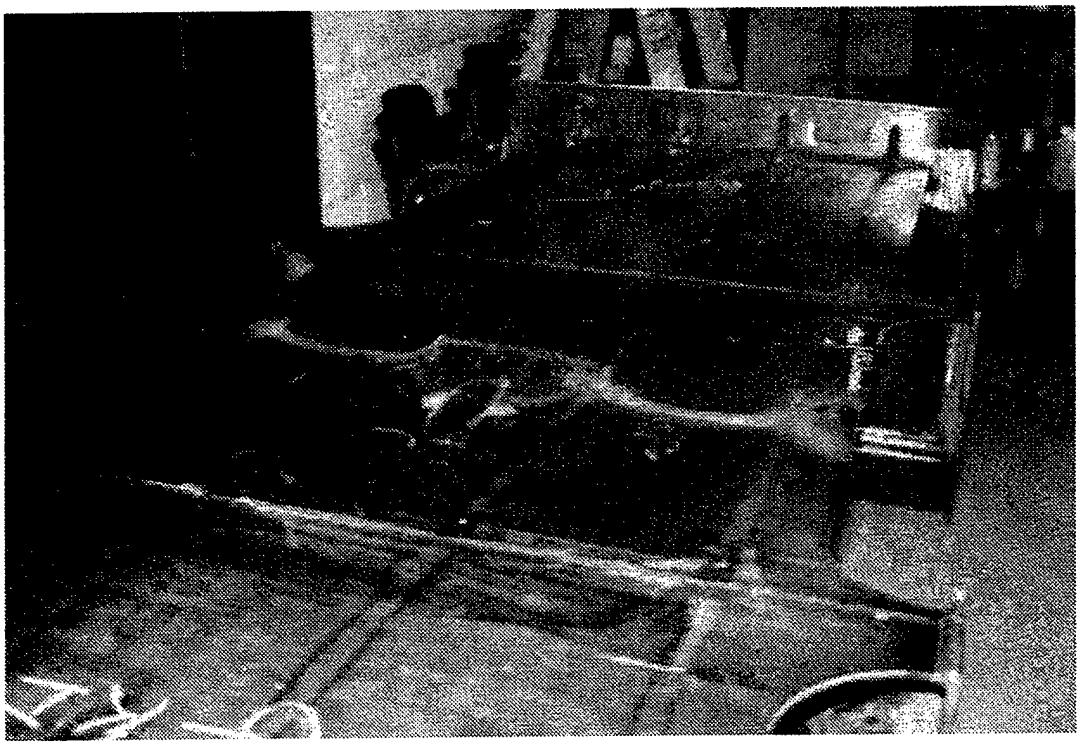

Figure 13b - Plate Side of Grillage 0494 after Collapse

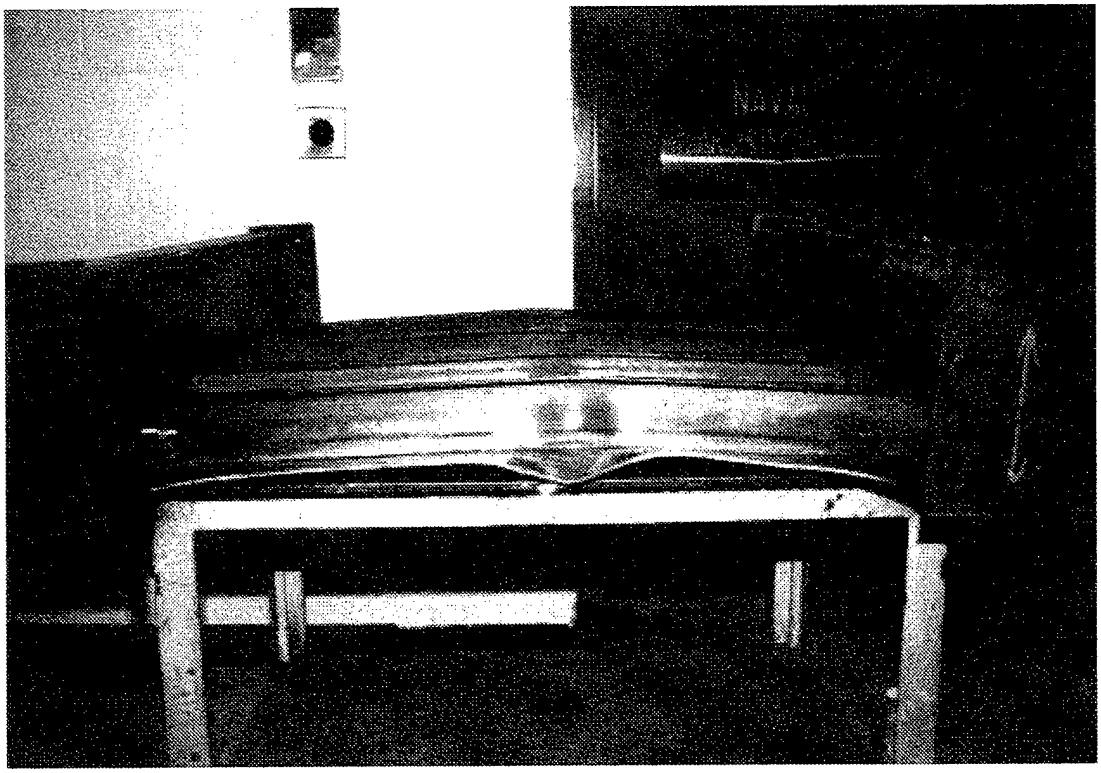

Figure 13c - Side View of Grillage 0494 after Collapse

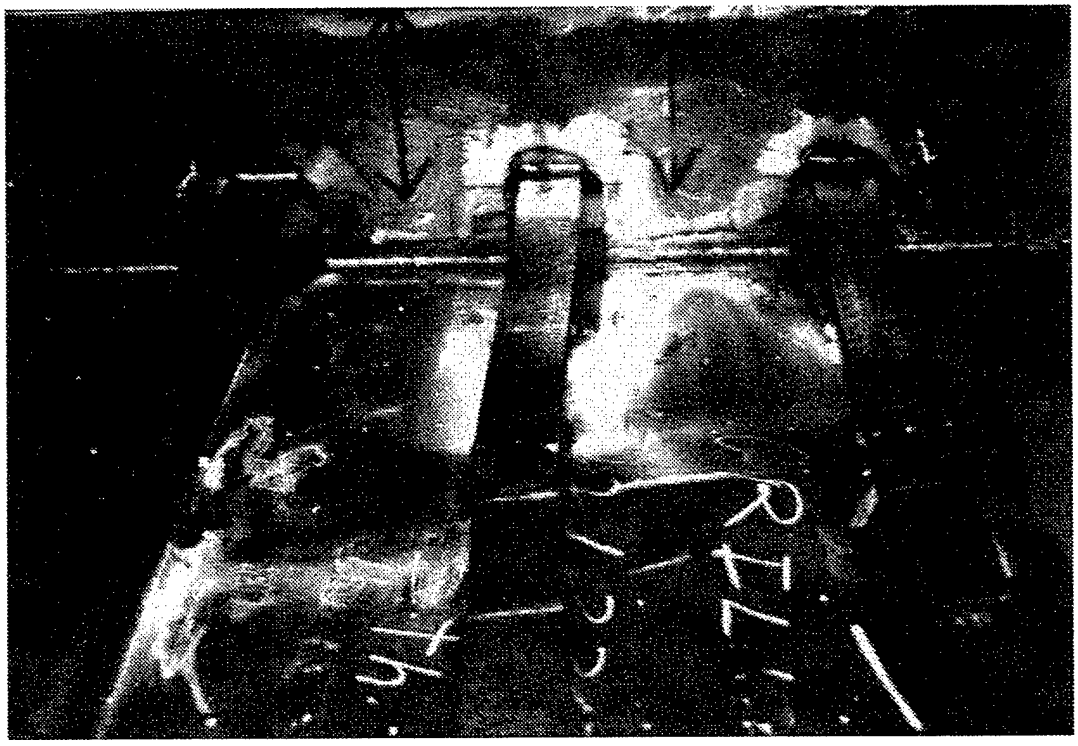

Figure 13d - Detail of Stiffeners on Grillage 0494

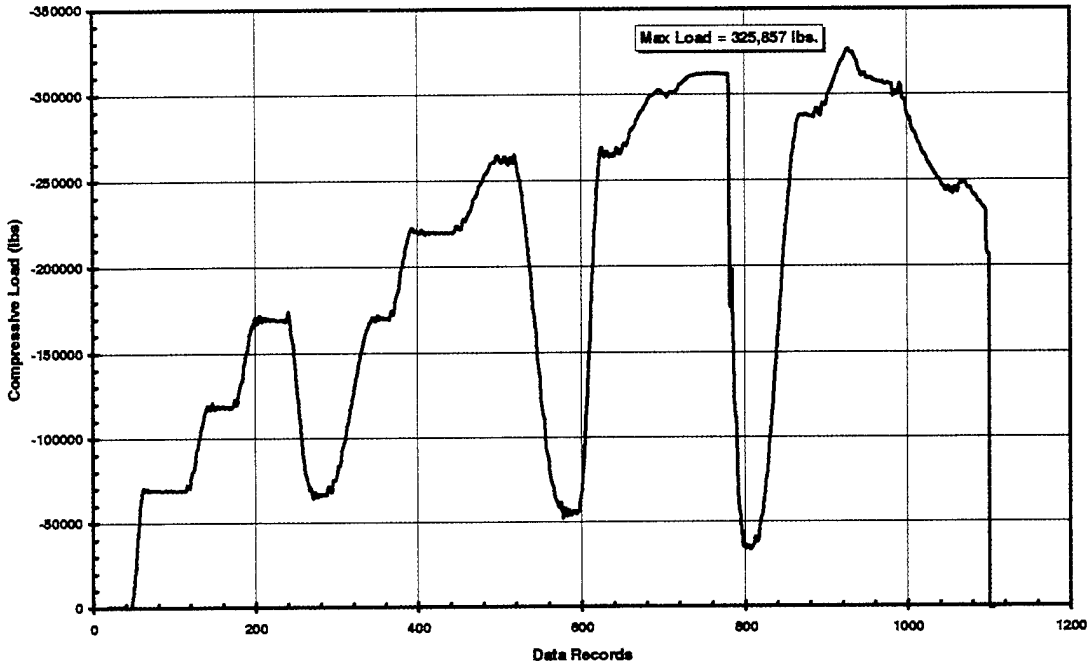


Figure 14a - Load History for Grillage 0494

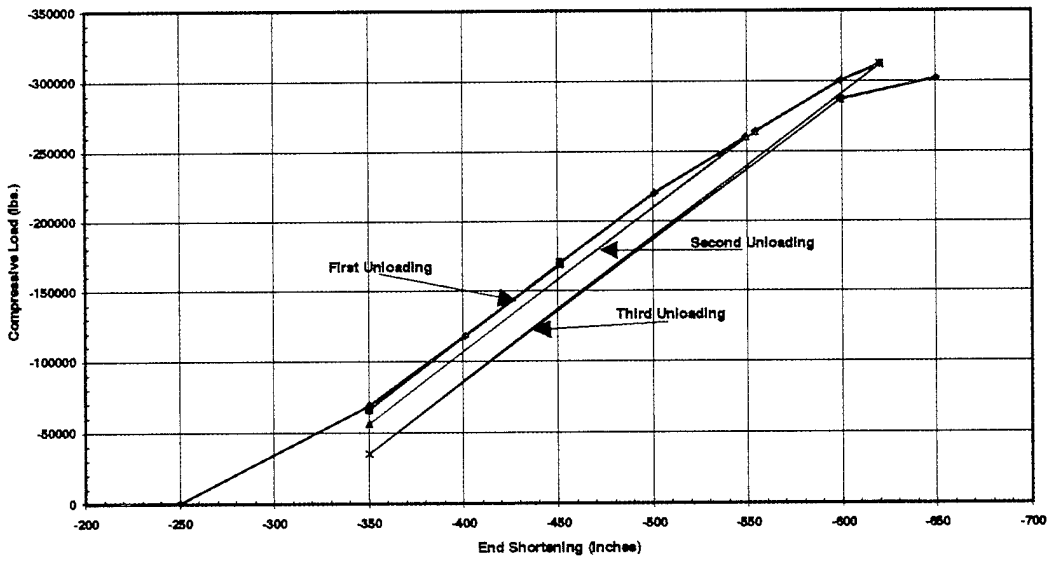


Figure 14b - Load versus End Shortening for Grillage 0494

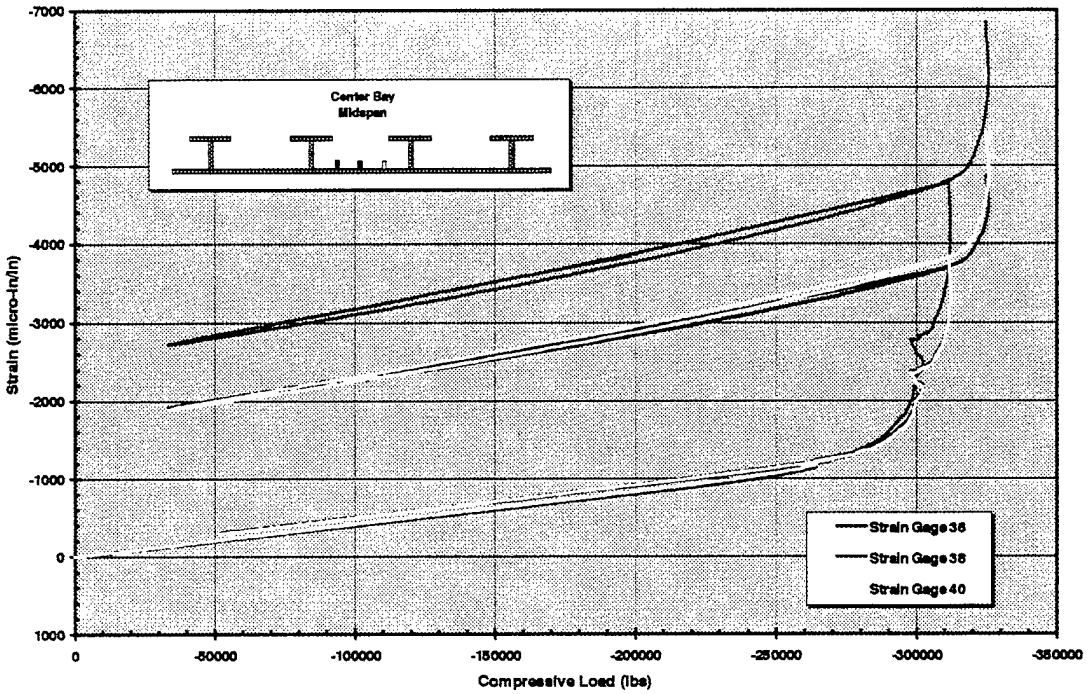


Figure 15a - Measure Strains in Center Bay - Stiffener Side

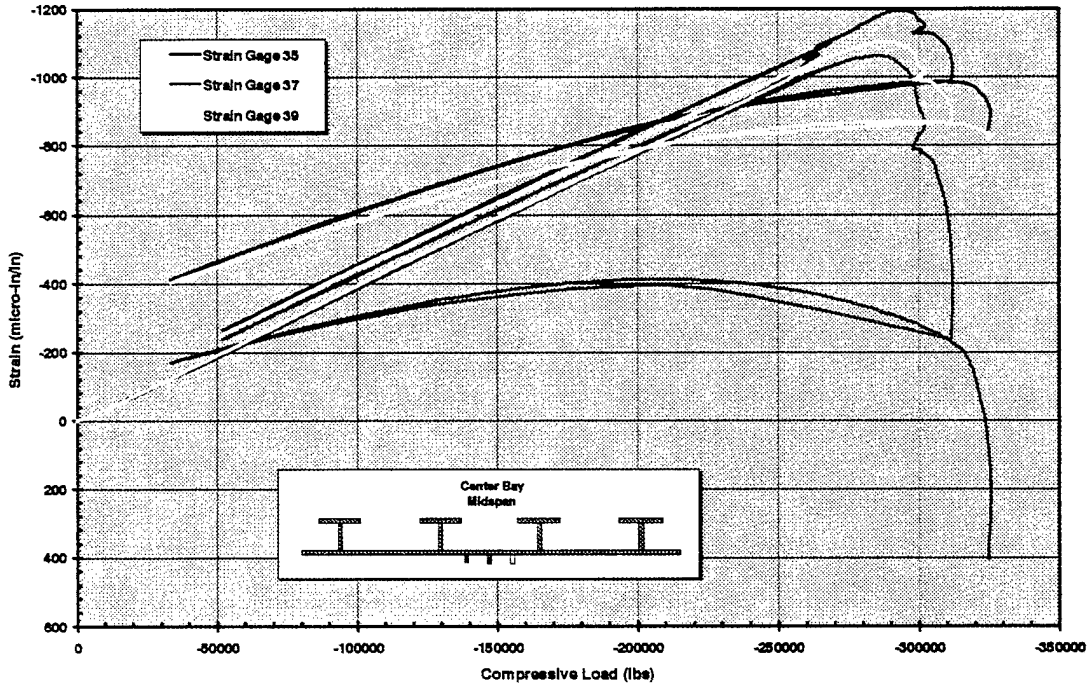


Figure 15b - Measure Strains in Center Bay - Plating Side

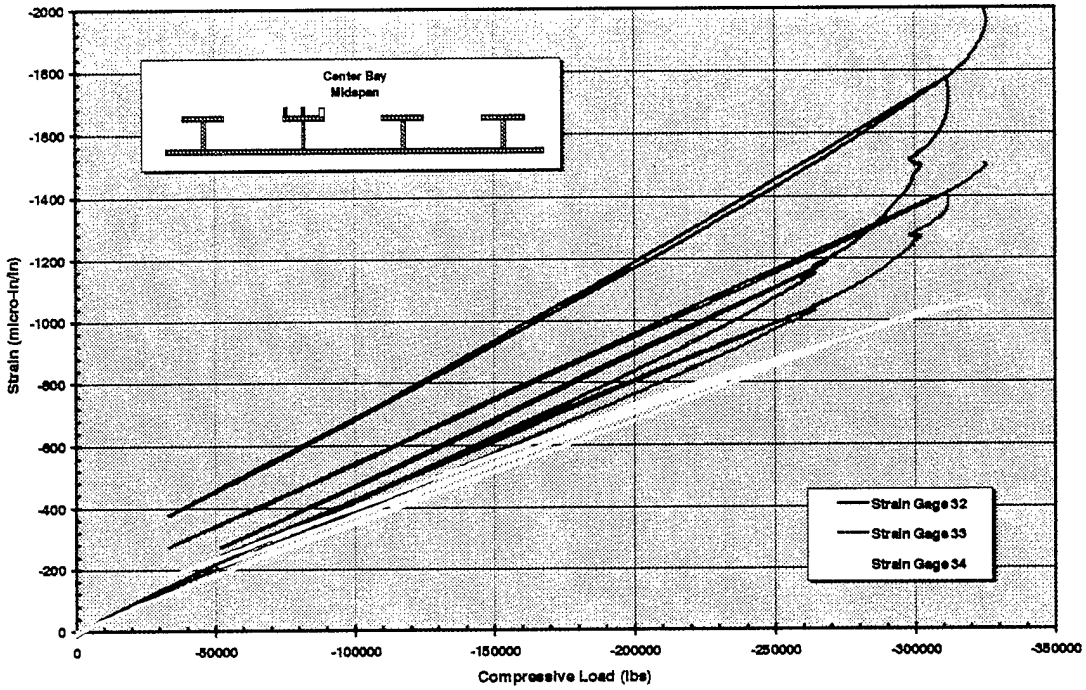


Figure 16a - Measured Strains in the Port Stiffener Flange

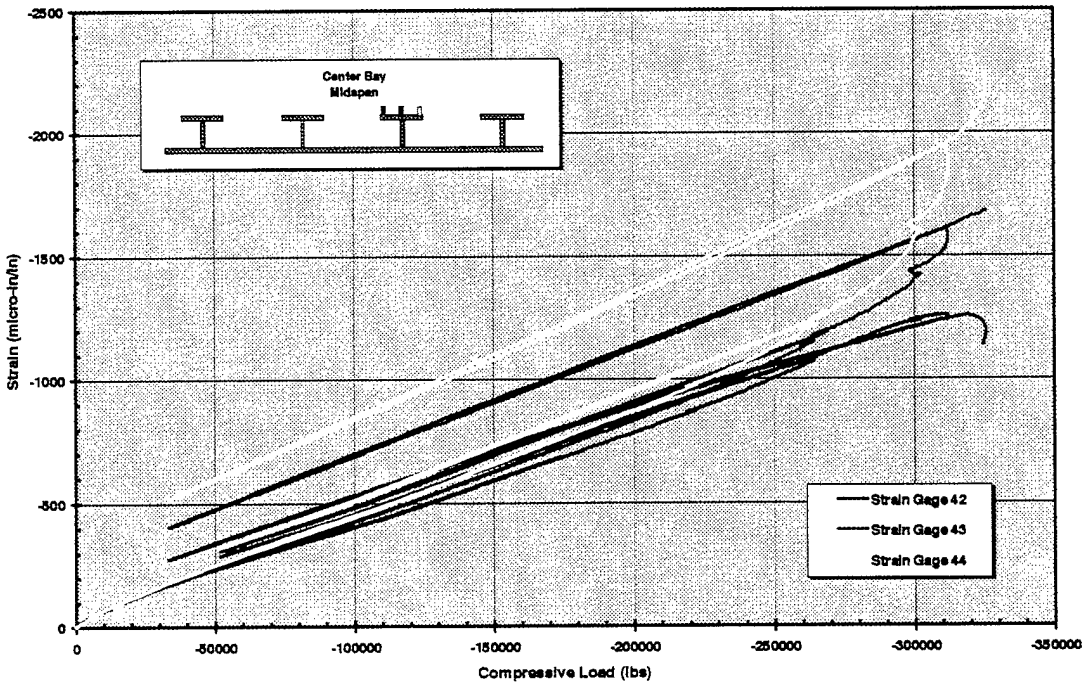


Figure 16b - Measured Strains in the Starboard Stiffener Flange

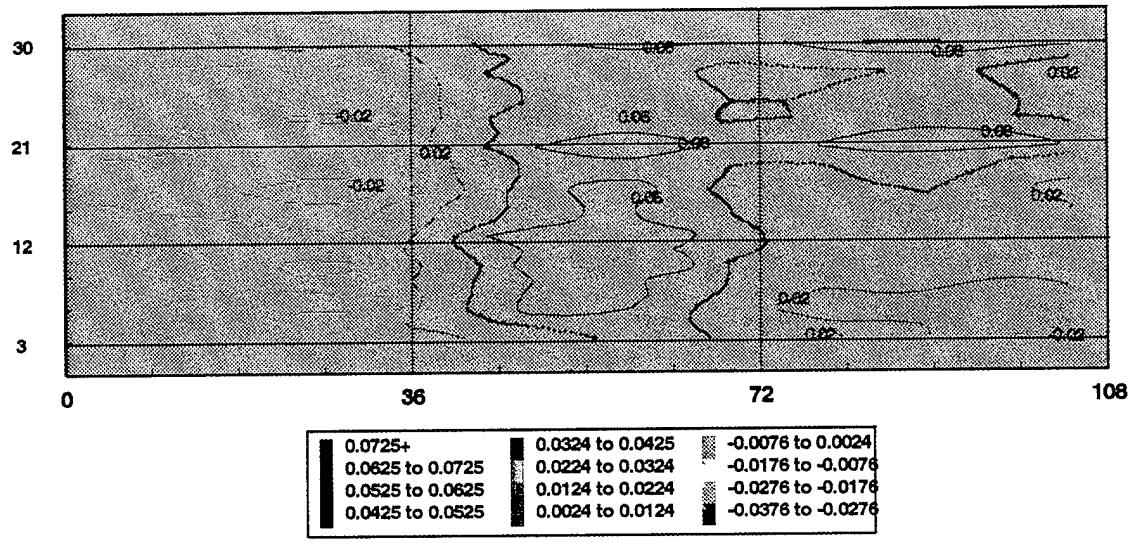


Figure 17a - Contour Plot of Initial Deflections of Grillage 0494

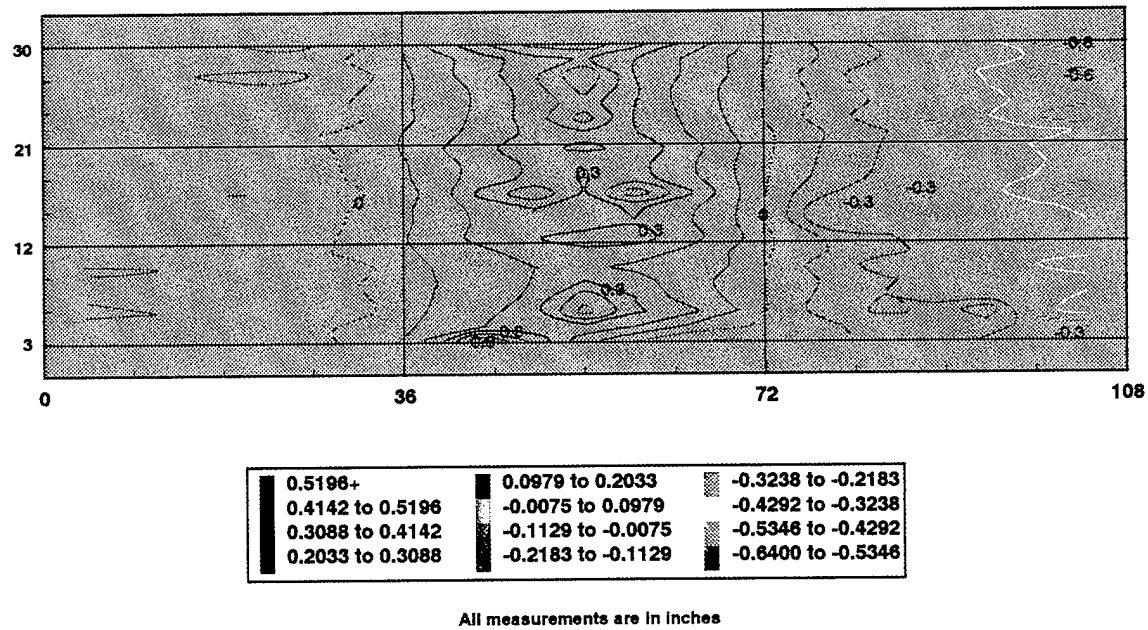


Figure 17b - Contour Plot of Final Deflections of Grillage 0494

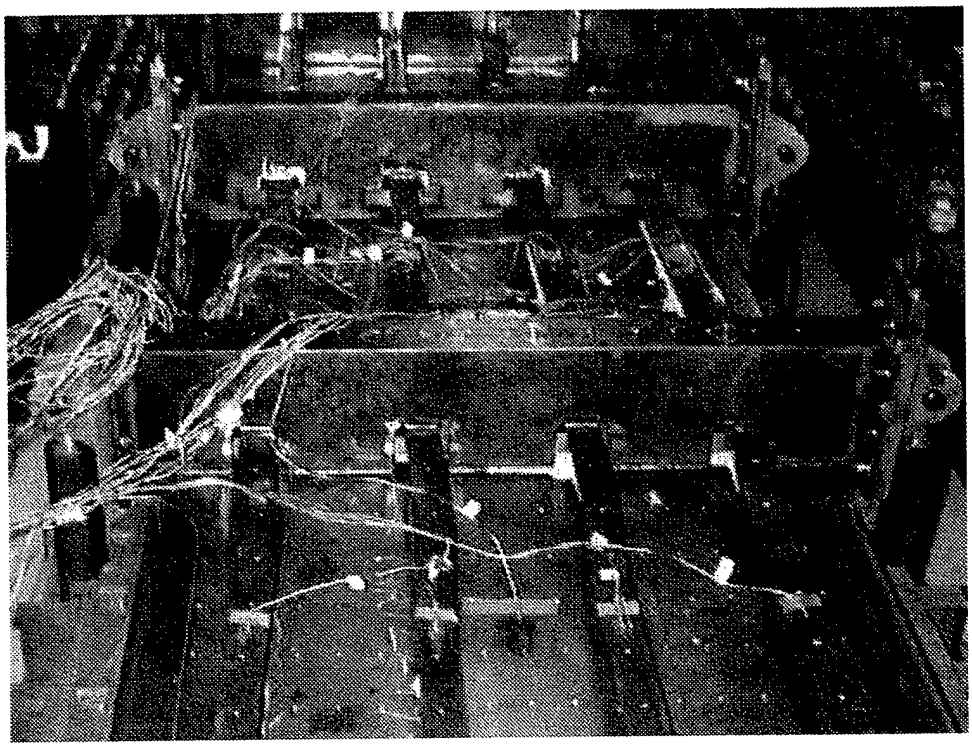

Figure 18a - Grillage 0894 in Test Fixture after Collapse - Top View

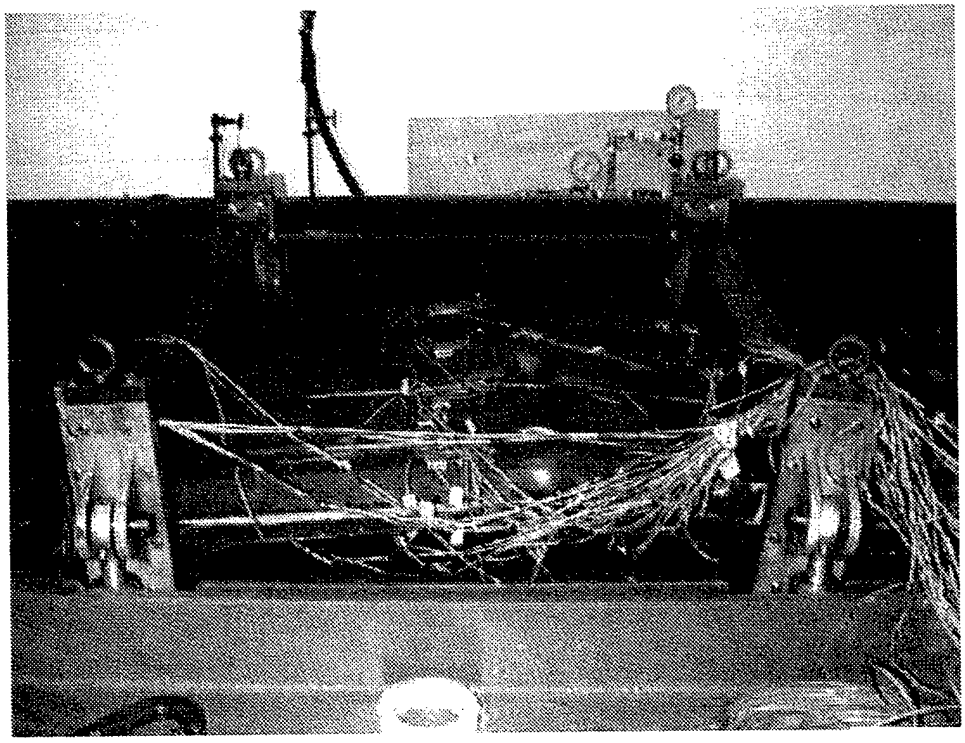

Figure 18b - Grillage 0894 in Test Fixture after Collapse - Side View

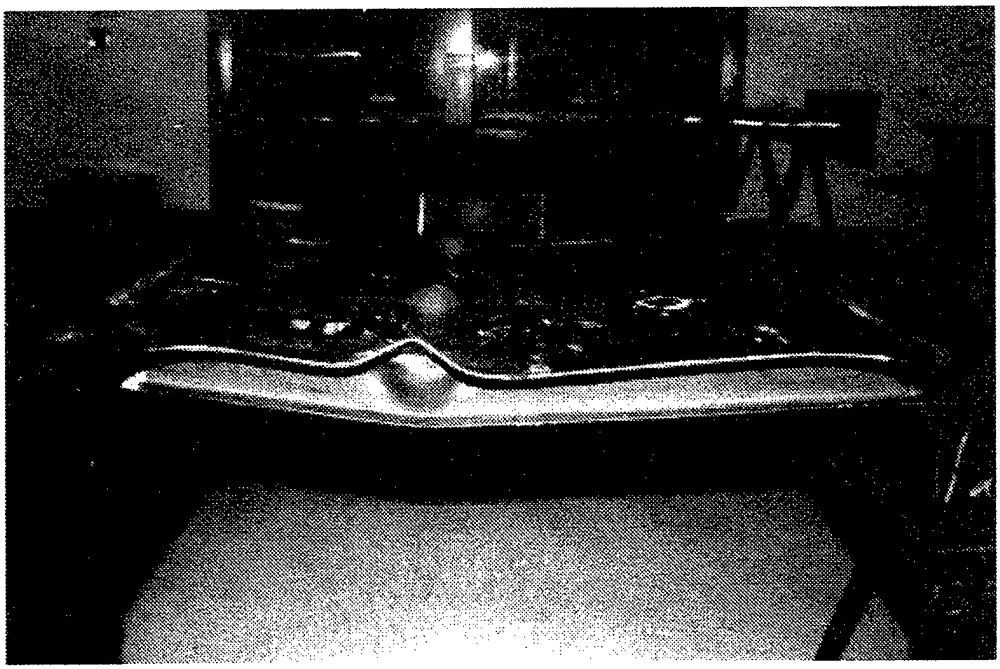

Figure 18c - Grillage 0894 - View of the Plate Side

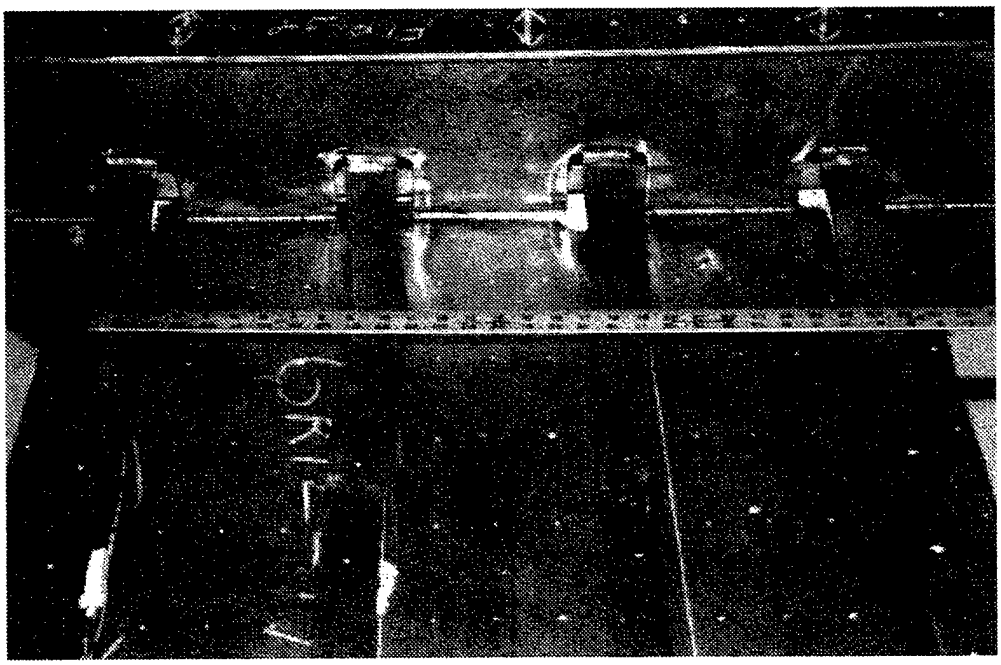

Figure 18d - Grillage 0894 - Detail of Stiffener Collapse

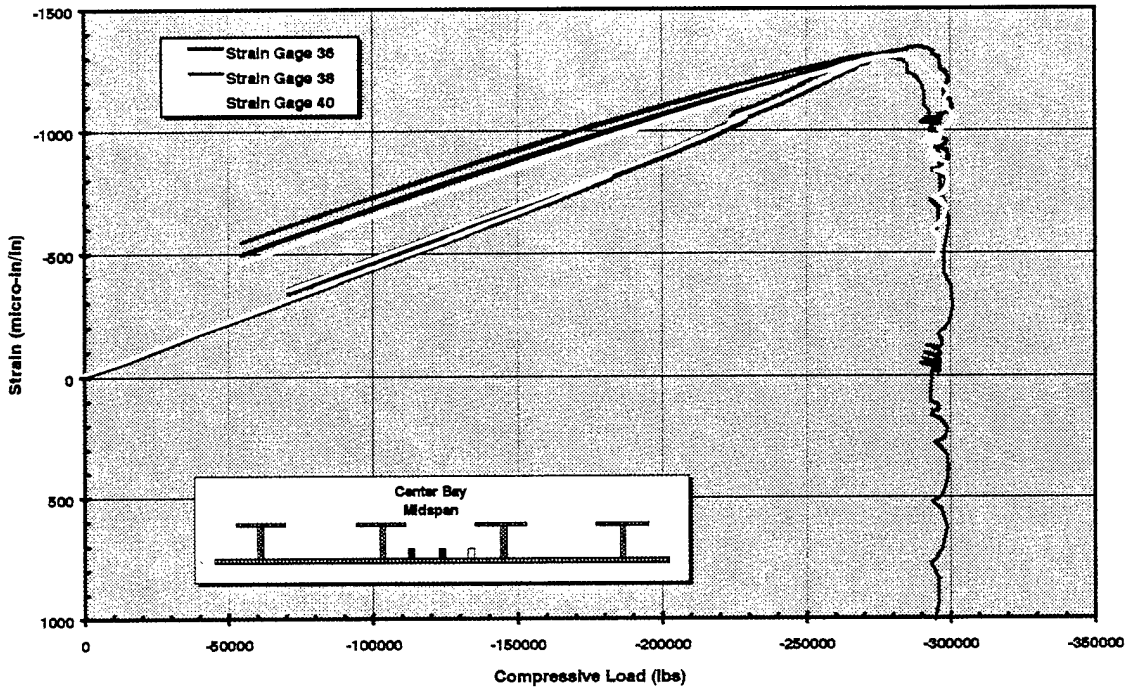


Figure 20a - Measured Strains in Center Bay on the Stiffener Side - Grillage 0894

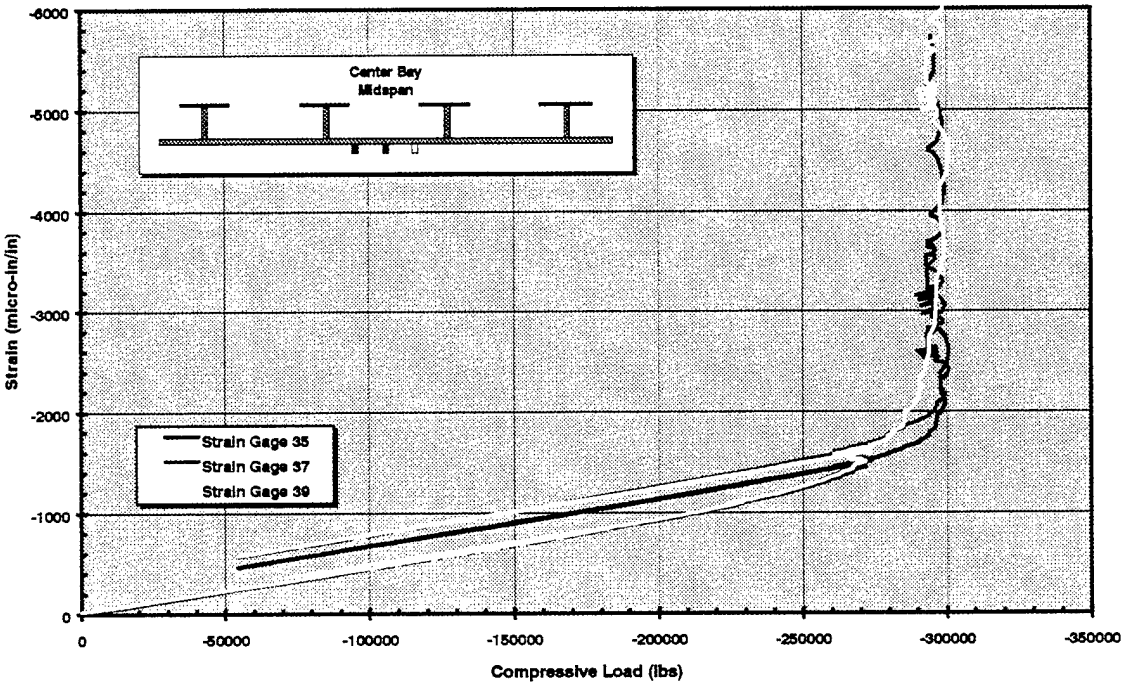


Figure 20b - Measured Strains in Center Bay on the Plate Side - Grillage 0894

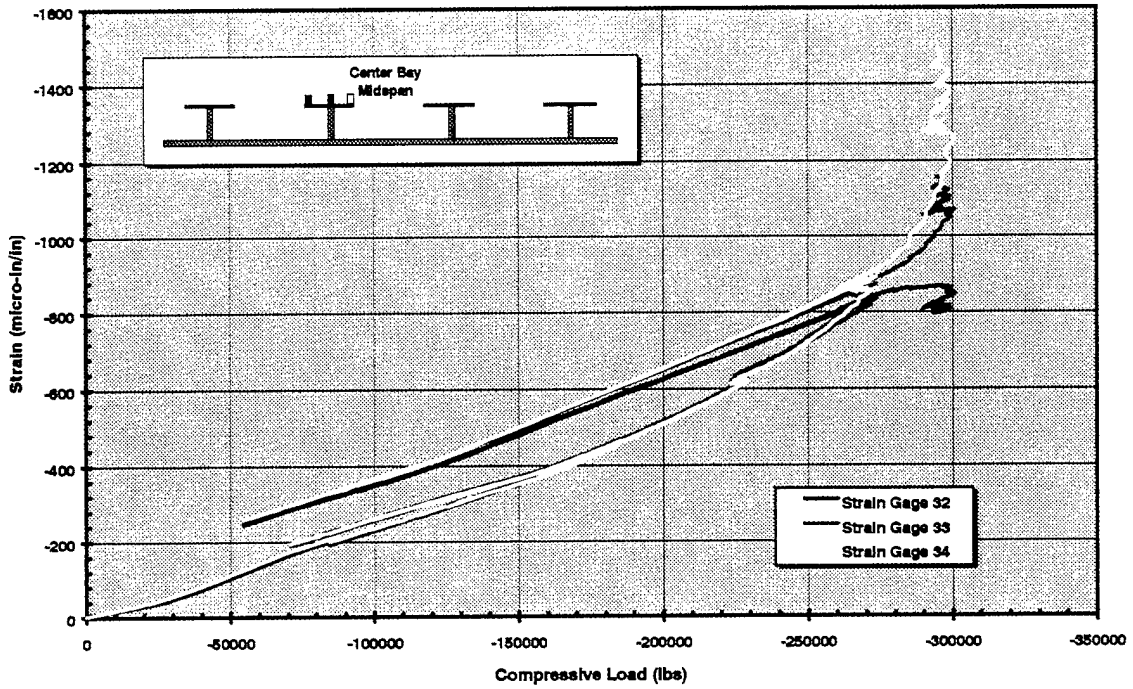


Figure 21a - Measured Strains on Port Stiffener - Grillage 0894

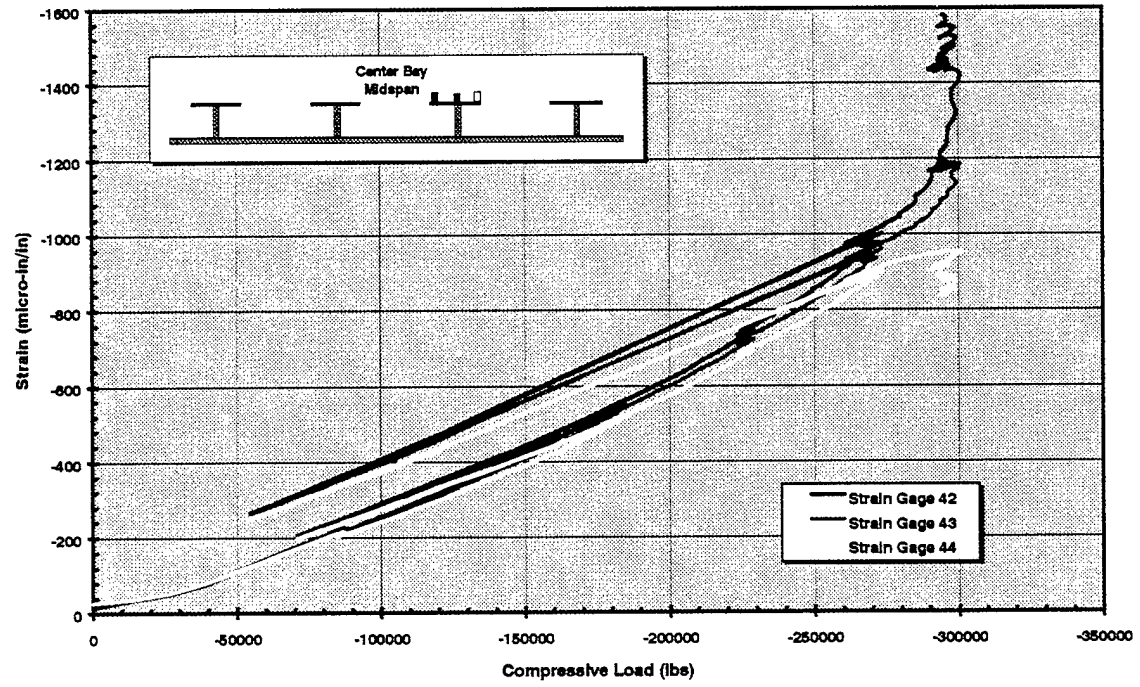


Figure 21b - Measured Strains on Starboard Stiffener - Grillage 0894

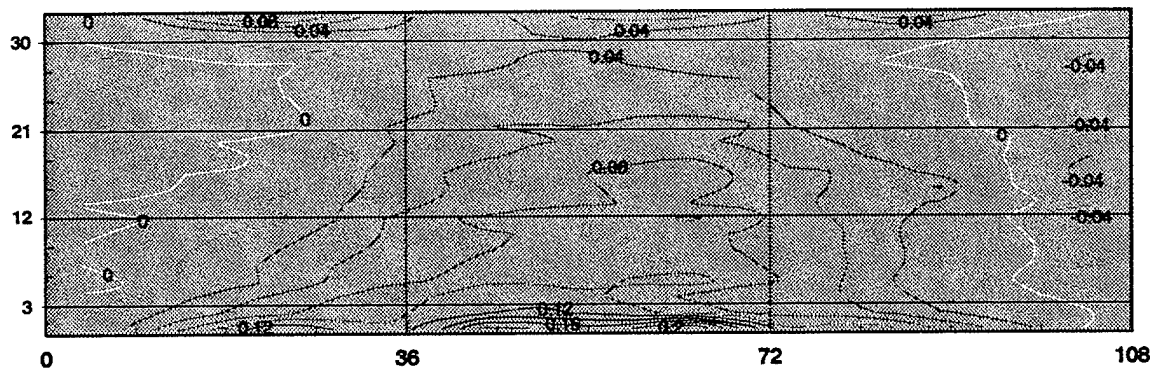


| | | |
|---|---|---|
| 0.1967+ | 0.1033 to 0.1267 | 0.0100 to 0.0333 |
| 0.1733 to 0.1967 | 0.0800 to 0.1033 | -0.0133 to 0.0100 |
| 0.1500 to 0.1733 | 0.0567 to 0.0800 | -0.0367 to -0.0133 |
| 0.1267 to 0.1500 | 0.0333 to 0.0567 | -0.0600 to -0.0367 |

All measurements in inches

Figure 22a - Contour Plot of Initial Deflections for Grillage 0894

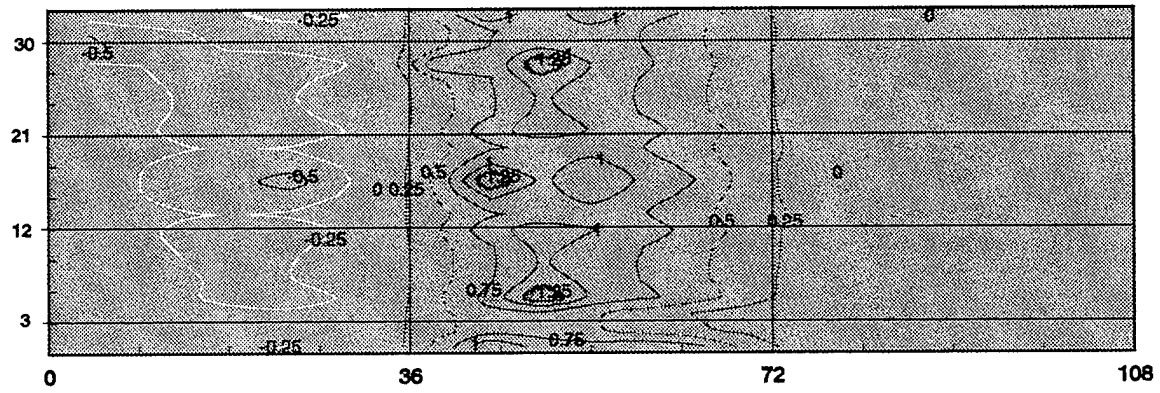


| | | |
|---|---|---|
| 1.2838+ | 0.5989 to 0.7701 | -0.0859 to 0.0853 |
| 1.1126 to 1.2838 | 0.4277 to 0.5989 | -0.2571 to -0.0859 |
| 0.9414 to 1.1126 | 0.2565 to 0.4277 | -0.4284 to -0.2571 |
| 0.7701 to 0.9414 | 0.0853 to 0.2565 | -0.5996 to -0.4284 |

All measurements in inches

Figure 22b - Contour Plot of Final Deflections for Grillage 0894

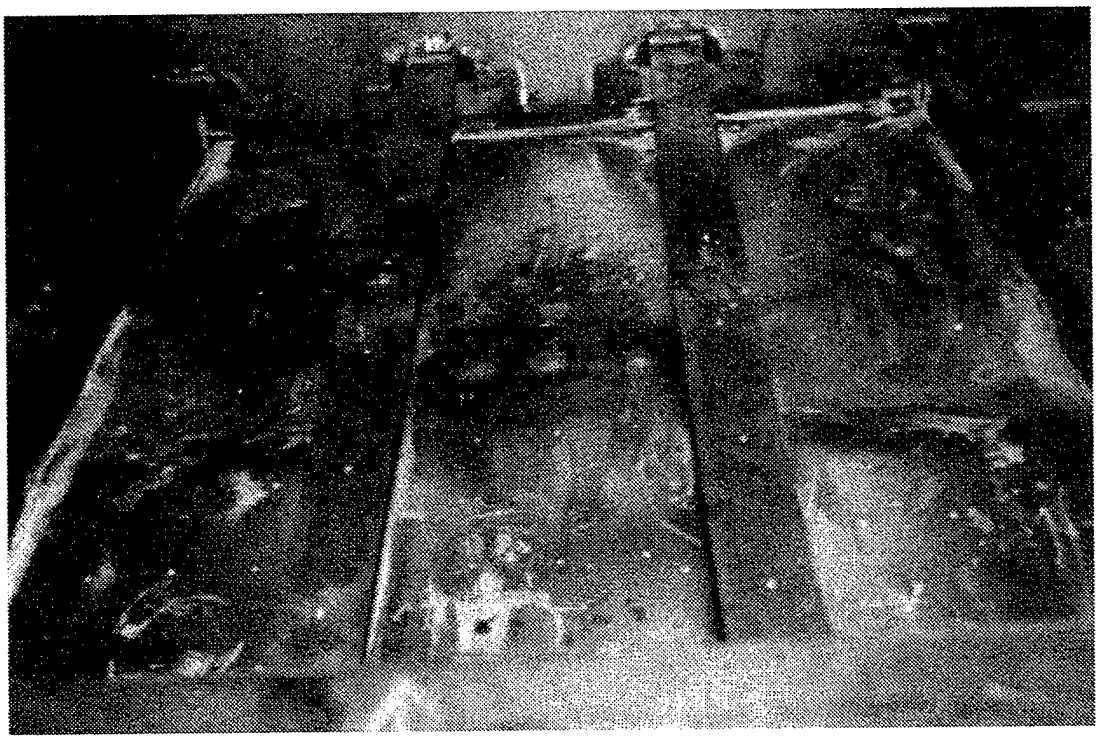

Figure 23a - Post Test Deformations on Stiffener Side of Grillage 1094

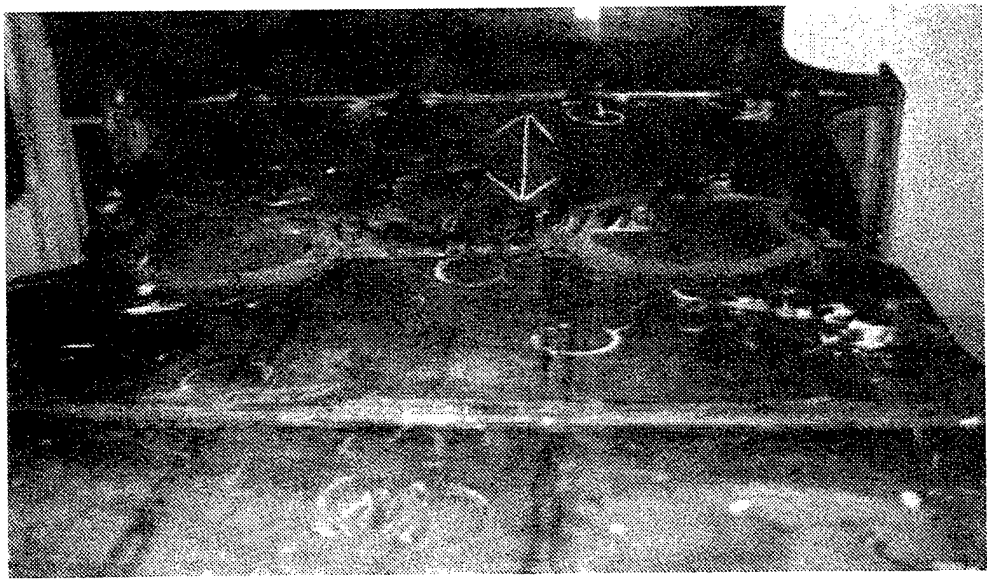

Figure 23b - View of the Deformations on the Plate Side of Grillage 1094

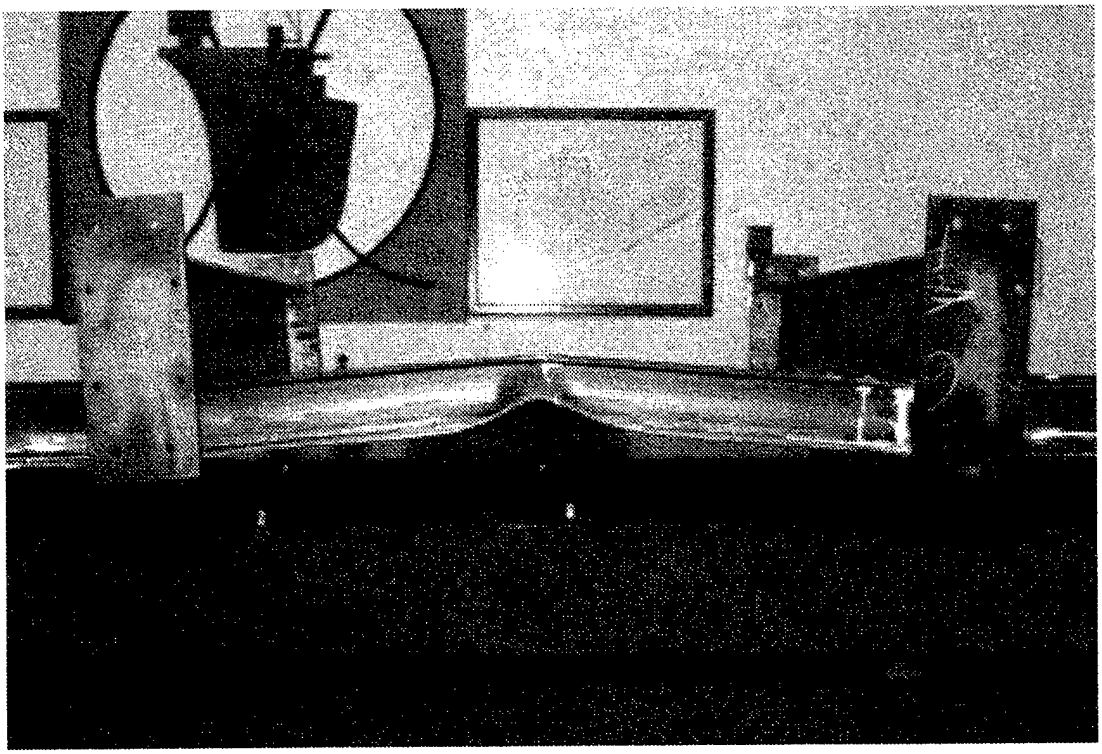

Figure 23c - Post Test Side View of Grillage 1094

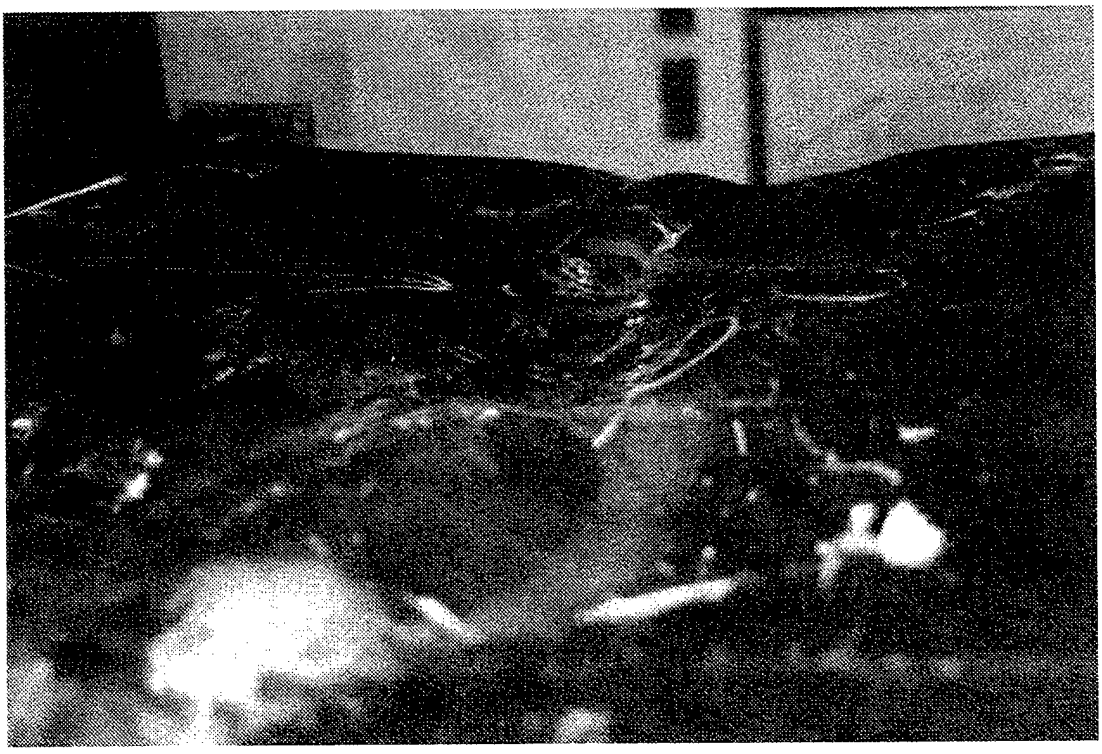

Figure 23d - Close-up of Plate Side Deformations

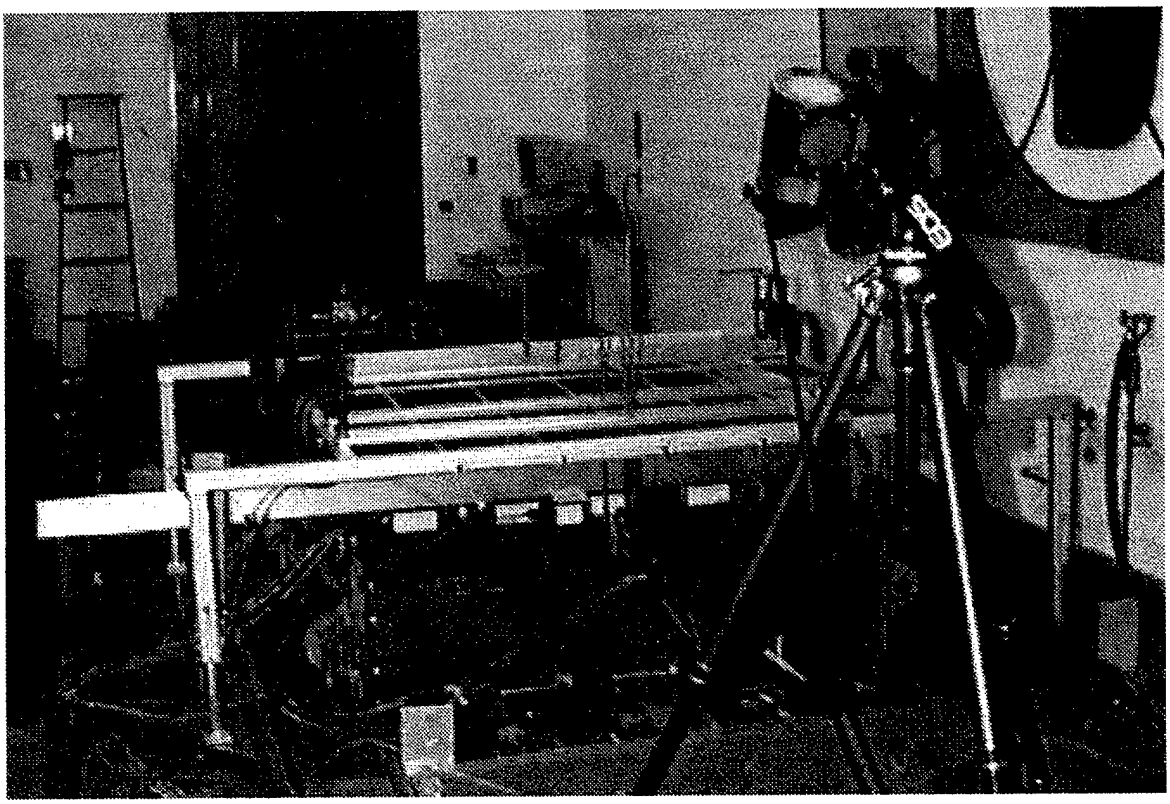

Figure 24a - Photo-elastic Measurement Equipment Setup During Testing

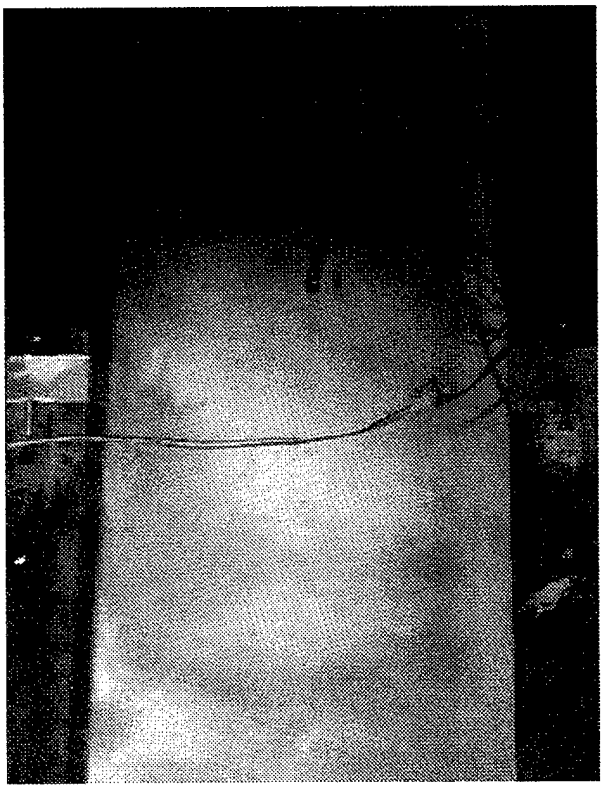

Figure 24b - Pattern in Photo-elastic Material During Testing of Grillage 1094

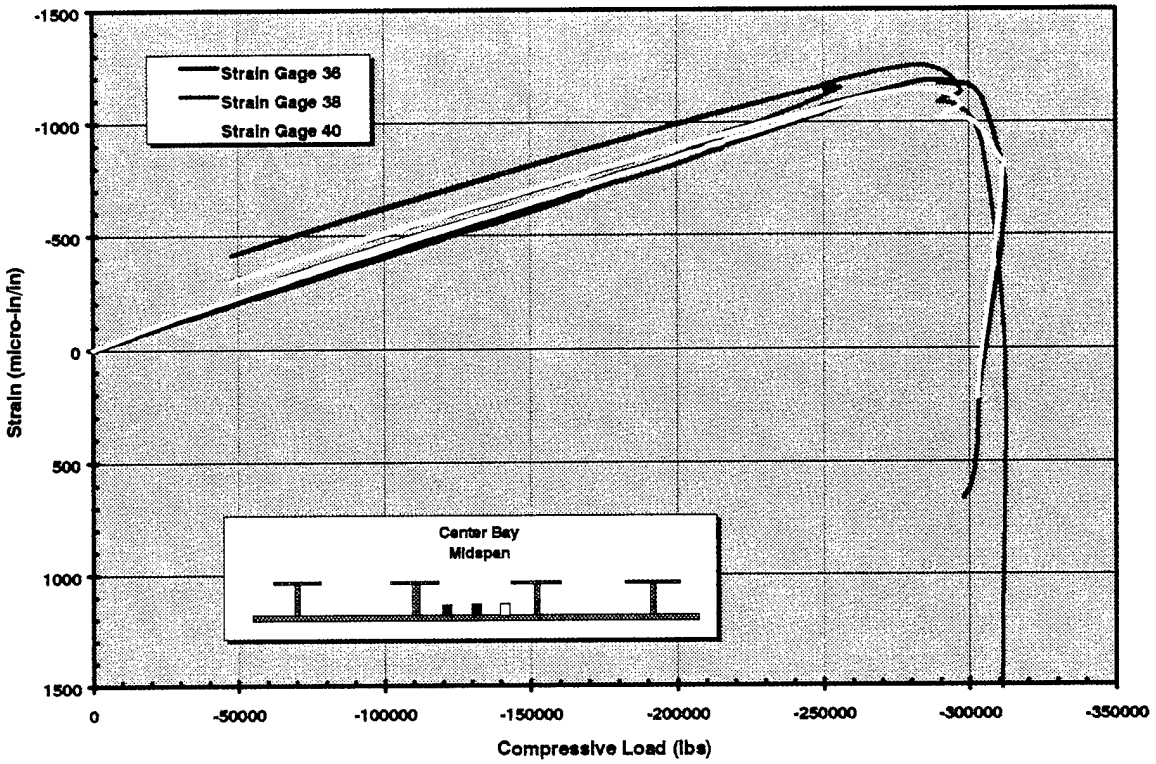


Figure 25a - Measured Strains in Center Bay on Stiffener Side for Grillage 1094

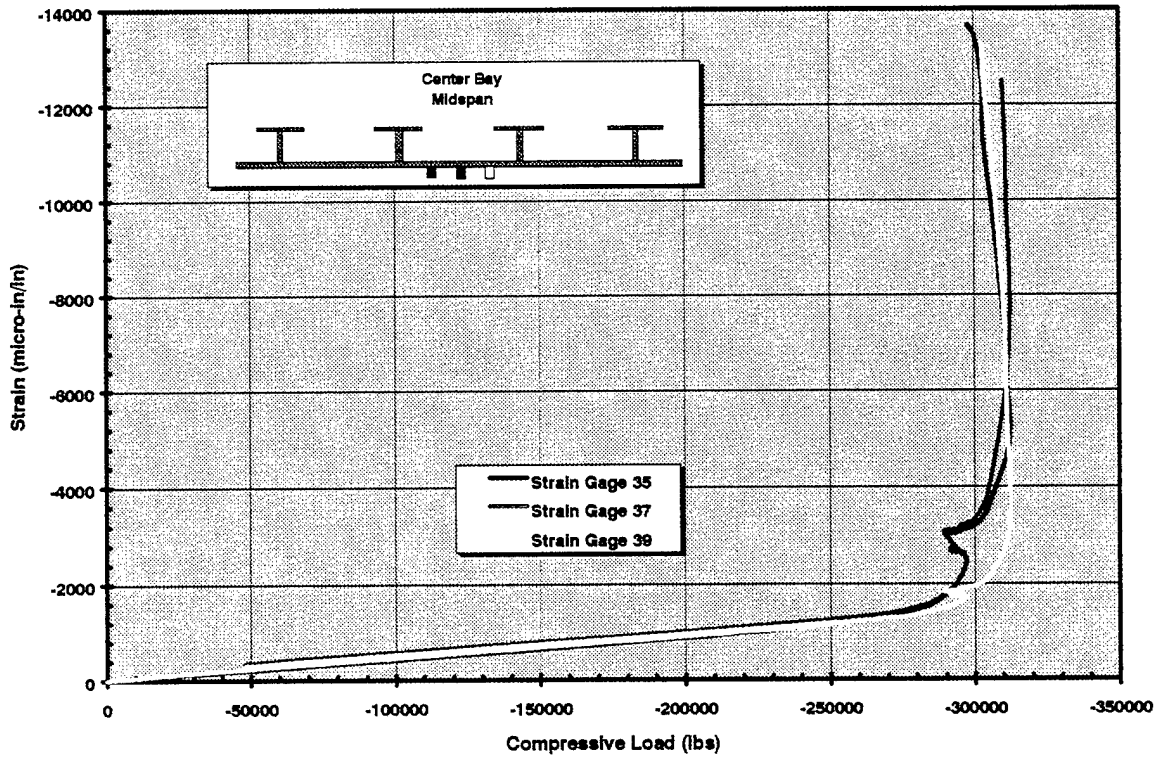


Figure 25b - Measured Center Bay Strains on Plate Side of Grillage 1094

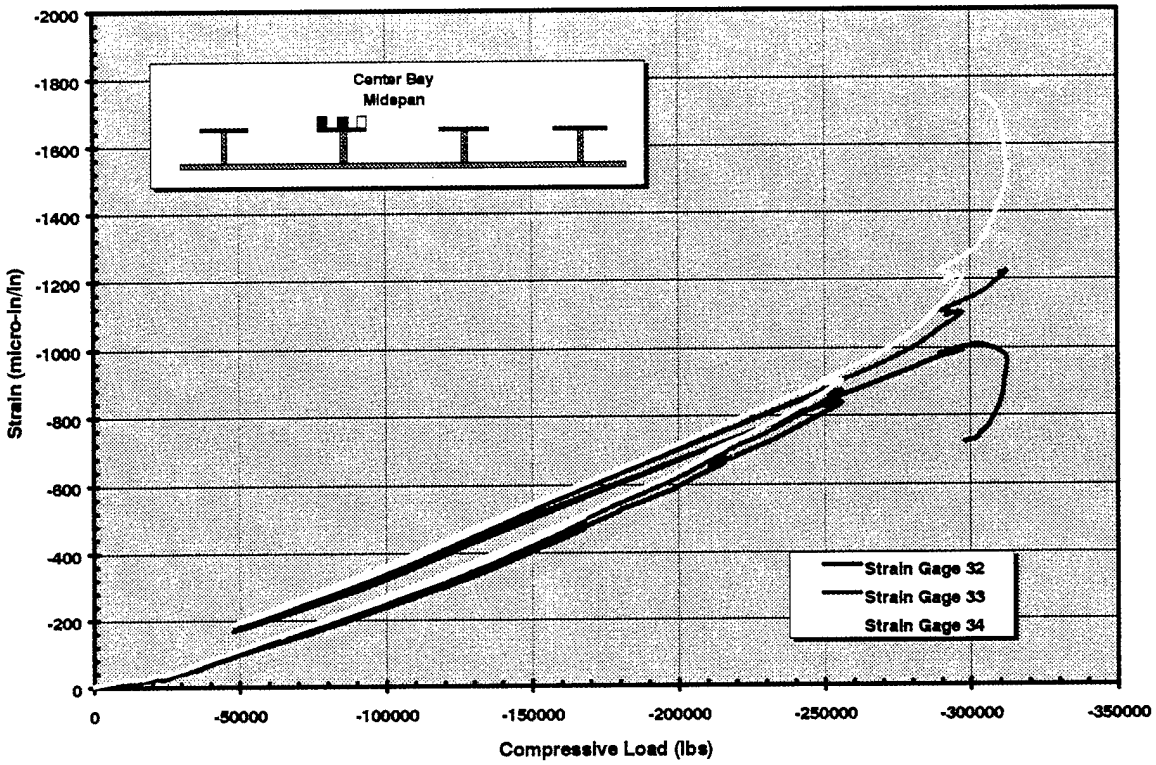


Figure 26a - Measure Strains on Port Stiffener - Grillage 1094

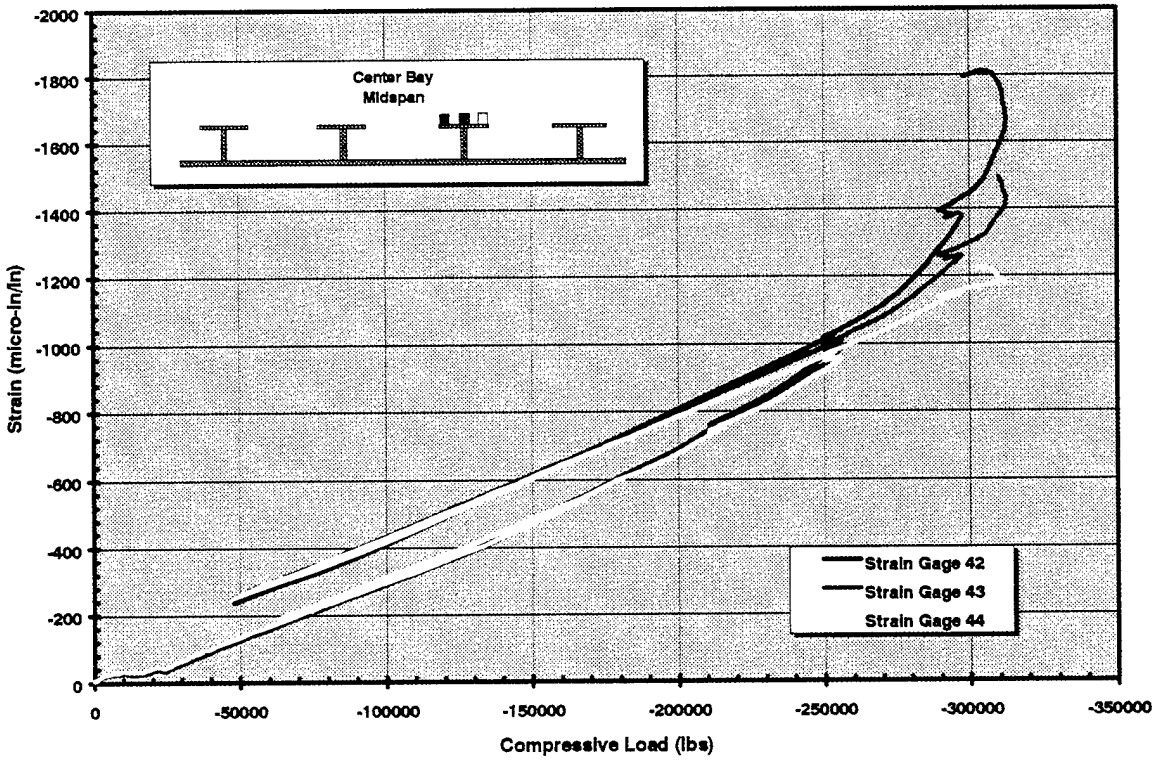


Figure 26b - Measured Strains on Stbd. Stiffener - Grillage 1094

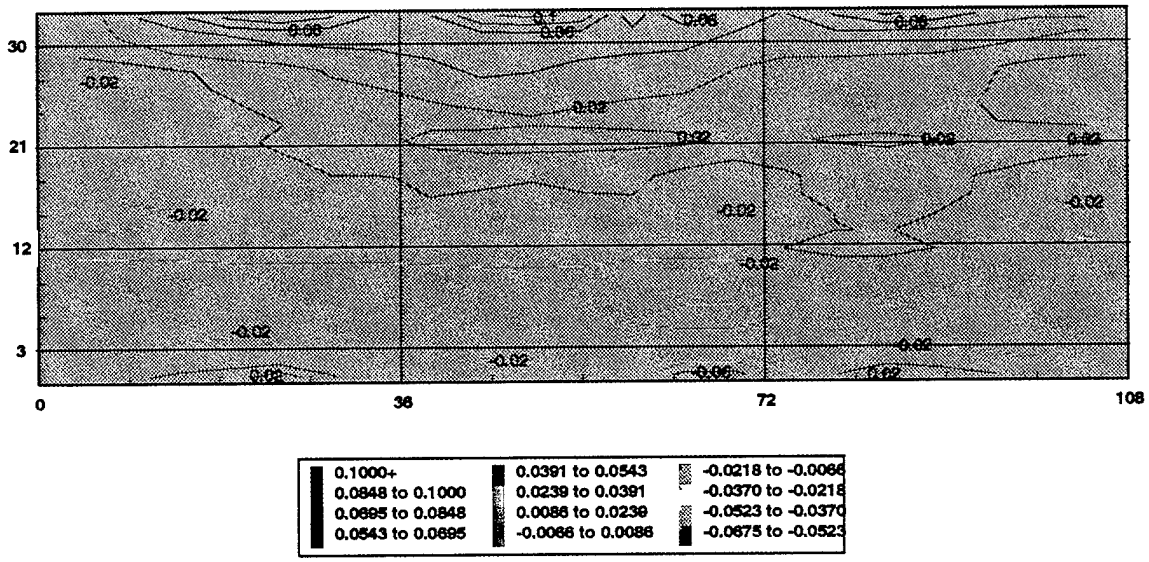


Figure 27a - Contour Plot of Initial Deflections for Grillage 1094

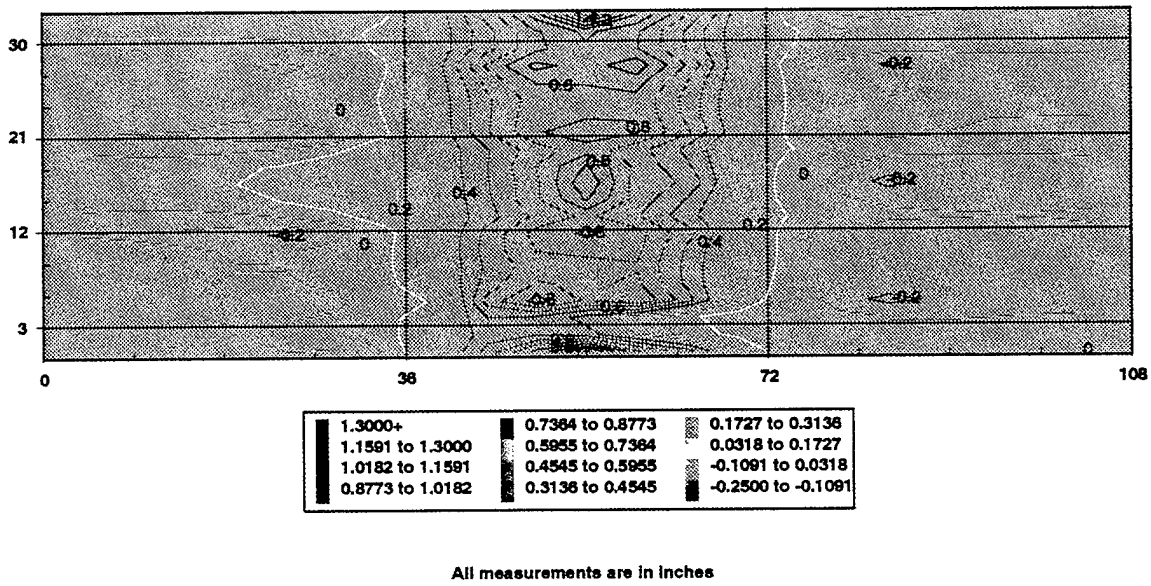


Figure 27b - Contour Plot of Final Deflections for Grillage 1094

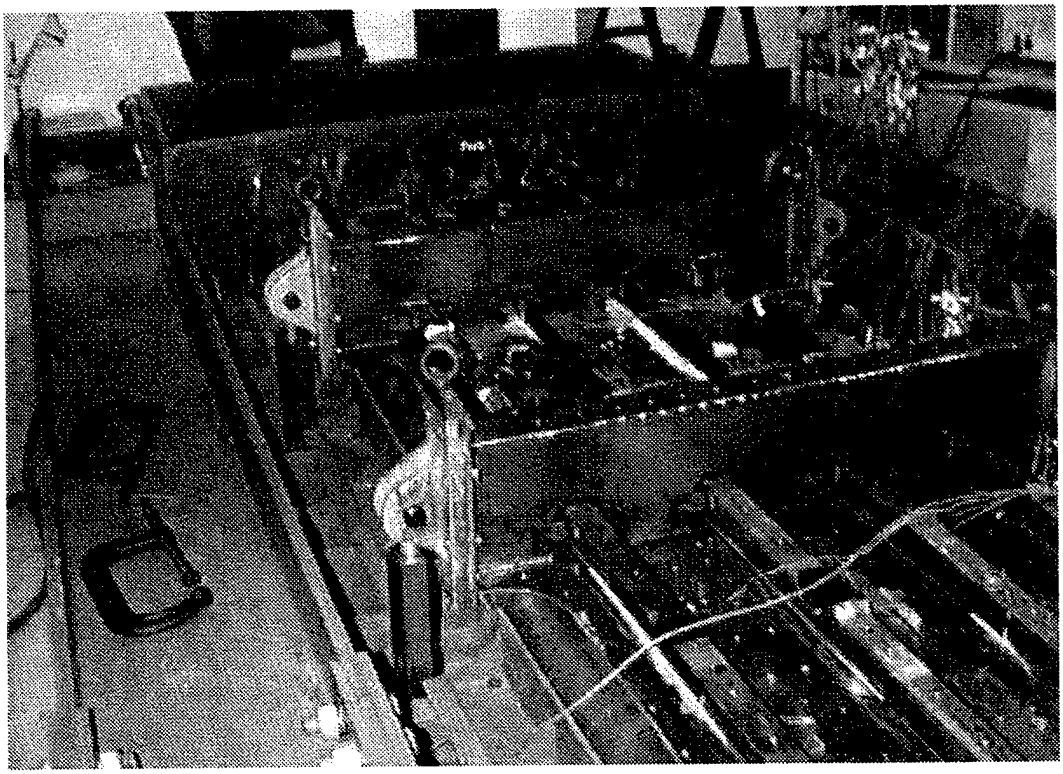

Figure 28a - Grillage 0595 in Test Fixture After Collapse

Figure 28b - Center Bay of Grillage 0595 Showing Stiffener and Plate Deformation

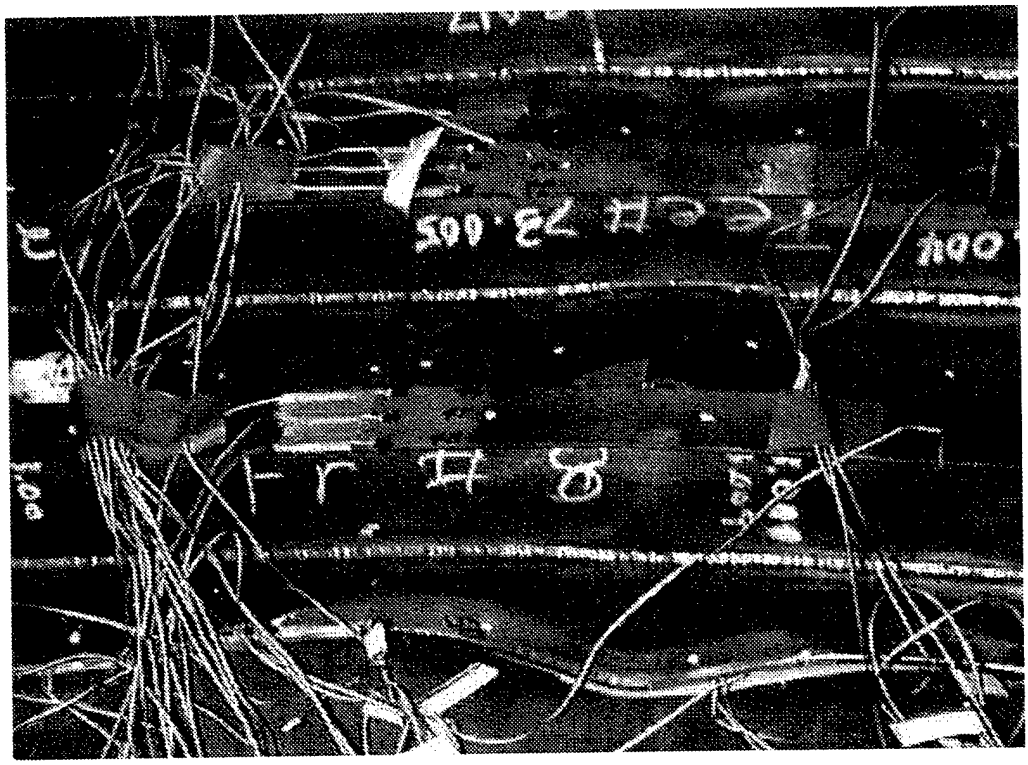

Figure 28c - Detail of Plate and Stiffener Deformations on Grillage 0595

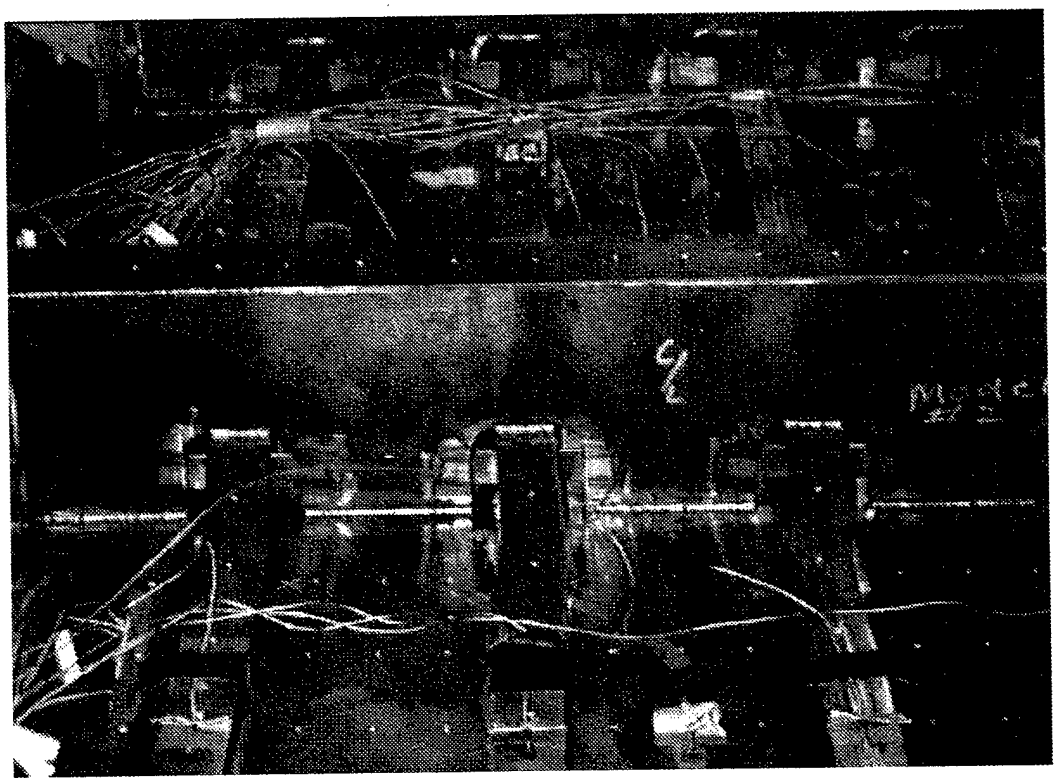

Figure 28d - Stiffener Failure in the Forward Bay of Grillage 0595

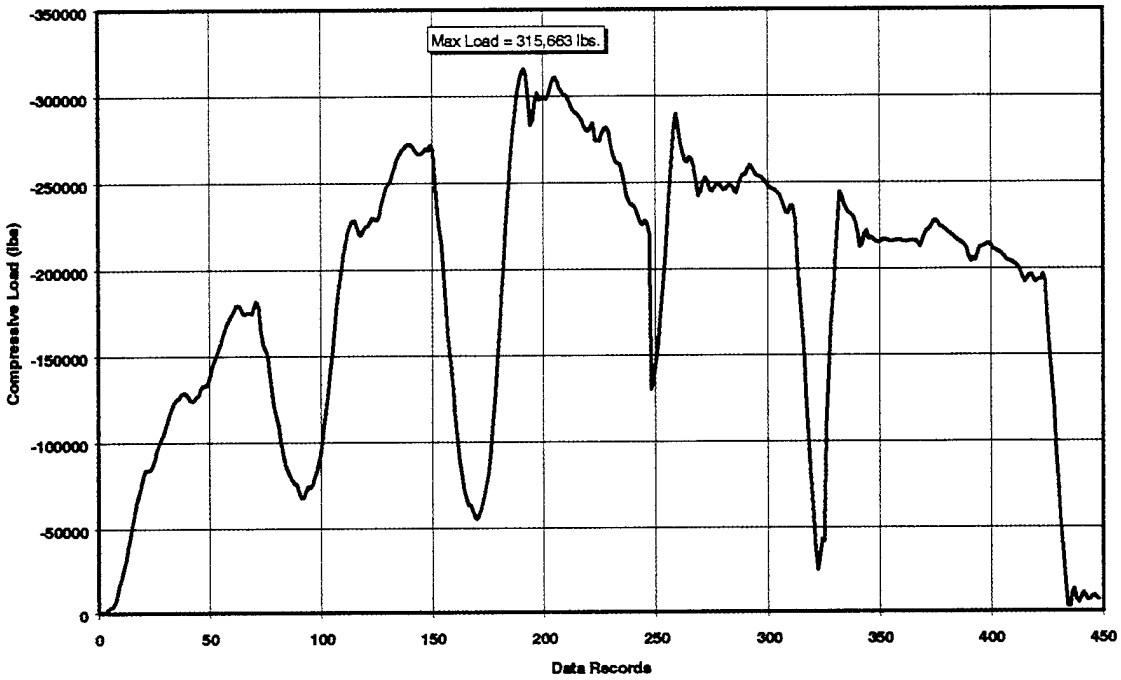


Figure 29a - Load History for Grillage 0595

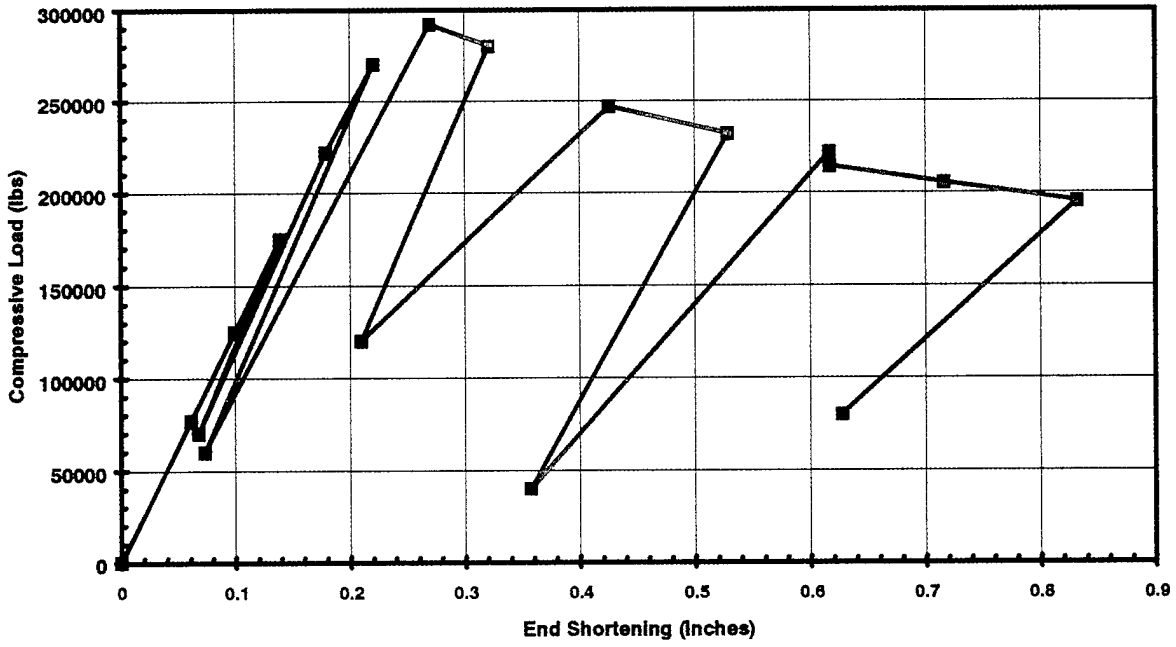


Figure 29b - Load vs. End Shortening for Grillage 0595

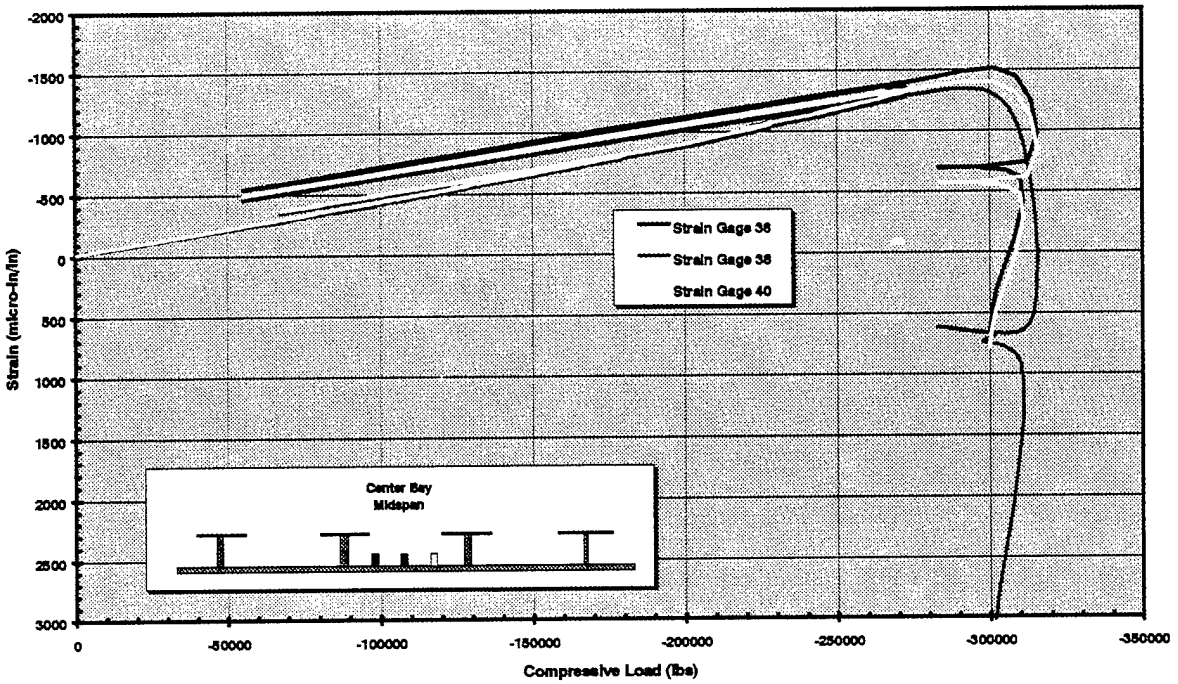


Figure 30a - Measure Strains in the Center Bay on the Stiffener Side on Grillage 0595

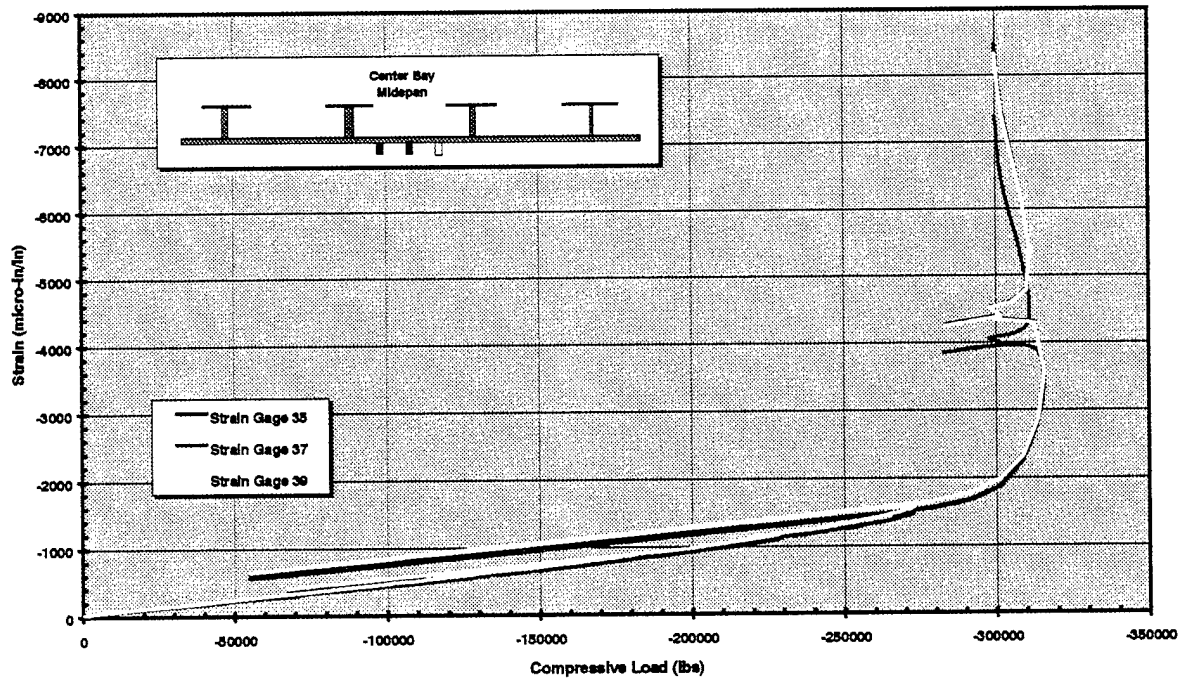


Figure 30b - Measured Strains in the Center Bay on the Plate Side of Grillage 0595

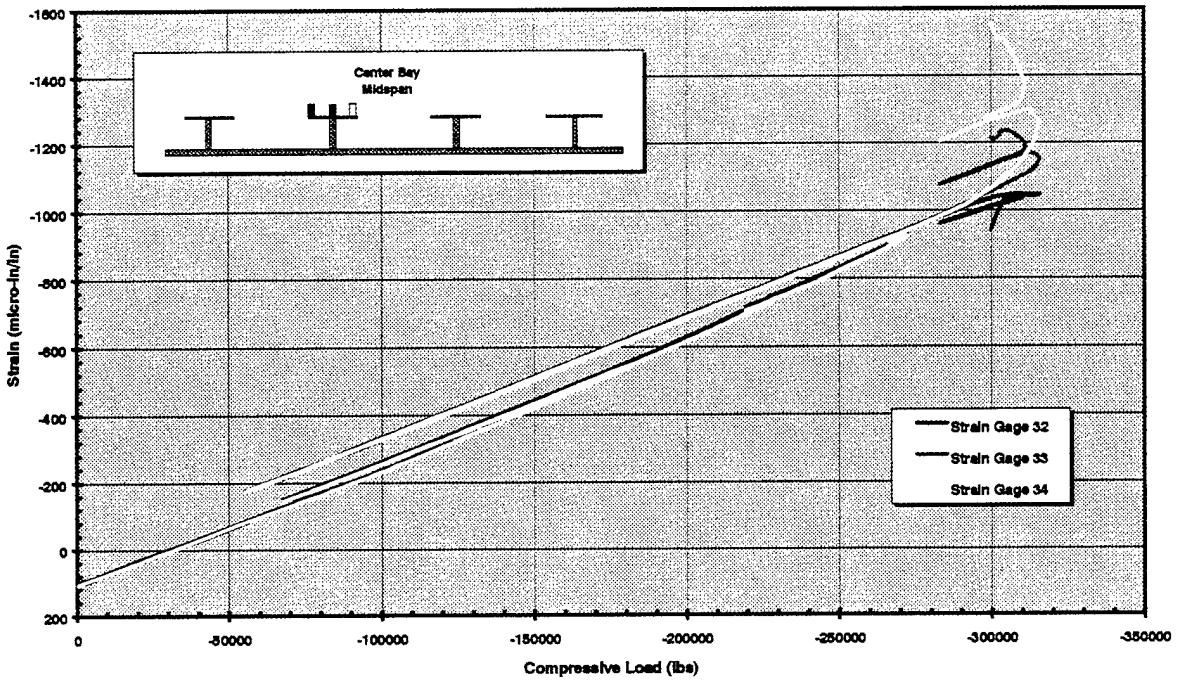


Figure 31a - Measured Strains on Port Stiffener - Grillage 0595

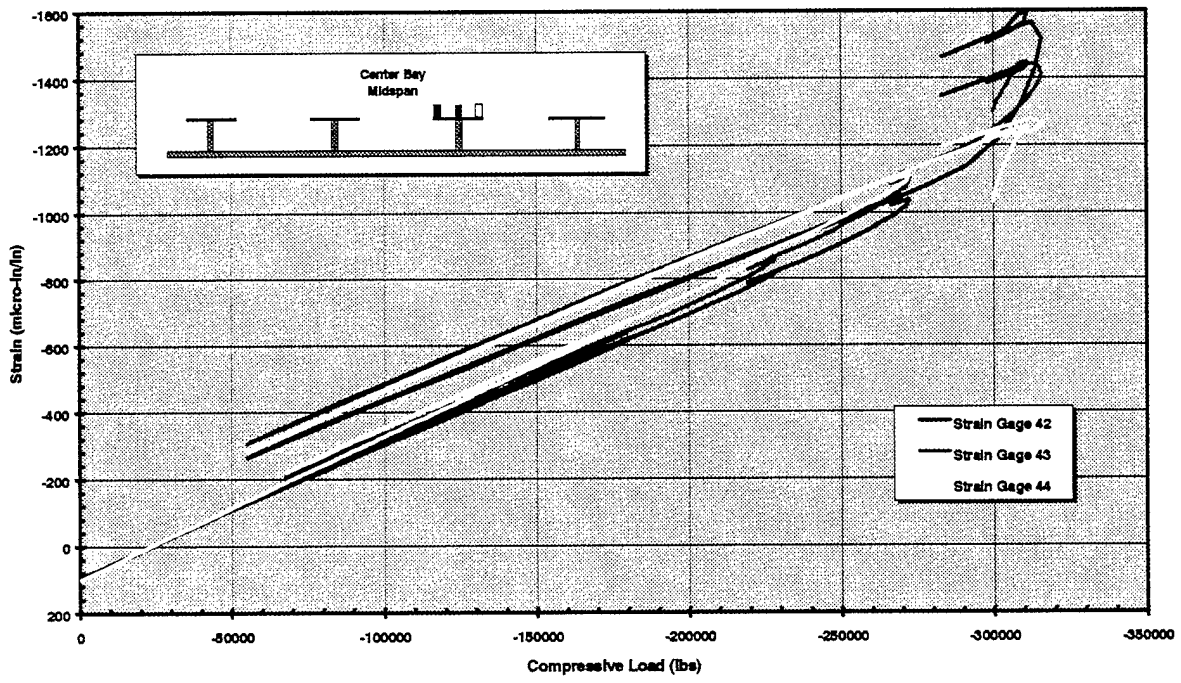


Figure 31b - Measured Strains on Stbd. Stiffener - Grillage 0595

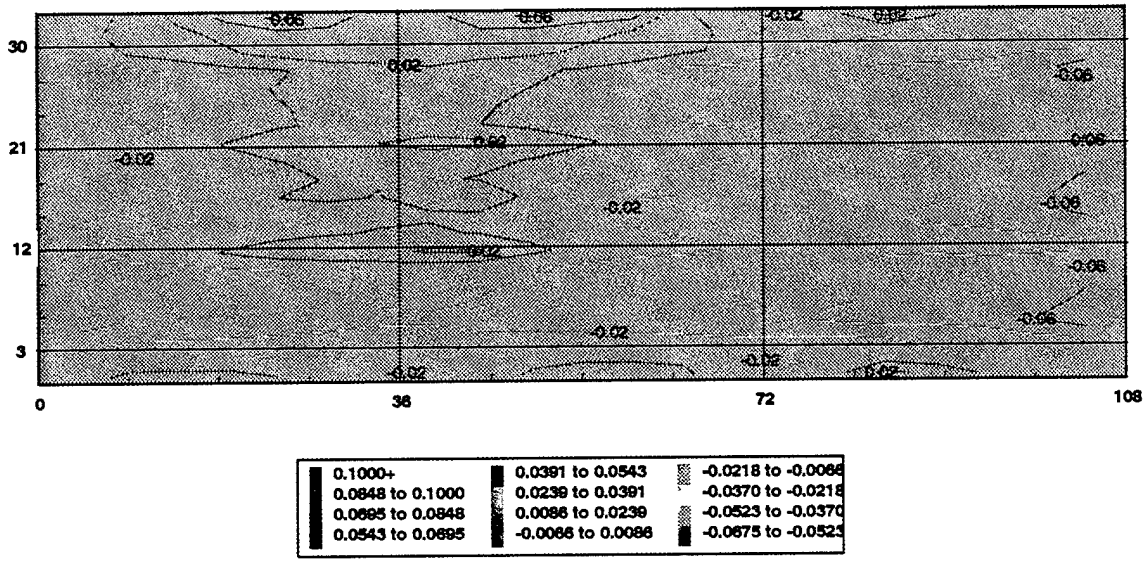


Figure 32a - Contour Plot of Initial Deflections for Grillage 0595

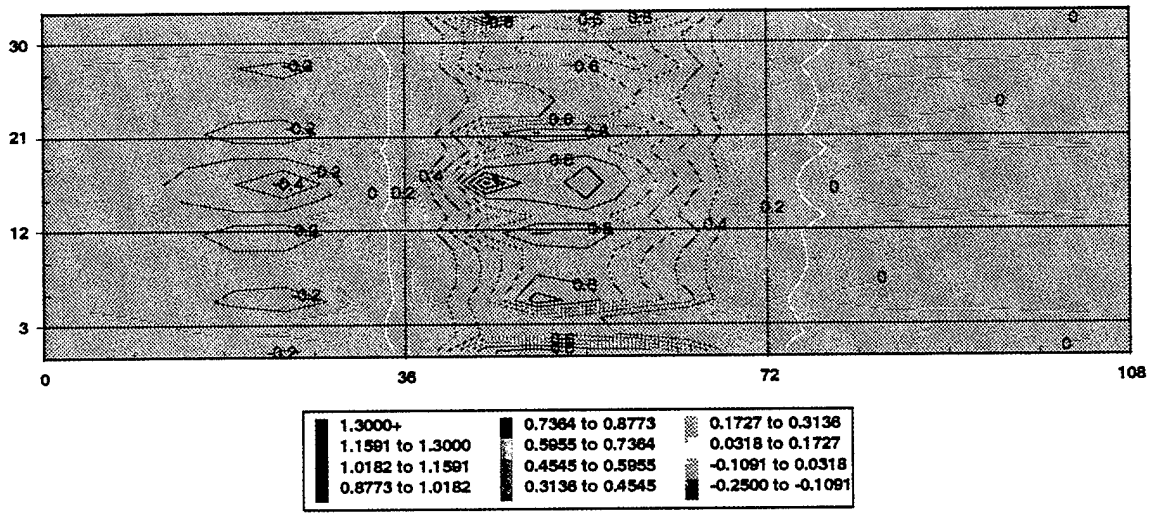


Figure 32b - Contour Plot of Final Deflections for Grillage 0595

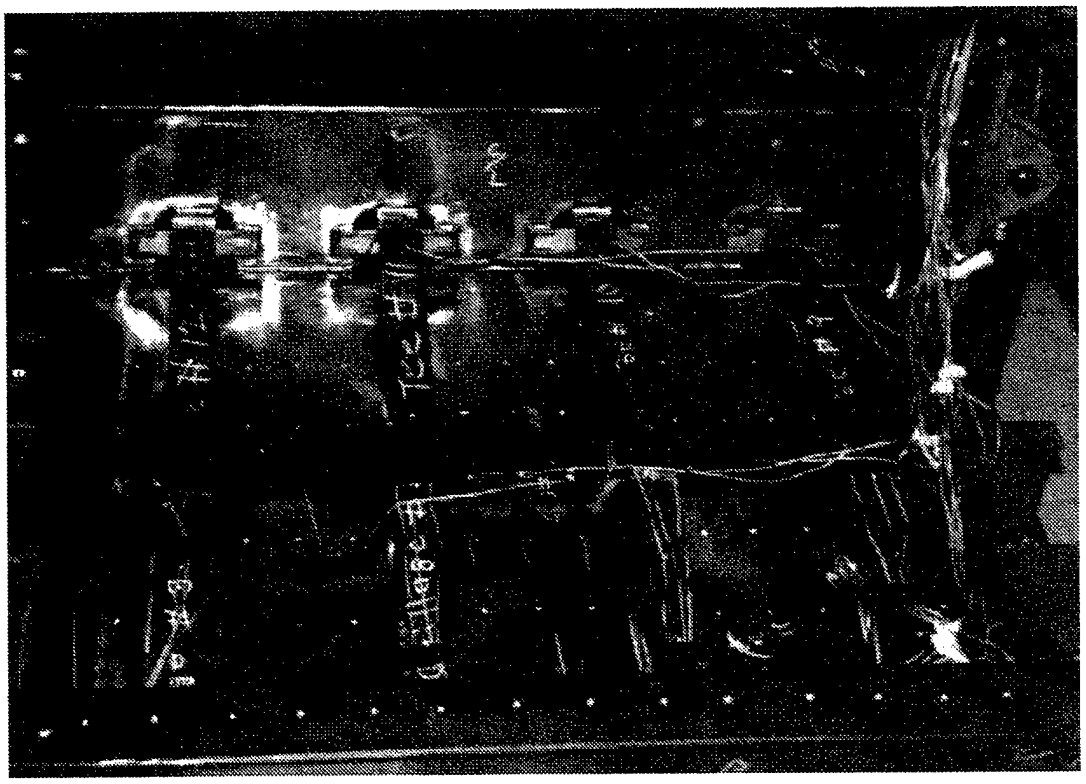

Figure 33a - Center Bay of Grillage 0695 After Collapse

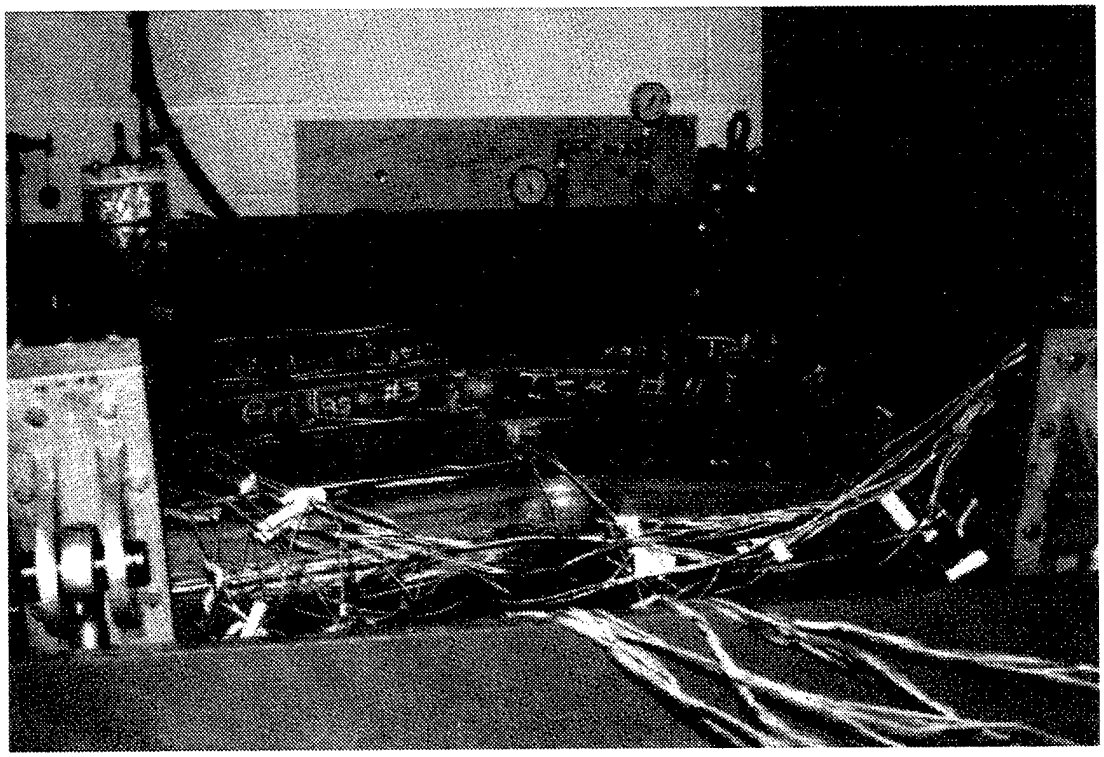

Figure 33b - Starboard Side of Grillage 0695 Showing Stiffener Deformation

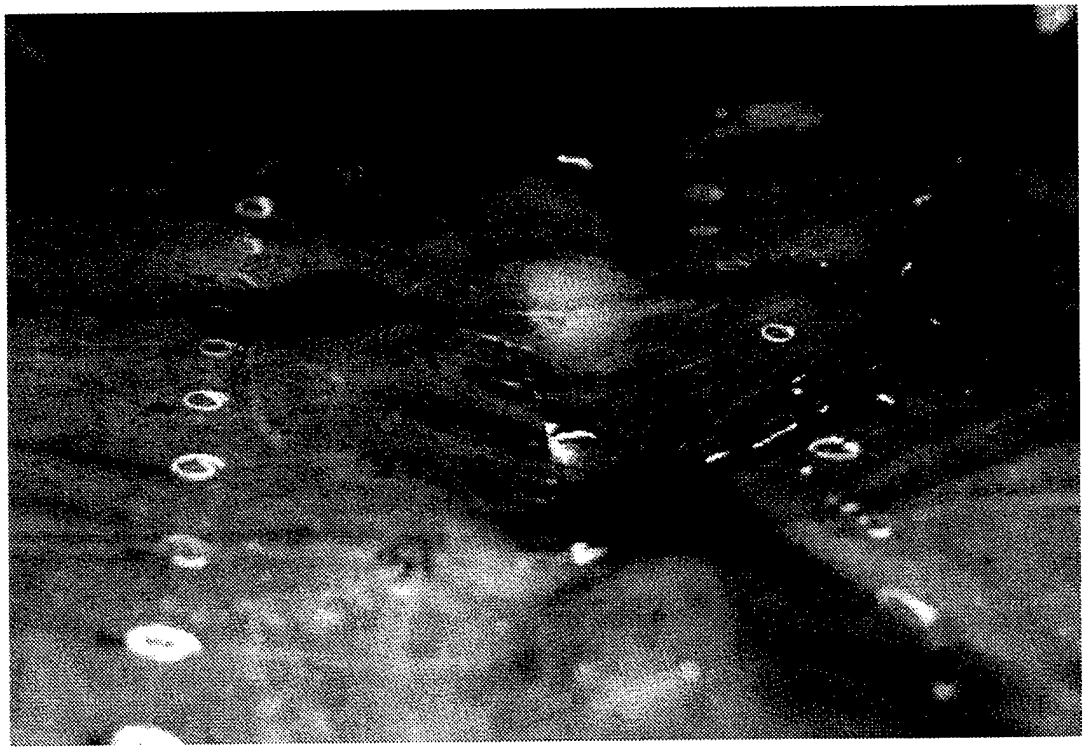

Figure 33c - Plate Side Showing Deformations on Grillage 0695

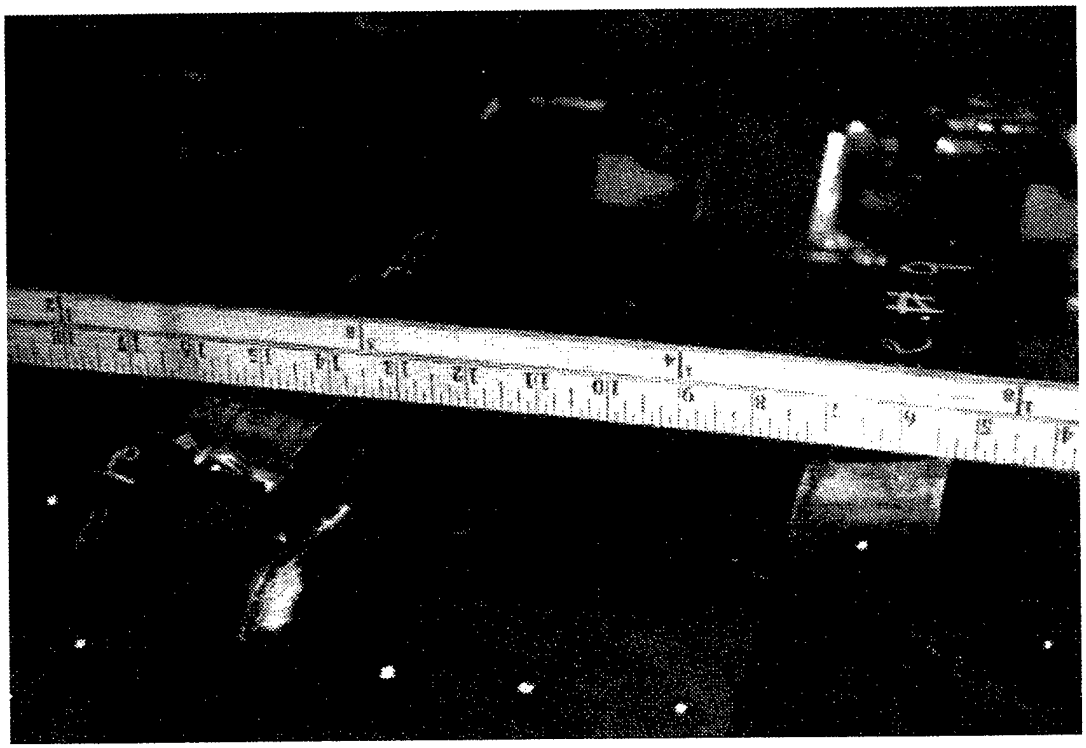

Figure 33d - Stiffener Rotation in the Center Bay of Grillage 0695

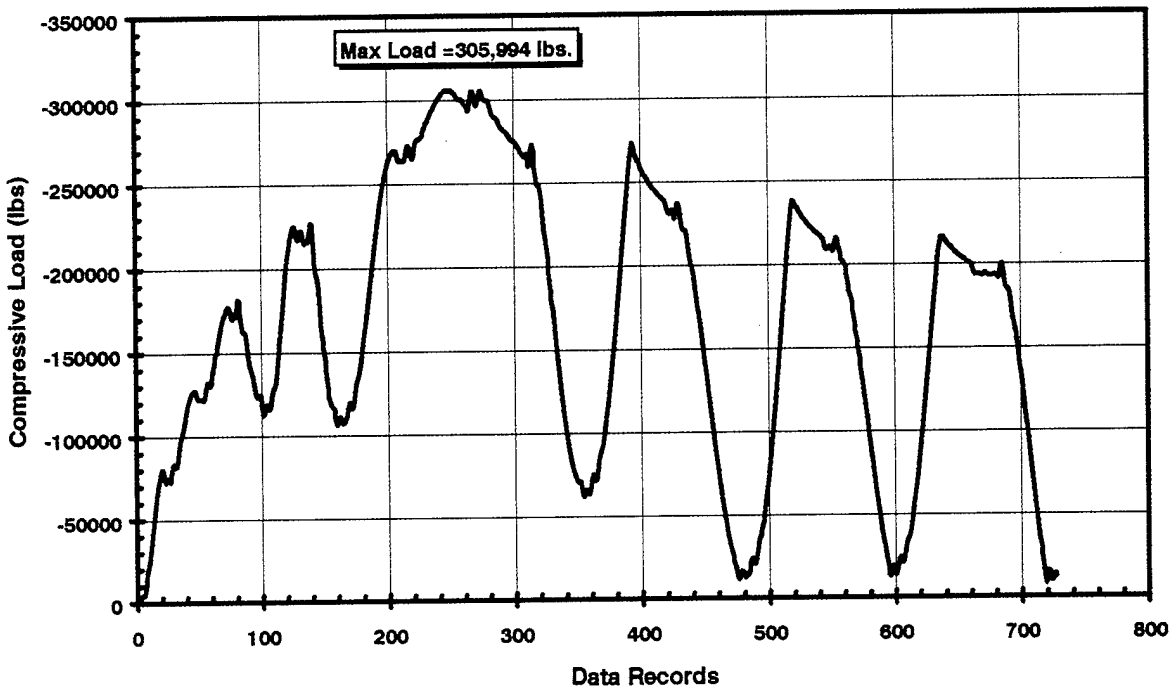


Figure 34a - Load History for Grillage 0695

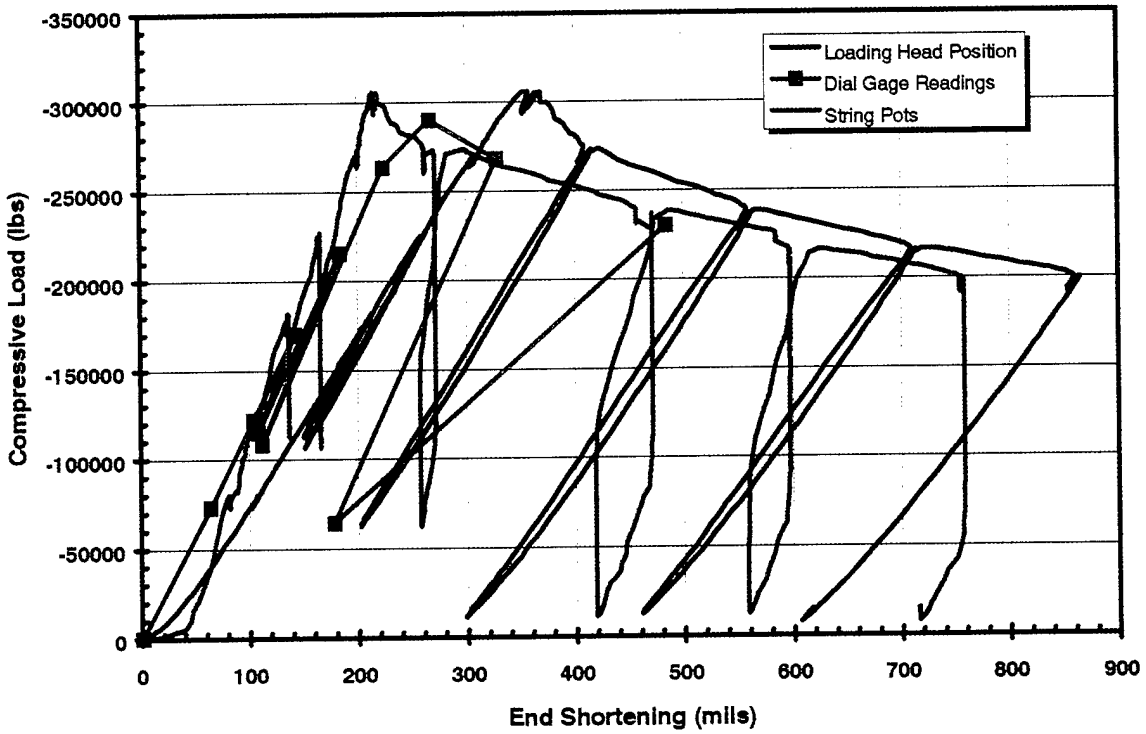


Figure 34b - Load vs. End Shortening for Grillage 0695

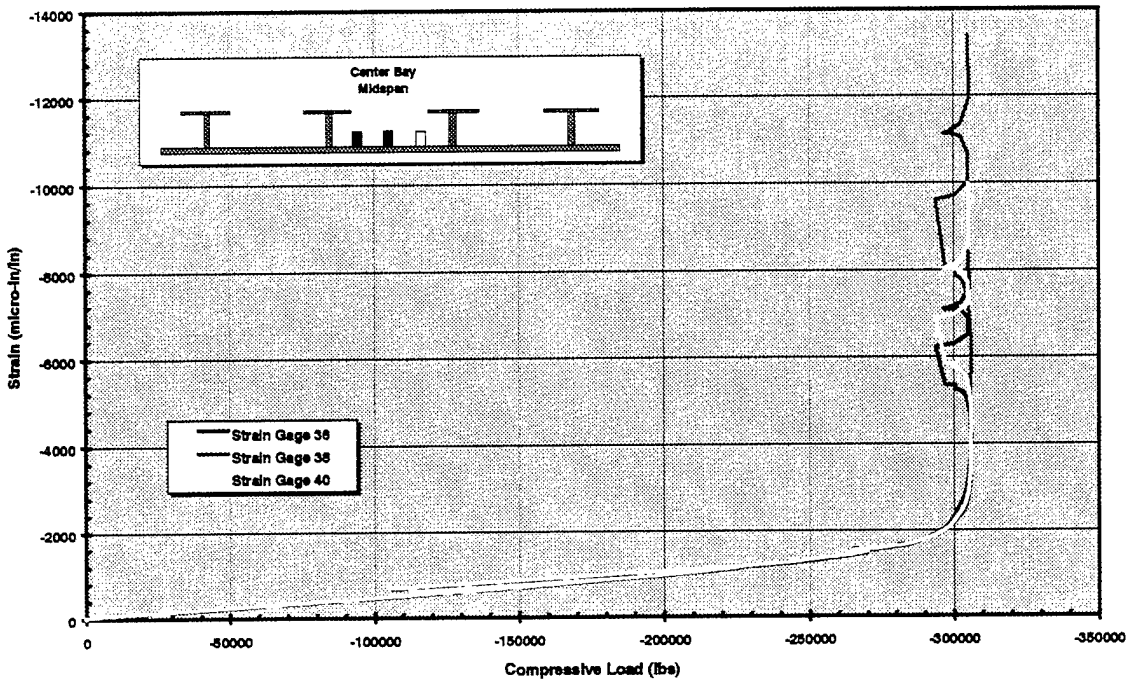


Figure 35a - Measure Strains in the Center Bay on the Stiffener Side on Grillage 0695

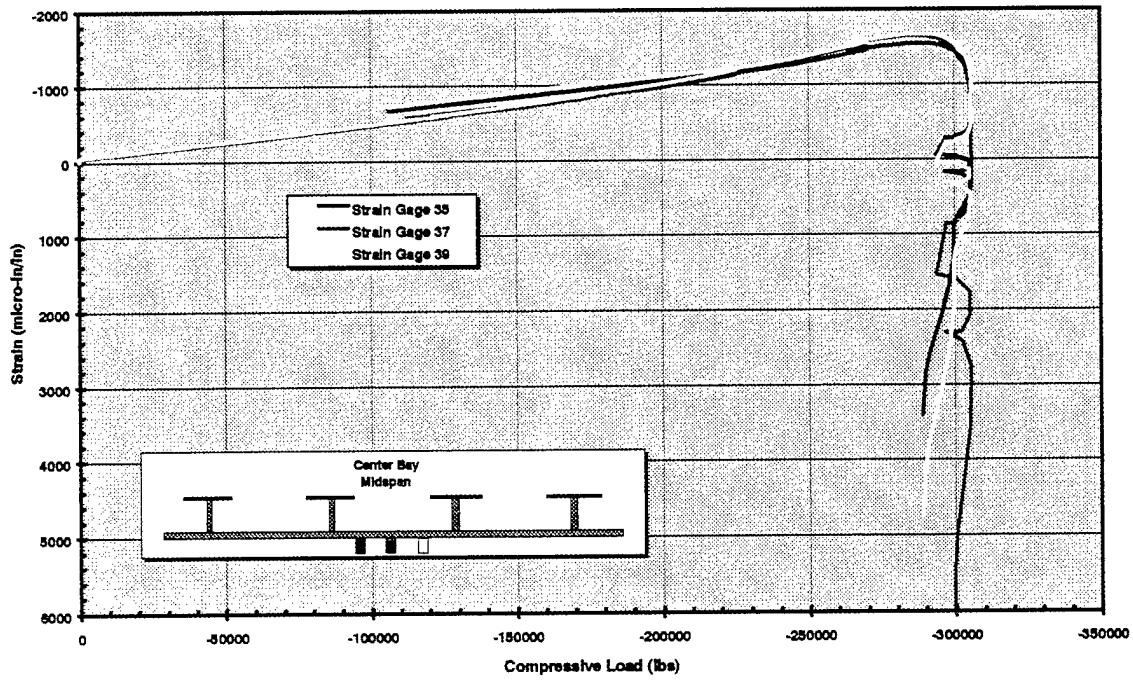


Figure 35b - Measured Strains in the Center Bay on the Plate Side of Grillage 0695

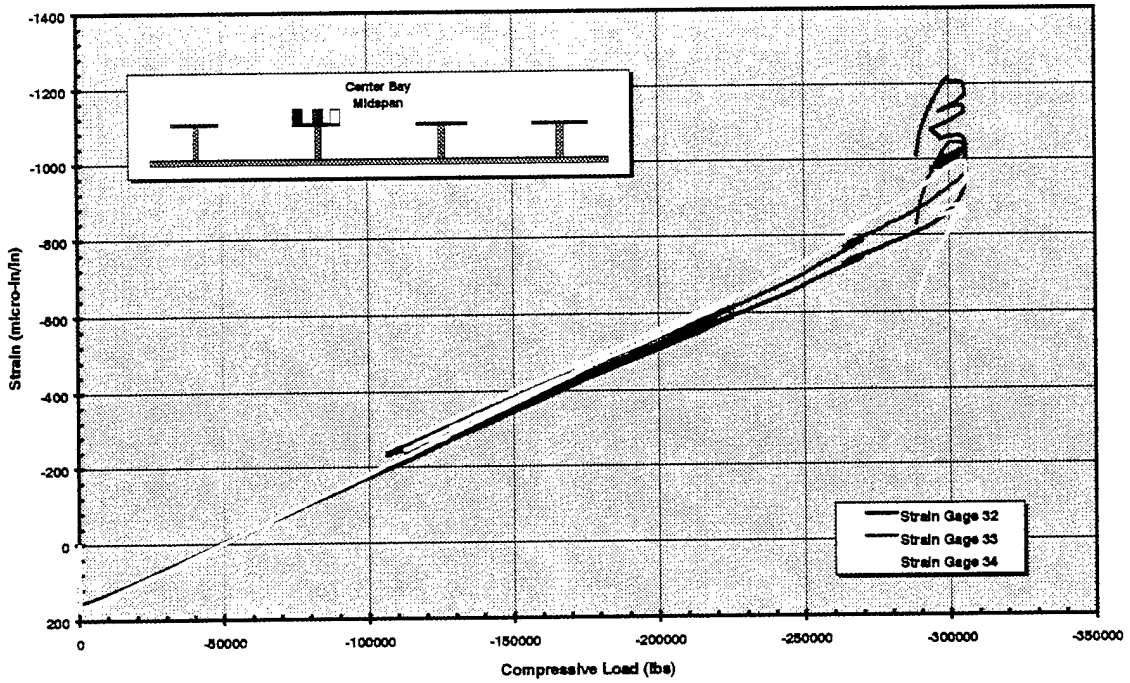


Figure 36a - Measured Strains on Port Stiffener - Grillage 0695

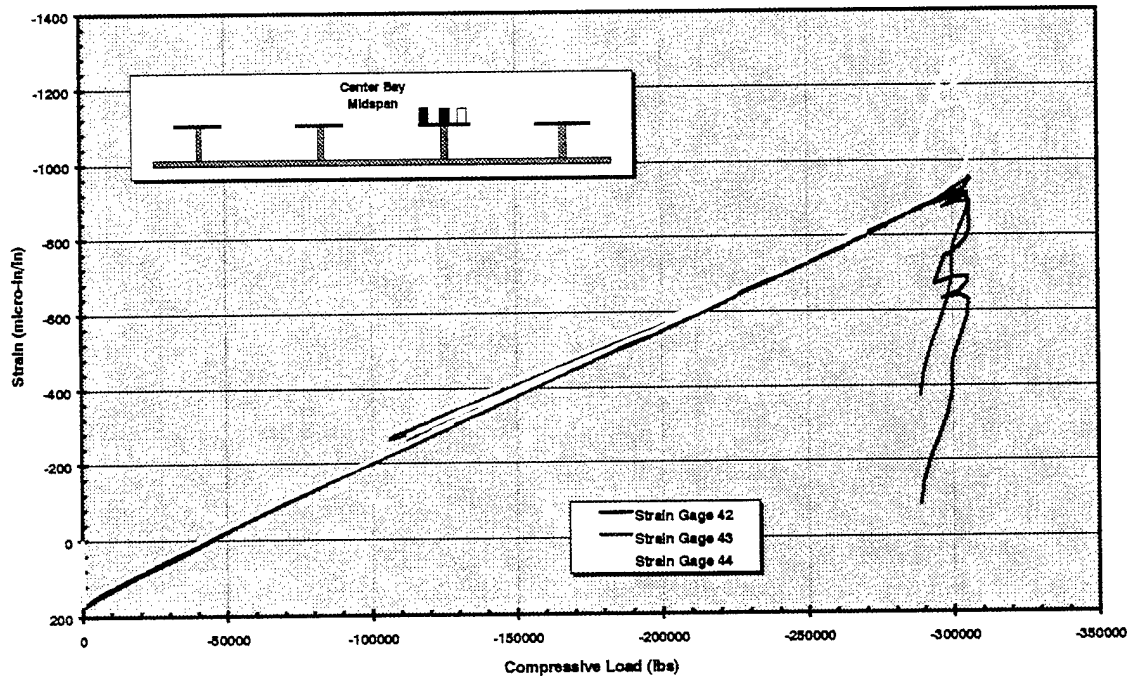


Figure 36b - Measured Strains on Stbd. Stiffener - Grillage 0695

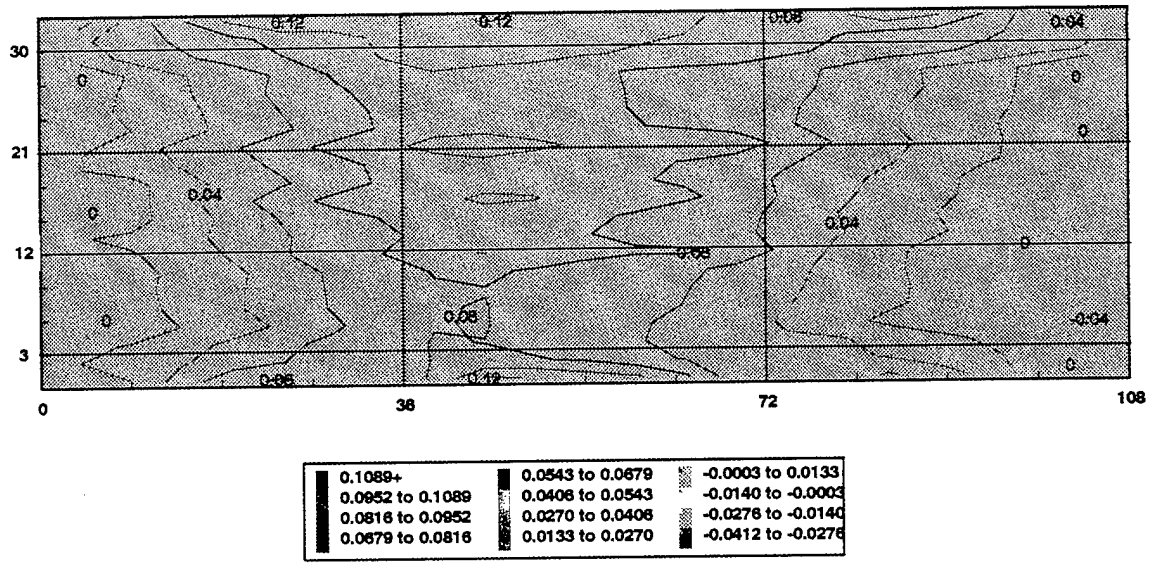


Figure 37a - Contour Plot of Initial Deflections for Grillage 0695

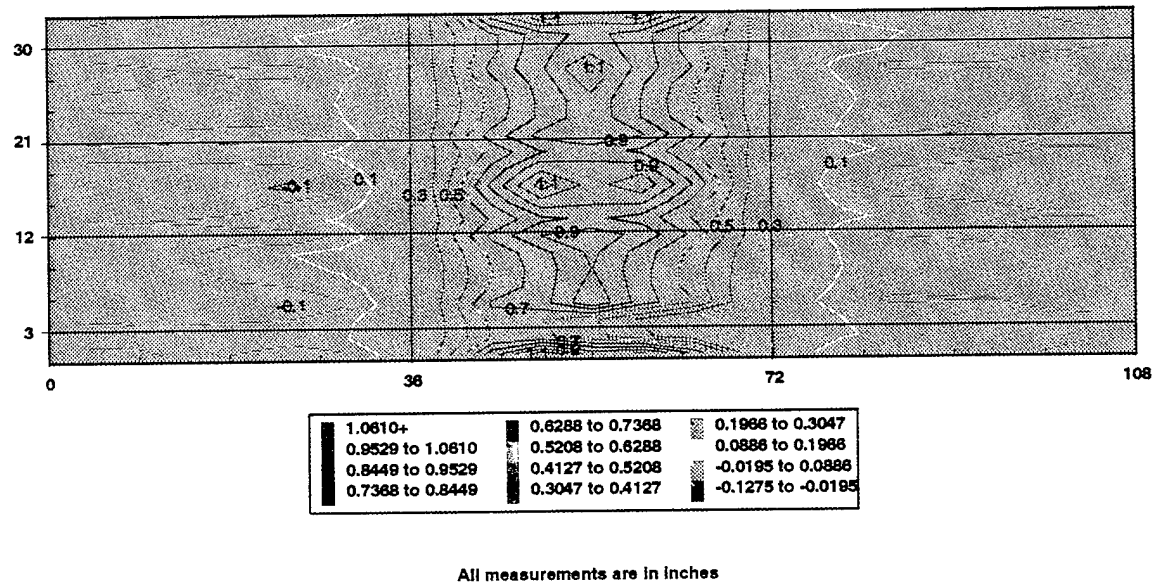


Figure 37b - Contour Plot of Final Deflections for Grillage 0695

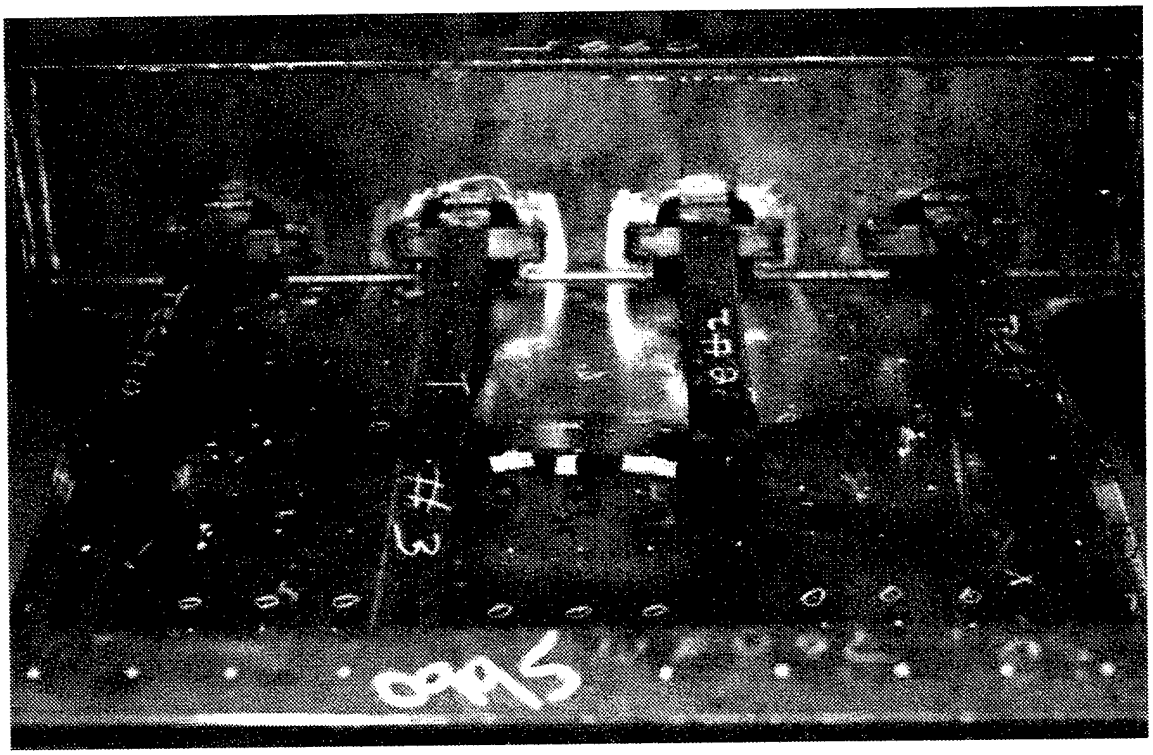

Figure 38a - Center Bay of Grillage 0995 in Test Fixture After Collapse

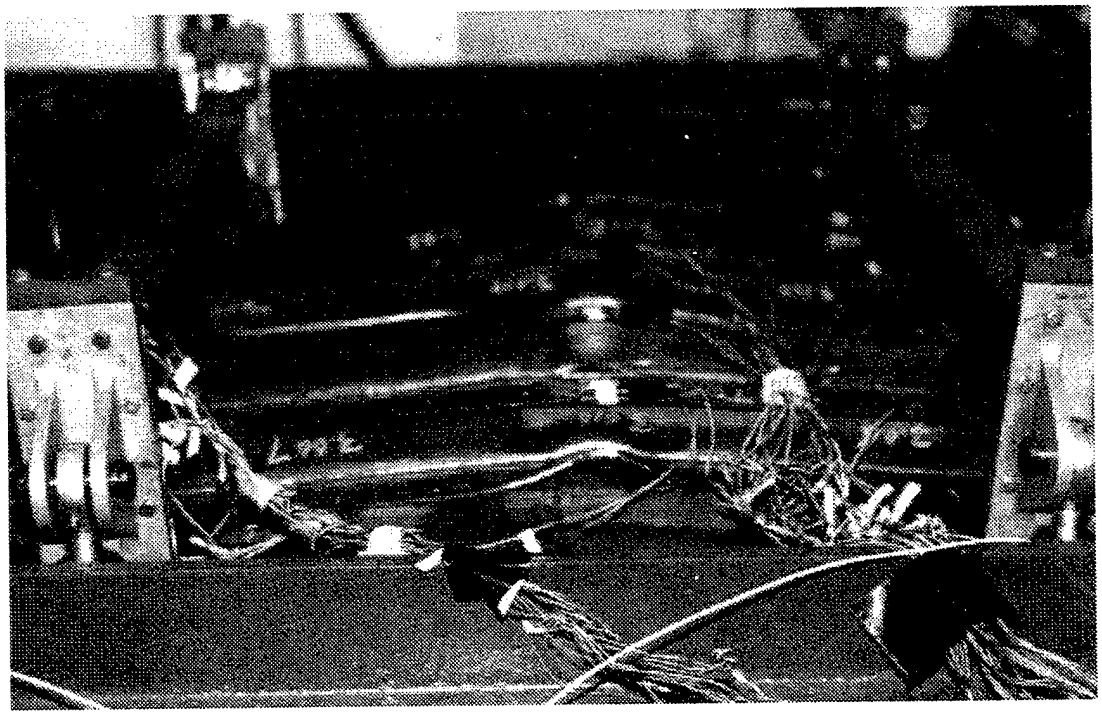

Figure 38b - Center Bay of Grillage 0995 Showing Stiffener and Plate Deformation

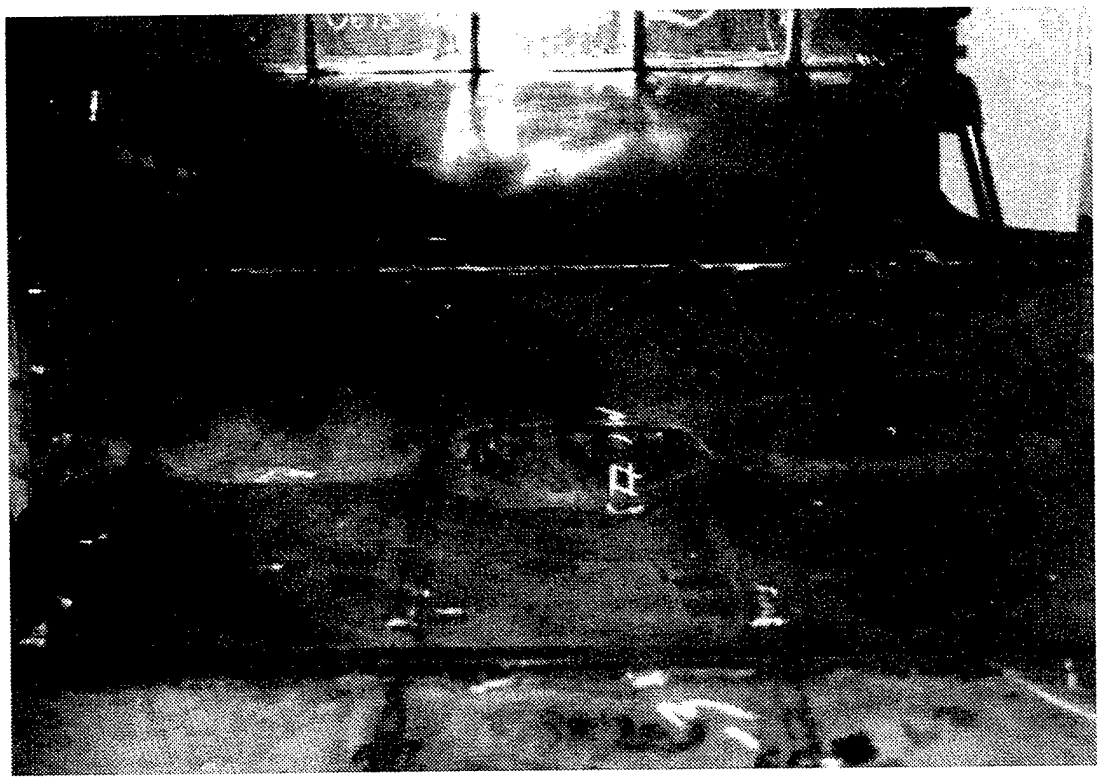

Figure 38c - Plate Deformations on Plating Side of Grillage 0995

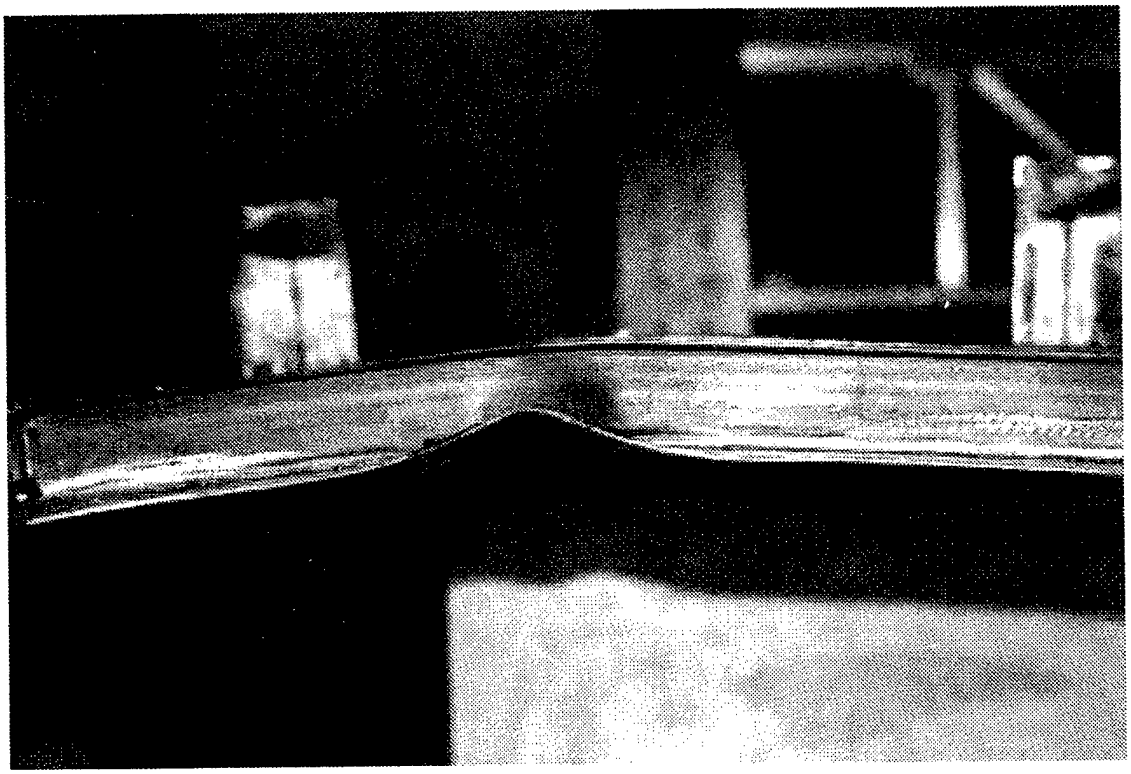

Figure 38d - Detail of Plate & Stiffener in the Center Bay of Grillage 0995

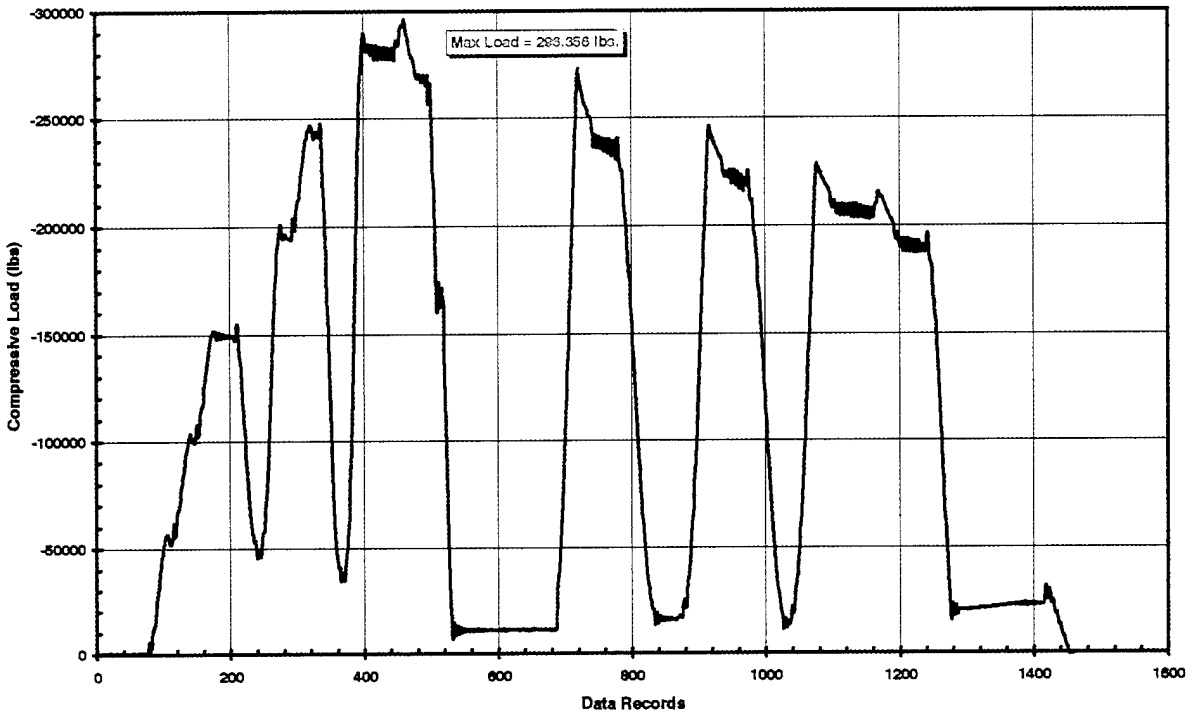


Figure 39a - Load History for Grillage 0995

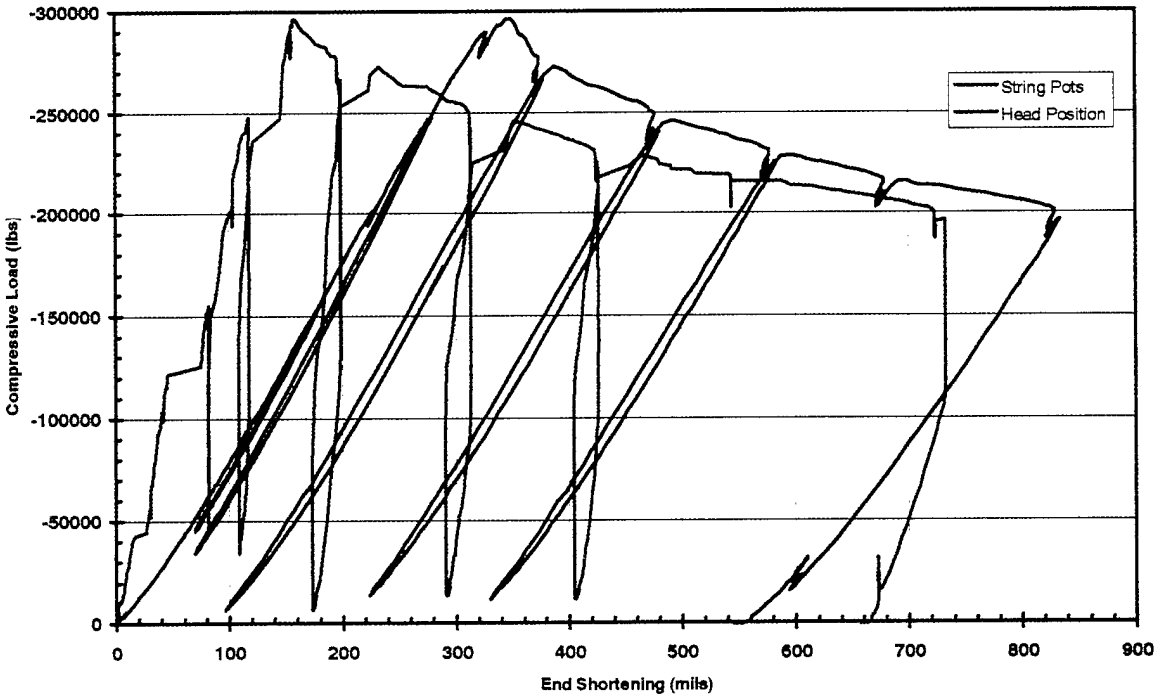


Figure 39b - Load vs. End Shortening for Grillage 0995

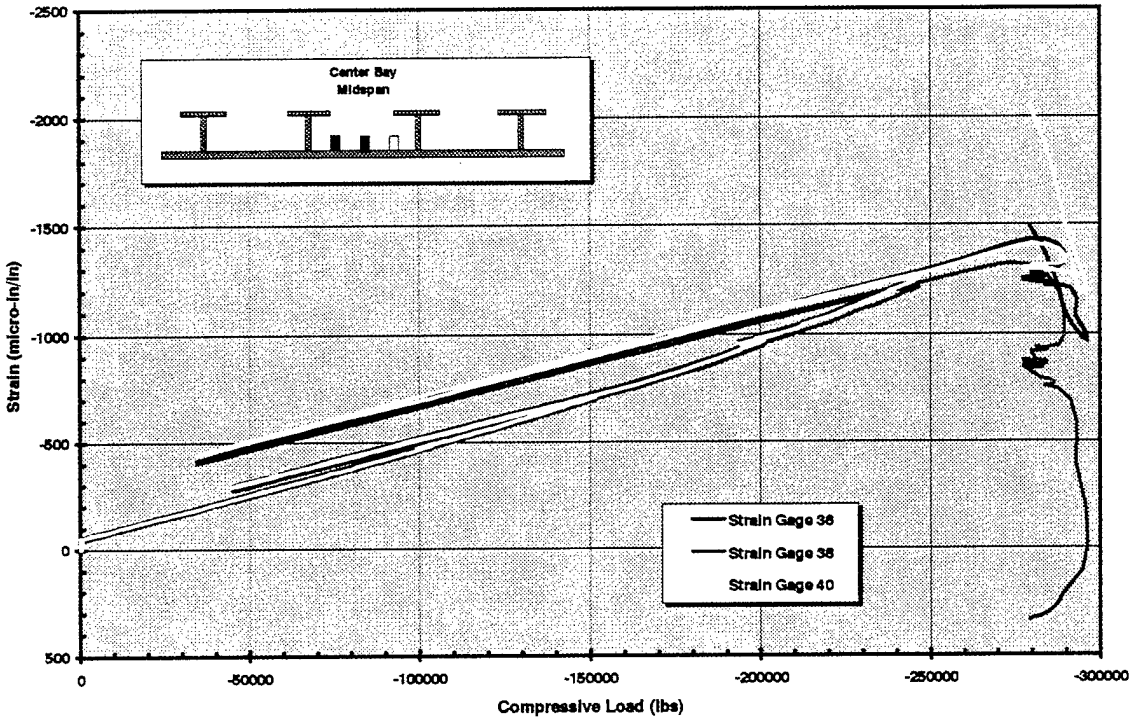


Figure 40a - Measure Strains in the Center Bay on the Stiffener Side on Grillage 0995

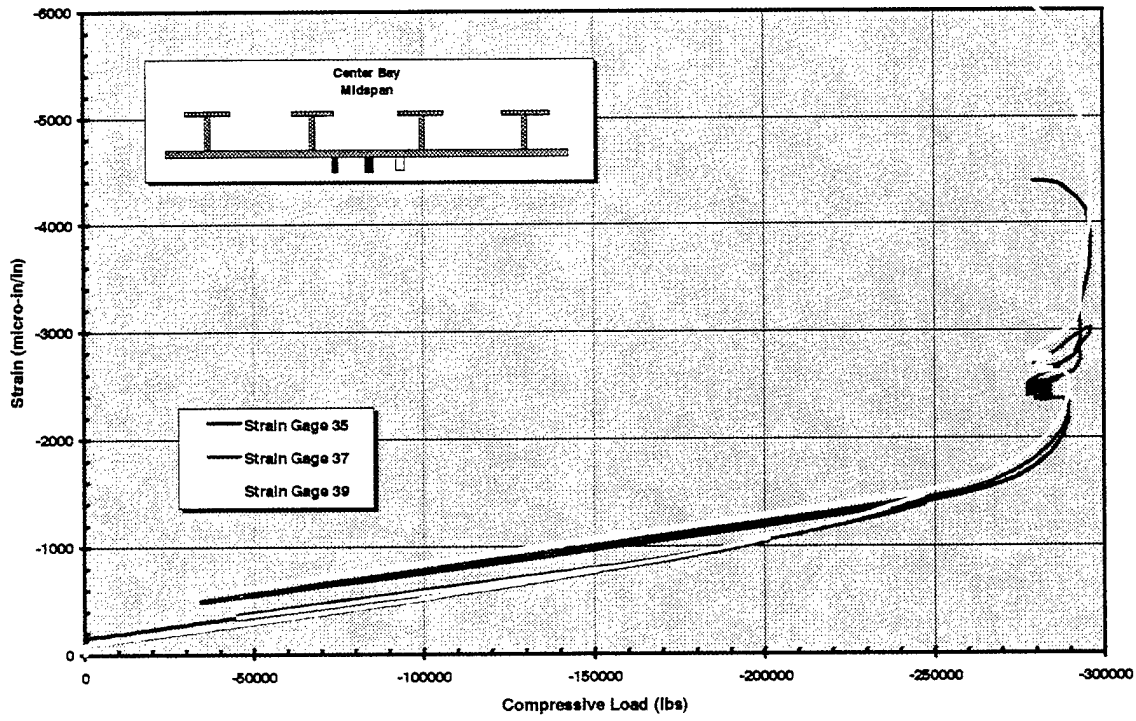


Figure 40b - Measured Strains in the Center Bay on the Plate Side of Grillage 0995

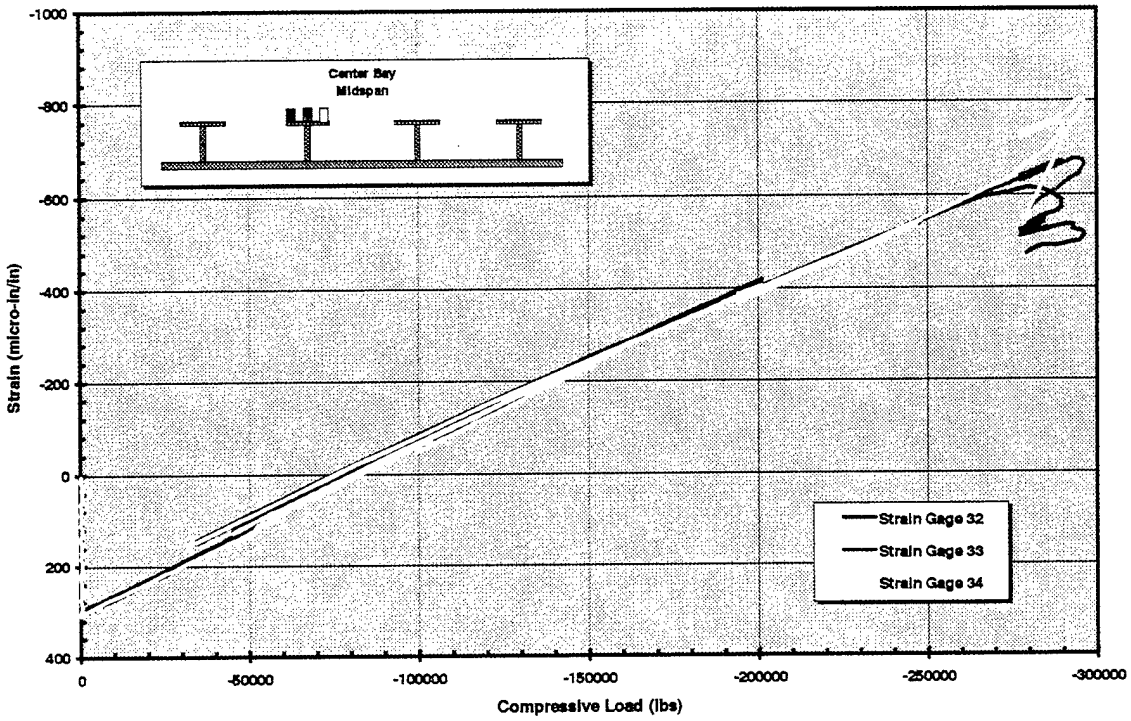


Figure 41a - Measured Strains on Port Stiffener - Grillage 0995

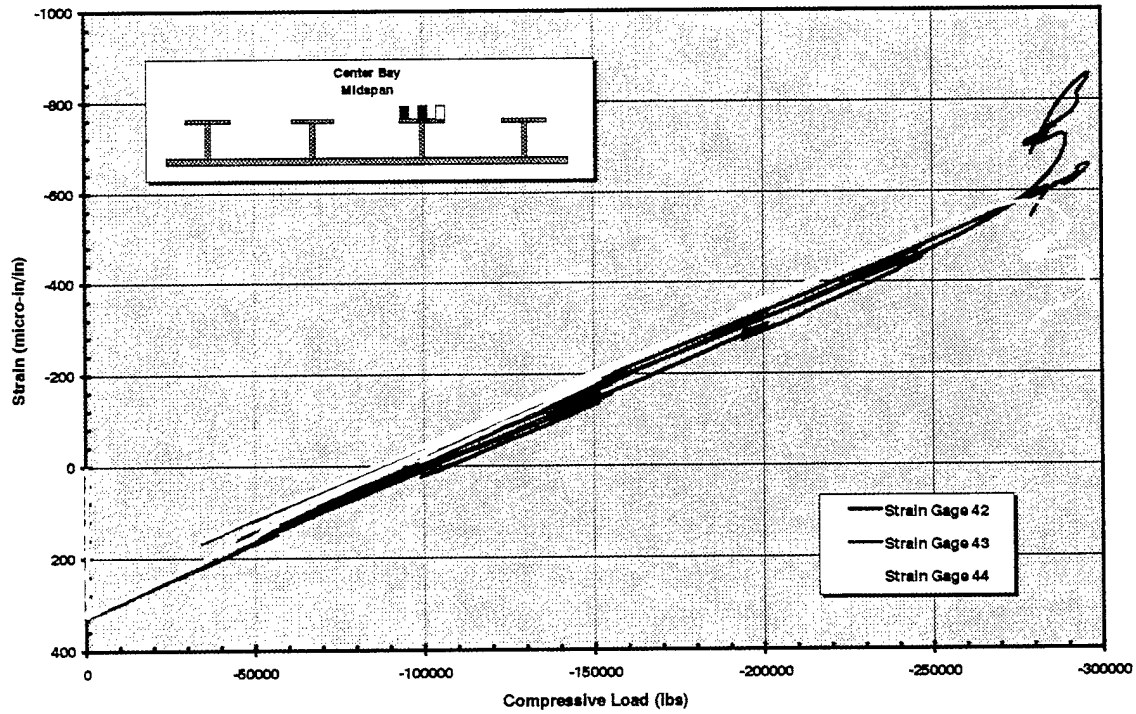


Figure 41b - Measured Strains on Stbd. Stiffener - Grillage 0995

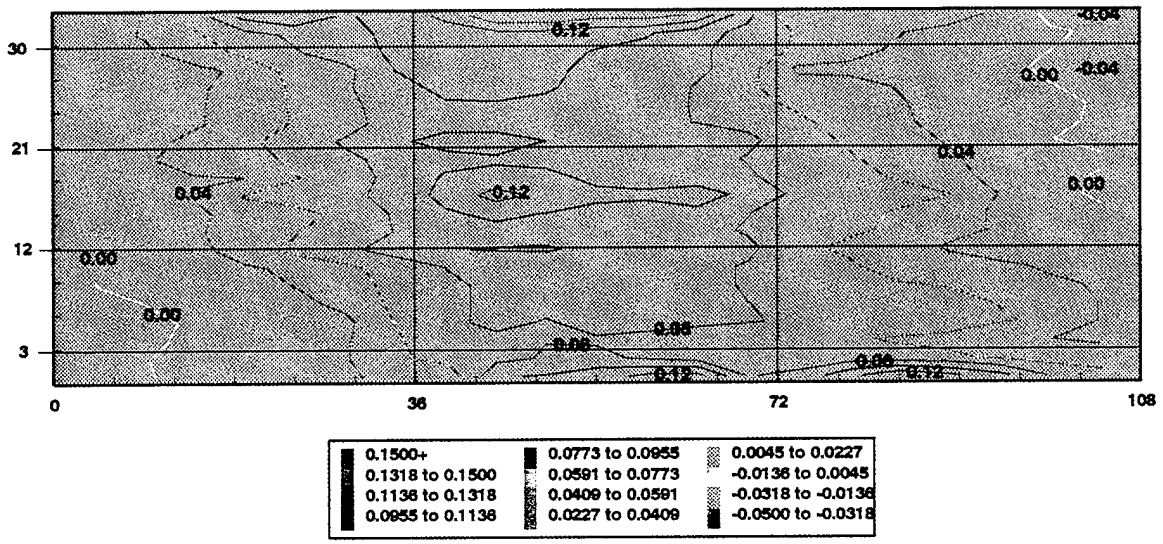


Figure 42a - Contour Plot of Initial Deflections for Grillage 0995

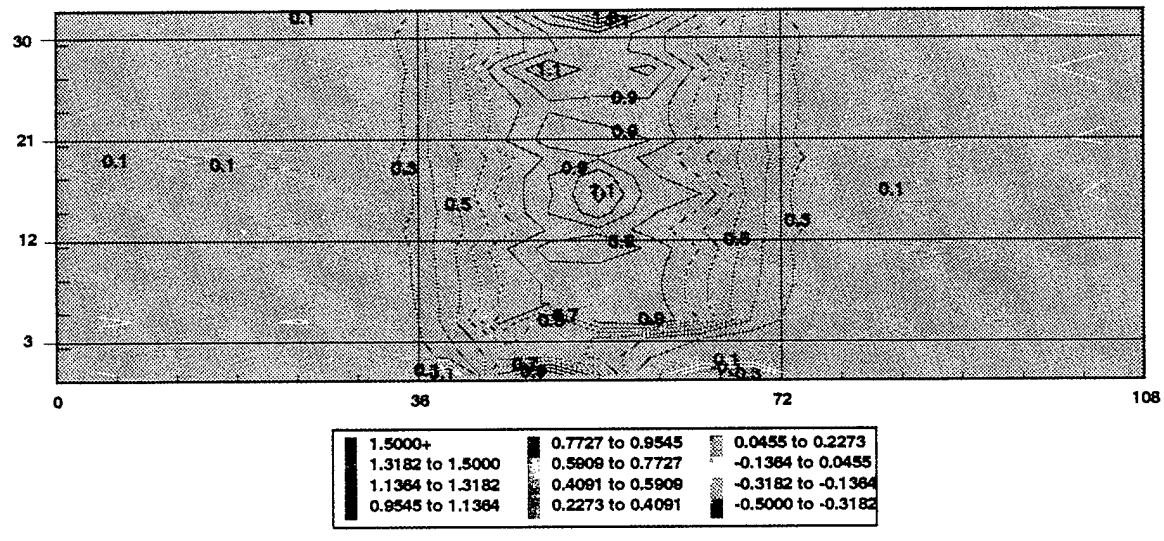


Figure 42b - Contour Plot of Final Deflections for Grillage 0995

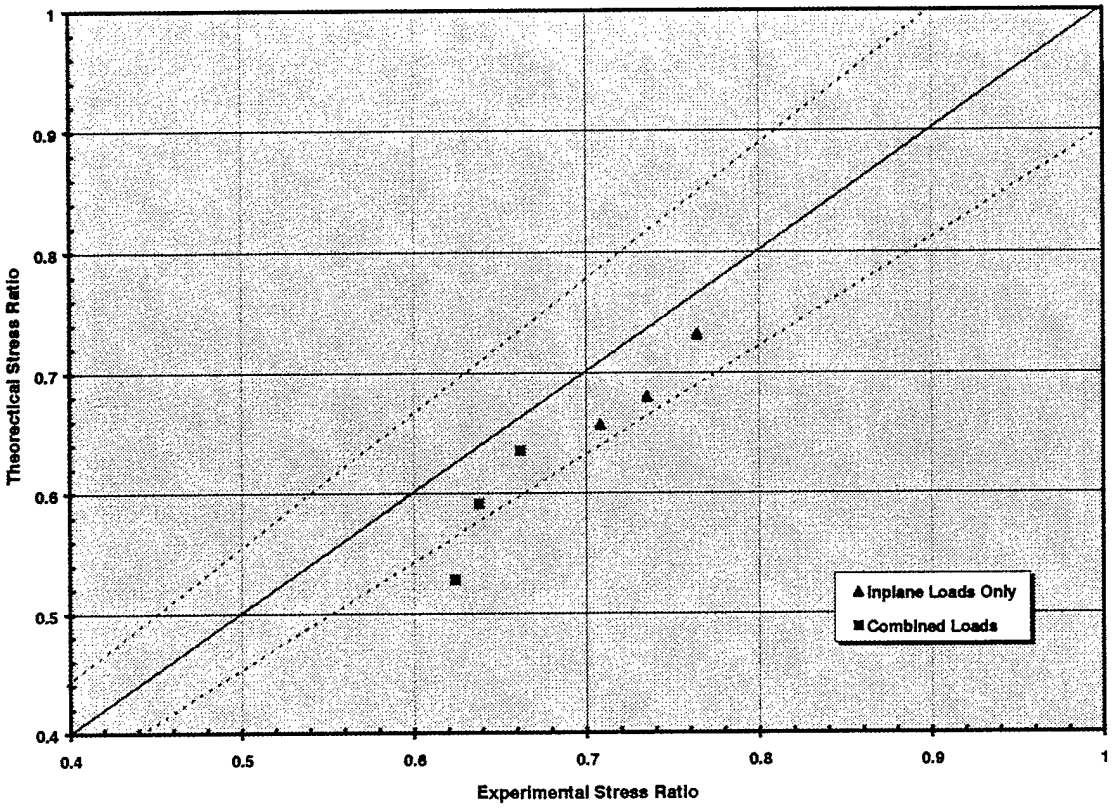


Figure 43 -Theory vs. Experiment for USNA Tests

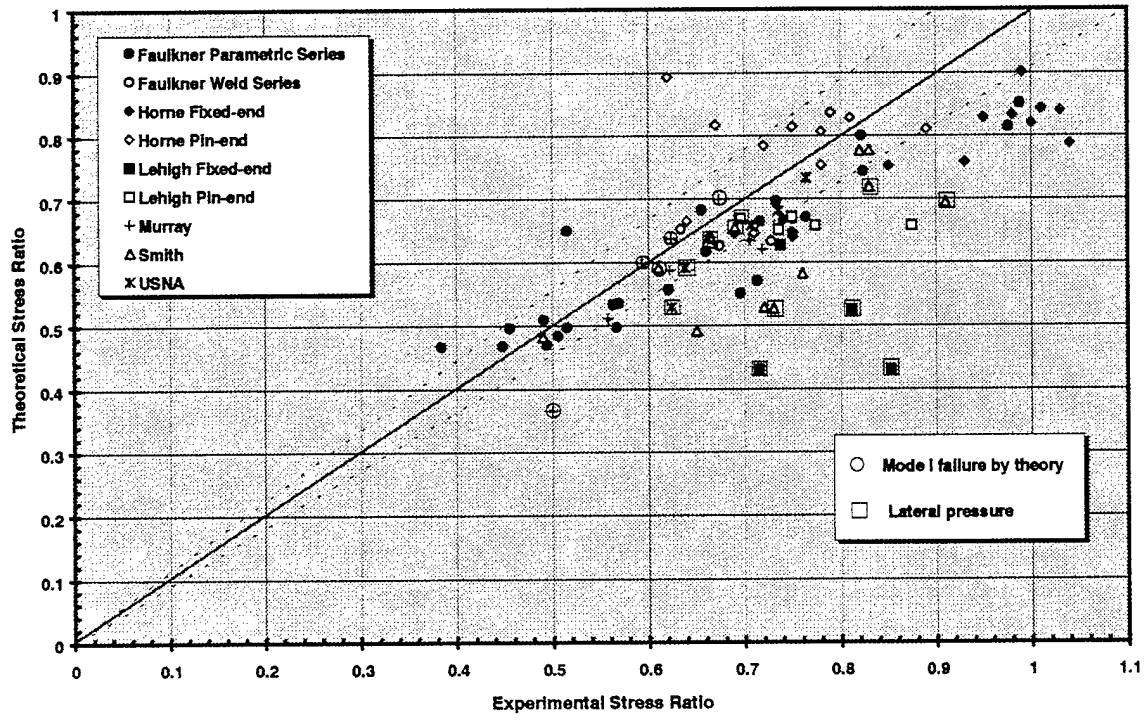


Figure 44 -Theory vs. Experiment for Test Database

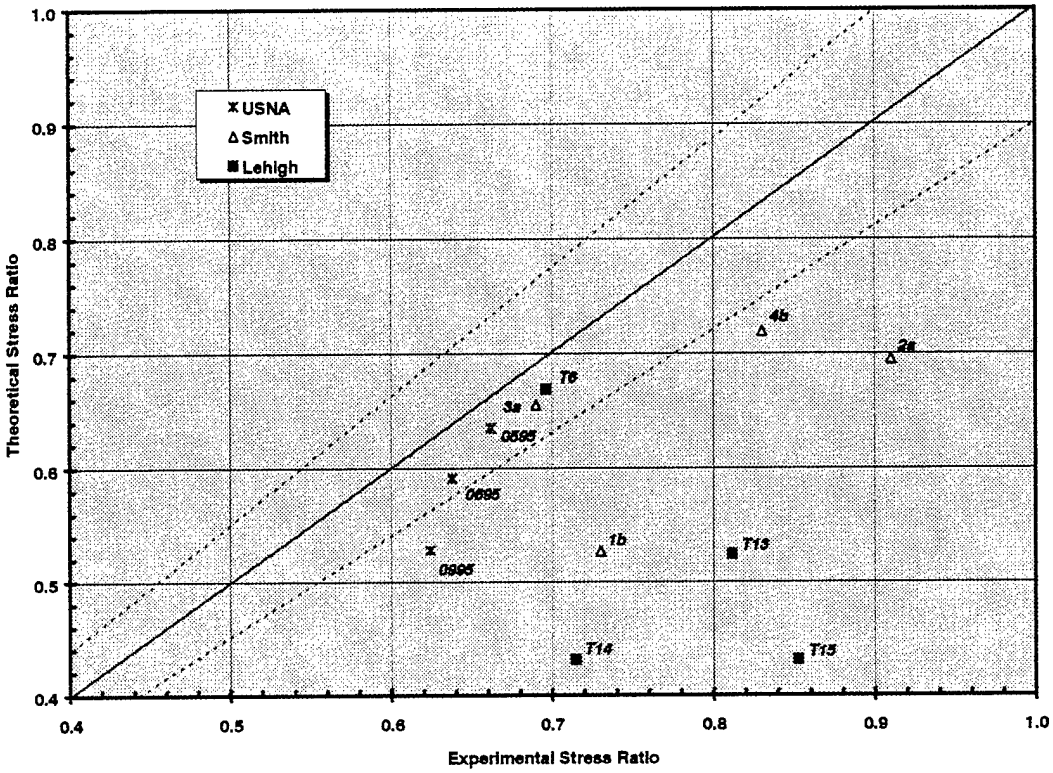


Figure 45 - Theory vs. Experiment for Combined Load Tests

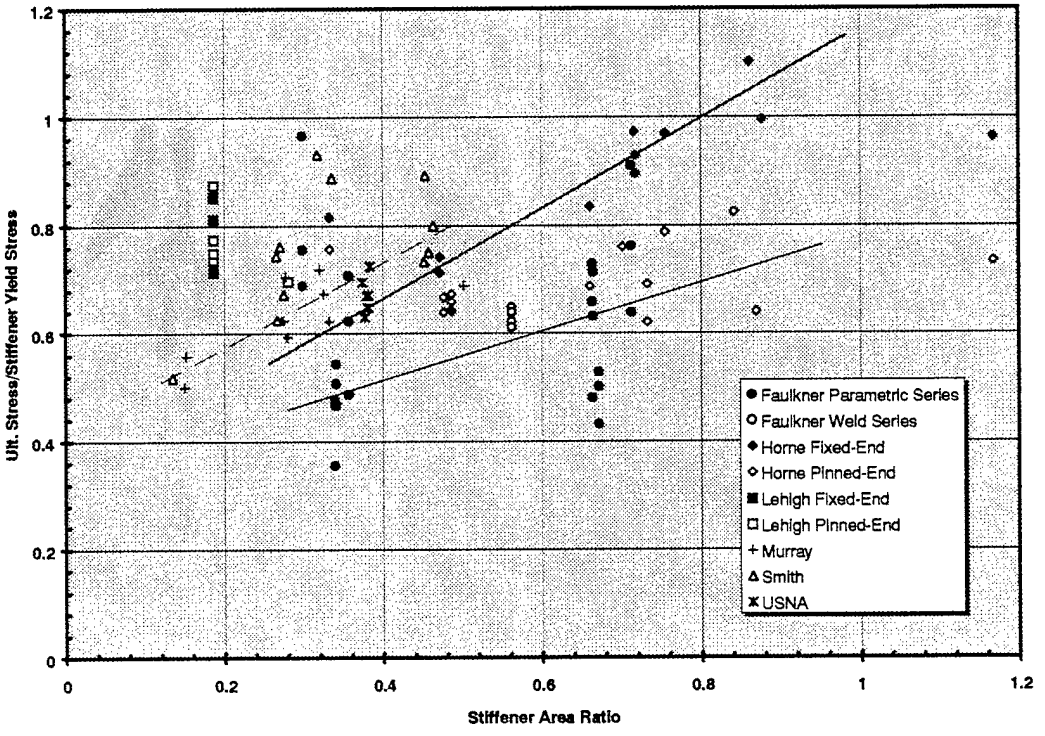


Figure 46 - Effect of Stiffener Area Ratio

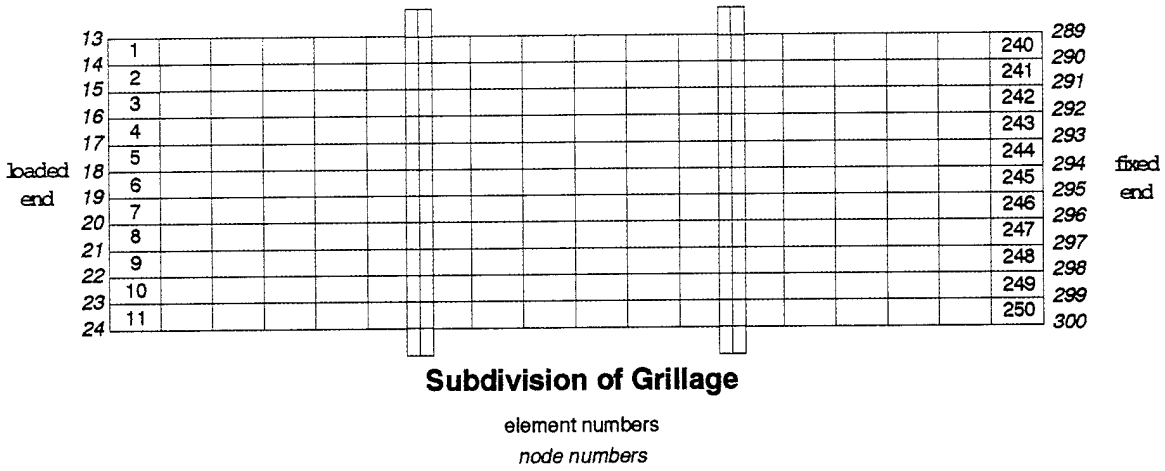


Figure 47 - Element Subdivisions of Grillage
All nodes and elements numbered consecutively

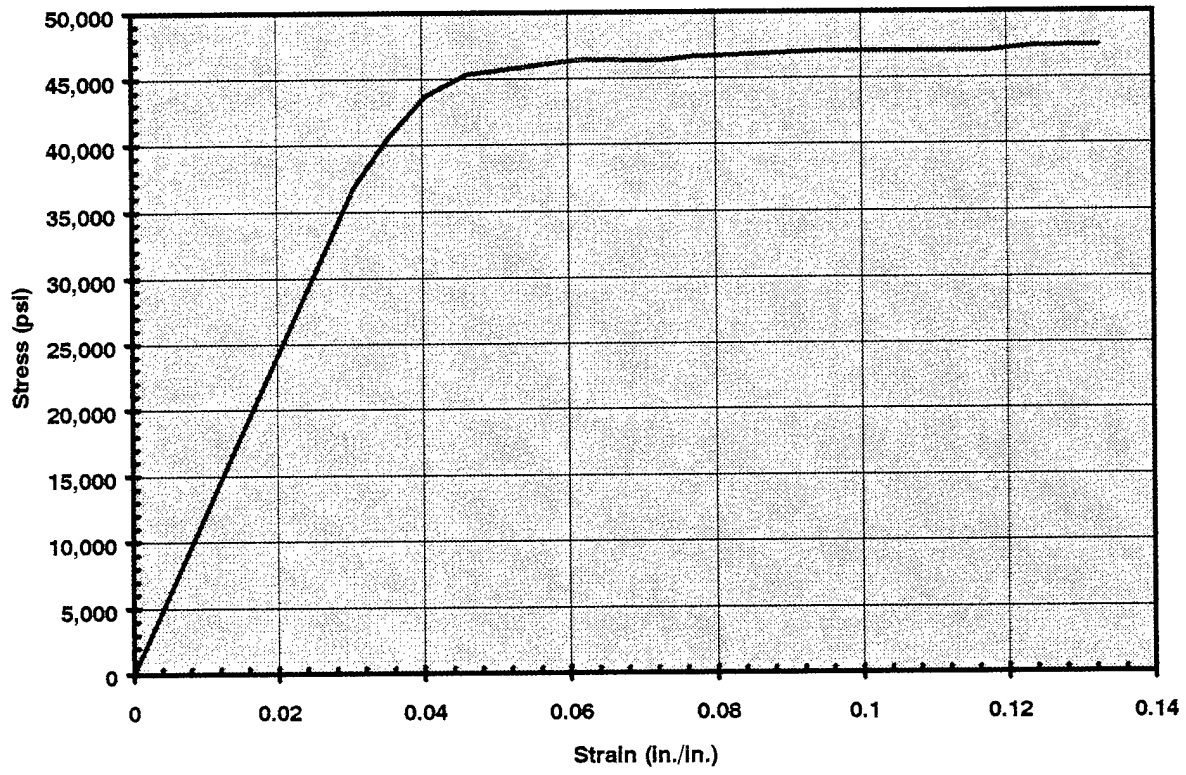


Figure 48 - Compressive Coupon Test for Center Plate

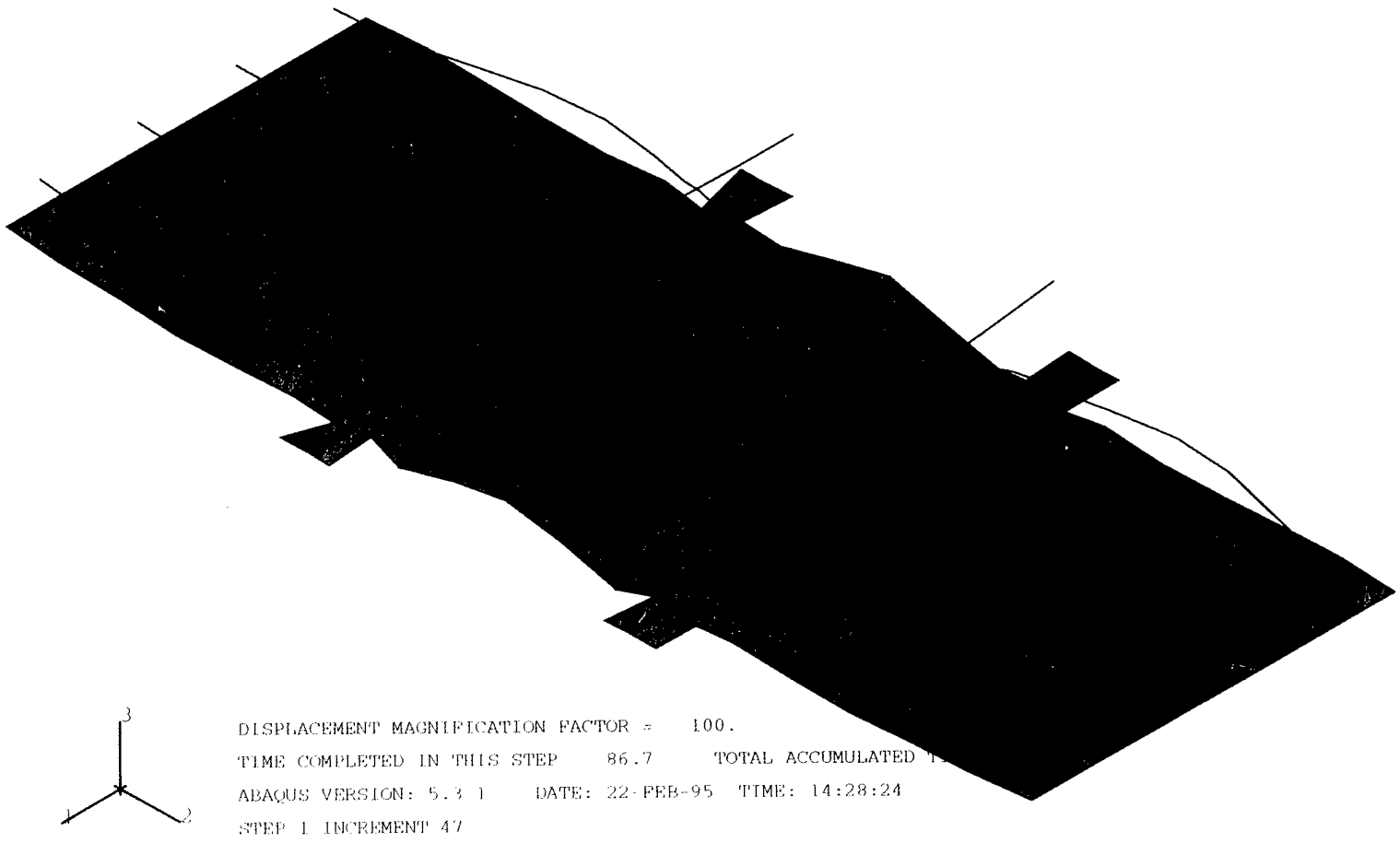


Figure 49 - FEA Displacement Results at the Ultimate Load Capacity

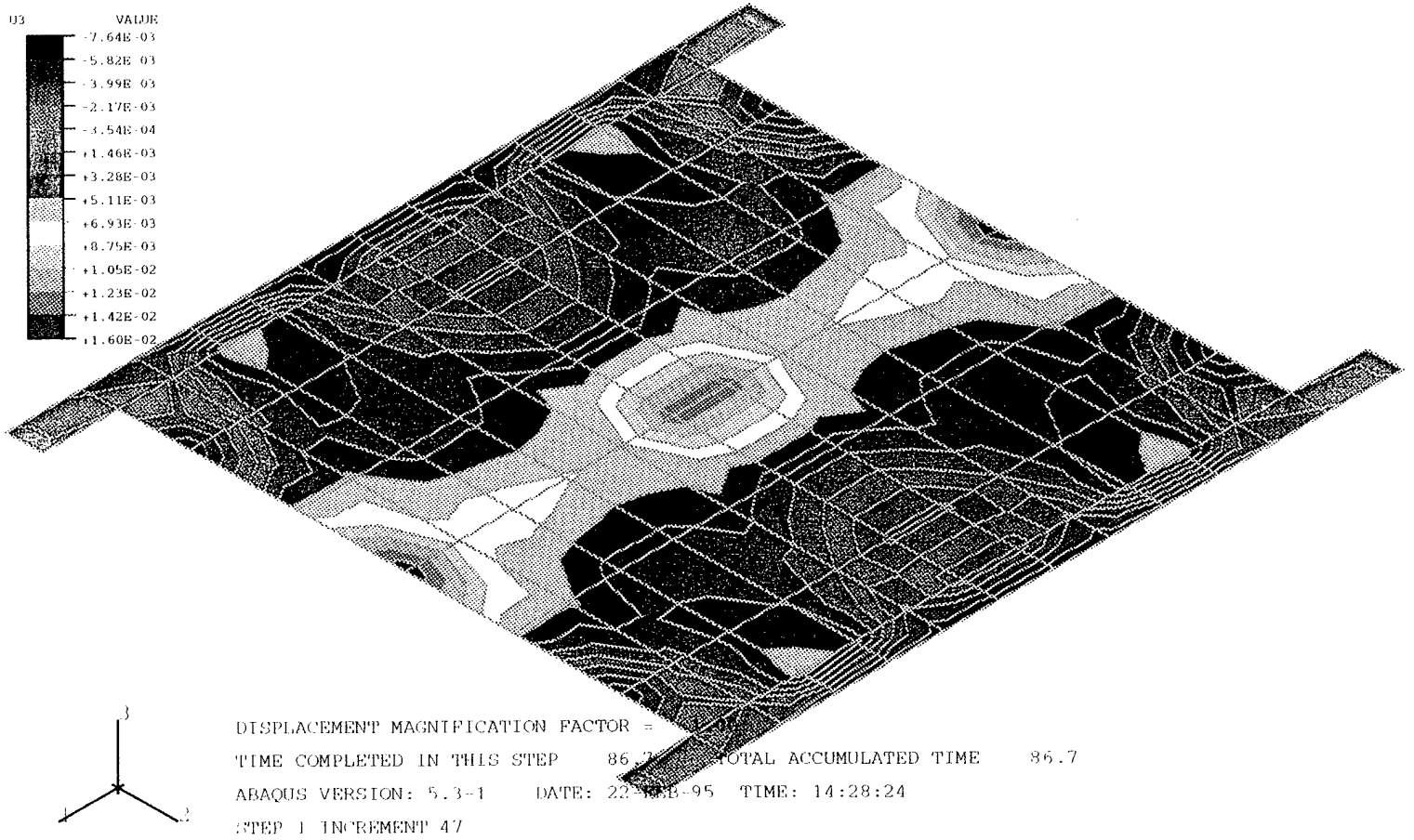


Figure 50 - FEA Contour Plot of Vertical Displacements in the Center Bay

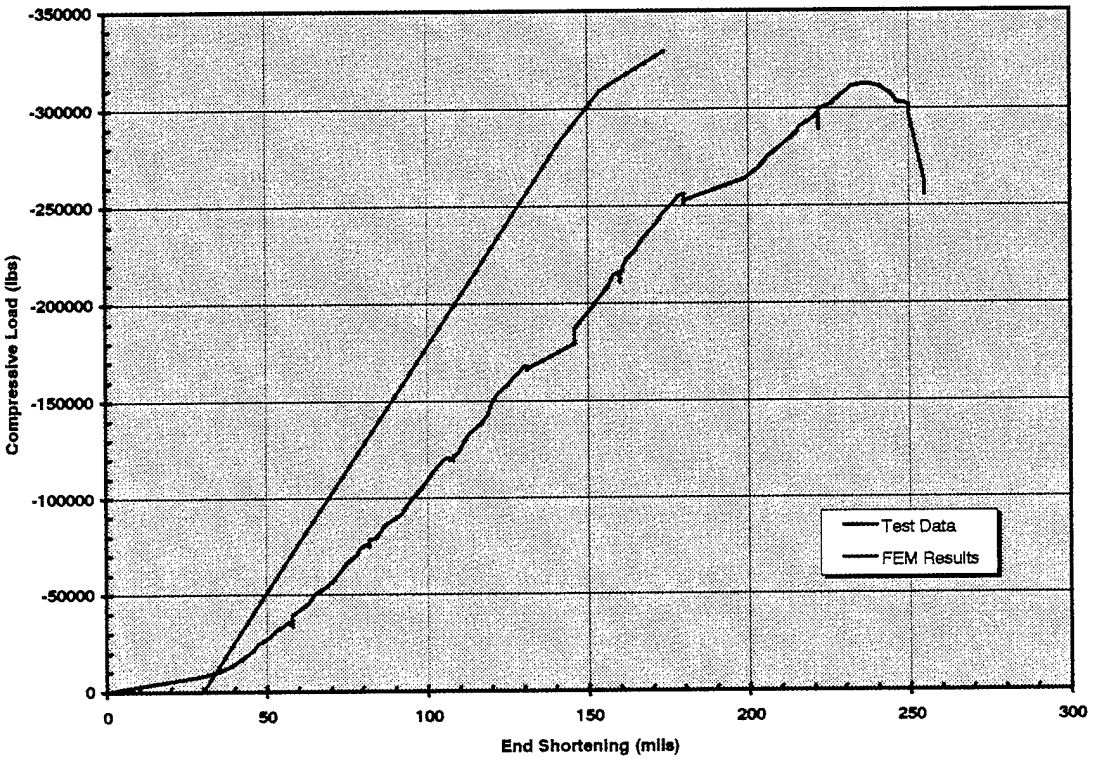


Figure 51 Comparison of FEA and Grillage Test Results

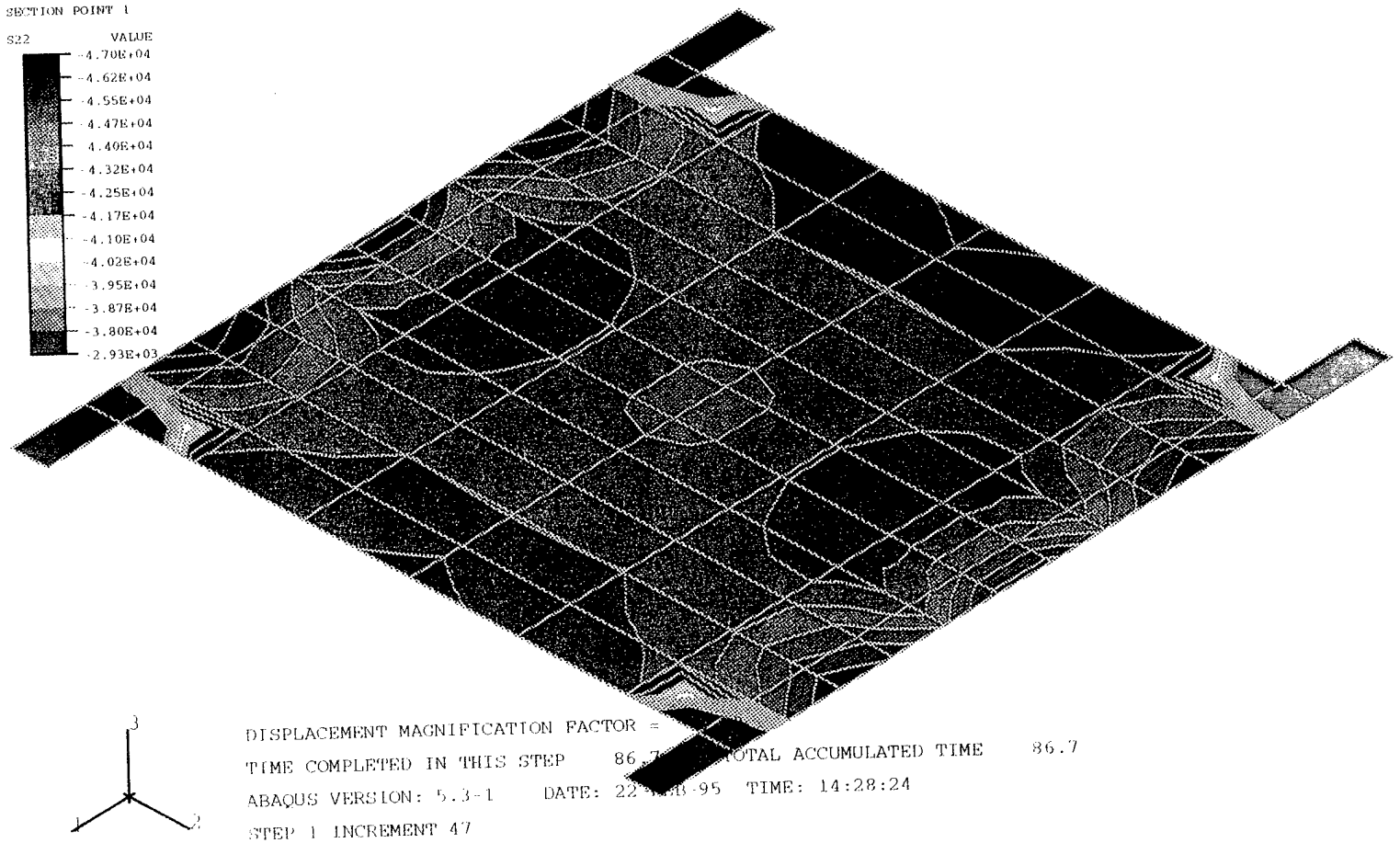


Figure 52 - Contour Plot of Stresses in Center Bay

References

1. Faulkner, D., Compression Tests on Welded Eccentrically Stiffened Plate Panels, Steel Plate Structures, ed. Dowling, P.J., et al, Crosby Lockwood, pp. 581-617, 1977.

2. Hughes, O.F., Ship Structural Design: A Rationally-Based, Computer-Aided, Optimization Approach, Society of Naval Architects and Marine Engineers, Jersey City, NJ, 1988.

3. White, G.J., R.H. Vroman, D.P. Kihl, and S.E. Mouring, An Experimental Investigation of the Ultimate Strength of Stiffened Panels - Volume 2, Test Data, NSWCCD-TR-65-97/18, April 1997.

4. British Standards Institution, BS5400: Steel, Concrete and Composite Bridges; Part 3: Code of Practice for Design of Steel Bridges, 1982

5. Hughes, O.F., E. Nikolaidis, B.M. Ayyub, G.J. White, and P. Hess, Uncertainty in Strength Models for Marine Structures, Ship Structure Committee Report SSC-375, Washington, DC, 1994.

6. Vroman, Robert H., An Analysis into the Uncertainty of Stiffened Panel Ultimate Strength, Trident Scholar Research Report No. 234, U.S. Naval Academy, Annapolis, MD., May, 1995.

7. Horne, M.R., P. Montague, and R. Narayanan, "Influence on Strength of Compression Panels of Stiffener Section, Spacing, and Weld Connection", Proceedings of the Institute of Civil Engineers, Part 2, 63, 1977.

8. Horne, M.R., and R. Narayanan, "Design of Axially Loaded Stiffened Panels," Journal of the Structural Division, ASCE, Vol. 103, pp. 2243-2257, 1977.

9. Kondo, J. and A. Ostapenko, Tests on Longitudinally Stiffened Plate Panels with Fixed Ends - Effect of Lateral Loading, Fritz Engineering Laboratory Report No. 248.12, Lehigh University, Bethlehem, PA, 1964.

10. Rampetstreiter, R.H., T. Lee, and A. Ostapenko, Tests on Longitudinally Stiffened Plate Panels - Effect of Residual Stress and Rotational Restraint by Stiffeners, Fritz Engineering Laboratory Report No. 248.5, Lehigh University, Bethlehem, PA, 1962.

11. Smith, C.S., "Compressive Strength of Welded Steel Ship Grillages," Transactions RINA, Vol. 117, pp. 325-359, 1975.

12. Murray, N.W., "Analysis and Design of Stiffened Plates for Collapse Load", The Structural Engineer, No. 3, Vol. 53, pp. 153-158, 1975.